AD-A070 291 ROYAL AIRCRAFT ESTABLISHMENT FARNBOROUGH (ENGLAND) F/6 17/7
TRIALS OF THE DOPPLER MICROWAVE LANDING SYSTEM AT MANCHESTER IN--ETC(U)
NOV 78 D WALKER

UNCLASSIFIED RAE-TR-78144 DRIC -BR-67351 NL

1 OF 2

AD
A070291

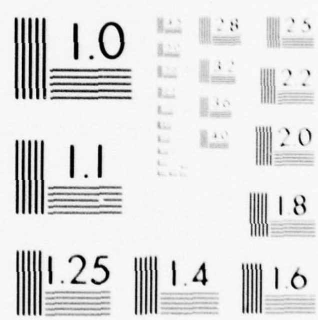


MICROCOPY RESOLUTION TEST CHART
NATIONAL BUREAU OF STANDARDS-1963-A

ROYAL AIRCRAFT ESTABLISHMENT

*

(9) Technical ~~Report~~ 78144

(11) November 1978

(12) 231p.

# (6) TRIALS OF THE DOPPLER MICROWAVE LANDING SYSTEM AT MANCHESTER INTERNATIONAL AIRPORT, OCTOBER/NOVEMBER 1977.

by

(10) D. Walker



*

Procurement Executive, Ministry of Defence
Farnborough, Hants

UDC 527.6 : 621.396.962.23 : 621.396.933.23 : 621.391.826.2

ROYAL AIRCRAFT ESTABLISHMENT

Technical Report 78144

Received for printing 29 November 1978

# TRIALS OF THE DOPPLER MICROWAVE LANDING SYSTEM AT MANCHESTER INTERNATIONAL AIRPORT, OCTOBER/NOVEMBER 1977

by

D. Walker

## SUMMARY

This Report describes tests performed at Manchester to determine the multipath environment at the airport, and to assess the accuracy and coverage of the Doppler Microwave Landing System in this environment.

High levels of azimuth system multipath were found close to runway threshold but azimuth systems with as small an aperture as 20 wavelengths (1.2 m) gave the equivalent of ILS Category III accuracy. No isolated sources of elevation multipath were found and a 39 wavelength aperture system (2.3 m) gave the equivalent of ILS Category III accuracy for $3^o$ approaches.

+ or -

The coverage requirement of 20 n mile range and $\pm 40^o$ azimuth was achieved at heights sufficient to give clear line of sight, but at elevation angles below about $1.5^o$, shadowing caused signal loss and large errors.

Autolands were demonstrated using the 54 wavelength aperture systems.

No specifically technique related effects were seen and the results are regarded as representative of typical C-band MLS performance.



Departmental Reference: Rad-Nav 67

# LIST OF CONTENTS

# 1 INTRODUCTION

## 1.1 Background

The trials of DMLS at Manchester International Airport formed part of a series conducted at operational airports during 1977/78. This series was in specific response to ICAO state letter SD 23/1-77/127 in which the Council encouraged proposers of MLS to carry out real trials at typical airports prior to the All Weather Operations Divisional Meeting scheduled for April 1978. The airports visited in the trials programme were Brussels[1], Stansted, Gatwick[2], Kjevik[3] (Norway), Manchester, Berne[4], Tehran, John F. Kennedy[5] (New York), and Dorval (Montreal) and each of these sites forms the subject of a separate report.

The primary information from these trials was submitted to ICAO prior to the April 1978 meeting in a series of working papers. This Report is intended as a more permanent and readily available record of the work and also looks at the results in more depth than the working paper. A full description of the Doppler Microwave Landing System used in these trials is given in Ref 6.

## 1.2 Local details

The DMLS equipment was tested at Manchester International Airport on runway 24 from 23 October to 9 November 1977. This included site preparation and clearance. The tasks were done in conjunction with the Plessey Company who installed and maintained the equipment, and the Civil Aviation Authority (TELS N3) who made planning arrangements for the trials and acted as liaison with the Airport Authorities. RAE RN2 Division conducted ground and flight tests (using Andover XS646) and FS2 Division demonstrated autolands in the RAE Bedford HS748. Flight checks of the ILS were done by the Civil Aviation Flying Unit before and after the MLS installation. Photographs of the DMLS equipment and of the local airfield environment were taken by Printing Branch, RAE.

The primary objectives of the tests at Manchester were:

(a) to investigate the performance of standard and reduced aperture systems on a humped-runway site;

(b) to demonstrate and record the autoland performance on a humped-runway site;

(c) to obtain further general data on typical performance in an operational environment to extend the data base for ICAO.

The opportunity was also taken to film the equipment installation and air-
144 craft autolands for a television programme (Tomorrow's World) and for a publicity film.

## 2 SITE DESCRIPTION

Manchester International Airport has one two-directional operational runway, 06-24 of length 2744 m (9000 ft), and the DMLS equipment was installed to serve the 24 direction which has a Category II ILS installation. Fig 1 shows the ICAO approach chart for this runway, Fig 2 shows a plan of the airport with the positions of the MLS installation, and Fig 3 gives detailed siting. A significant feature of the Manchester site was the runway hump, the profile of which is shown in Fig 4. Also shown are measured azimuth multipath levels near threshold (see section 4). Line of sight from the DMLS azimuth was blocked for aircraft below a height of 40 ft at threshold on an approach to runway 24, thus giving rise to significant attenuation of the guidance signal in the threshold region. The terrain in front of the DMLS arrays was level ground covered in short grass, which under the prevailing wet conditions gave strong reflection of the C-band signal at low elevation angles. A view from the azimuth transmitter site along the runway centre line shows the runway lights, and a marker post which was used to set the array centre line with respect to the runway centre line (Fig 5). It is seen that the lighting pattern was slightly offset relative to the array centre line.

The site included several structures of interest from the multipath point of view. Building 521 was a large hangar parallel to the runway and half way along, and gave rise to reflected azimuth system energy in the threshold region. A view of the hangar is shown in Fig 6a with a close-up of the surface detail in Fig 6b. Another feature, which affected azimuth guidance signals in orbital flights, was the brickworks' chimney in Fig 7a. This was at an azimuth angle of $32^{\circ}$ left (as seen from the aircraft) and subtended an elevation angle of $3.9^{\circ}$. Additional items were the control tower building, Fig 7b, and a radar tower, which again affected azimuth orbital data. A general sky-line elevation angle survey is shown in Figs 8 and 9 for the azimuth and elevation sites respectively. Also shown are orbital flight paths and flag details (see section 5.4). Apart from the chimney already mentioned, the highest elevation angles subtended by obstructions in the airfield vicinity were approximately $1.5^{\circ}$ and were associated with trees within or just outside the airfield boundary. The high ground of the Pennines (maximum height 550 m (1800 ft)) is beyond 20 n mile range and thus subtends elevation angles lower than the objects in the immediate vicinity of the airfield.

## 3 DIARY OF EVENTS

Single slab concrete bases and power supply lines were installed prior to equipment arrival.

| | | |
|---|---|---|
| Day 1 | October 23 | Concrete bases drilled |
| Day 2 | October 24 | Equipment arrived and unloaded into hangar |
| Day 3 | October 25 | Re-assembly of elevation switches and phase checking |
| Day 4 | October 26 | Installation of azimuth and elevation |
| Day 5 | October 27 | Continued installation, half of day lost due to vehicles stuck in mud |
| Day 6 | October 28 | Azimuth final alignment - no flying due to Andover engine fault. ILS flight calibration checks by CAFU. |
| Day 7-8 | October 29-30 | No flying at weekend |
| Day 9 | October 31 | No flying due to high cross winds |
| Day 10 | November 1 | Flight 155/14 and 155/15, 6 autolands |
| Day 11 | November 2 | Andover flight UT35 - autoland flights 155/17 and 155/18 |
| Day 12 | November 3 | Andover flight UT36 - tracked azimuth and coverage |
| Day 13 | November 4 | Andover flight UT37 - tracked elevation and CW runs |
| Day 14-15 | November 5-6 | Weekend - no flying |
| Day 16 | November 7 | Multipath tests on runway in RAE test van |
| Day 17 | November 8 | Andover flight UT38 - long range coverage and orbits |
| Day 18 | November 9 | Uplift equipment and pack ready for trials at Berne. |

It should be noted that the installation was done on an active runway (either 06 or 24 in operation) and in poor weather conditions. A flight check of the ILS localiser and glide path had to be done as soon as possible after the arrays were installed, so that the ILS could be restored to Category II operation. It was found that the presence of the MLS installation did not affect the accuracy of the ILS serving runway 24. The MIAA (Manchester International Airport Authority) provided excellent facilities including laying a temporary road to the azimuth
144 site when conditions became too muddy for installation work.

## 4 MULTIPATH CHECKS

It has been the practice, at each test site, to take measurements to determine multipath levels wherever possible. The first landing at Manchester in the RAE Andover indicated an increase in azimuth guidance noise just after threshold, and it soon became obvious that building 521 (Fig 6a&b) was the likely cause. A series of measurements was therefore planned to investigate this region in detail both in the air and on the ground, in addition to the normal multipath checks.

### 4.1 Ground-based multipath measurements

A vehicle-mounted mast was used for measurements up to a height of 9.1 m (30 ft) and a trailer-mounted pneumatic mast for measurements up to a height of 21.3 m (70 ft). A small horn antenna was used in each case with a coverage of $\pm 40^{\circ}$ between 3 dB points in azimuth. The azimuth pattern of the horn was flat to $\pm 12^{\circ}$, so that the multipath level from building 521 was unaffected, and a reduction of 1.0 dB occurred for multipath sources out at $\pm 25^{\circ}$ in azimuth. Three sets of measurements were made during vehicle runs along the runway, while using the vehicle mast:

(a) recording normal receiver output and AGC level;

(b) recording receiver AGC from a CW signal radiated from a single element of the azimuth array;

(c) recording signal code spectra from a calibrated spectrum analyser.

The trailer mast was used for spectra measurements at a fixed position on the runway.

#### 4.1.1 Vehicle runs recording receiver output

The results from the vehicle runs recording receiver output, are summarised in Fig 10a-c. It is seen that the signal level fell off sharply over the crest of the runway hump, and that the multipath signal from building 521 took over from the direct signal at distances beyond 2600 m from the azimuth transmitter. Error bars on the AGC and angle plots indicate peak to peak excursions. The receiver remained locked to the direct signal as far as 2800 m on the vehicle run away from the azimuth transmitter, due to the receiver confidence circuit which enabled the receiver to ignore a multipath greater than the direct signal for a predetermined length of time. Large angular variations ($0.3^{\circ}$ peak to peak) on the guidance signal were seen in the region 2700 m from the azimuth transmitter. A bad receiver
flag condition occurred during the change-over from direct to multipath signal. 144
Also shown on Fig 10a are theoretical values of signal level (see section 5.1.2).

#### 4.1.2 Vehicle runs recording receiver AGC from a CW transmission

Two vehicle runs were done recording a CW transmission from a single element of the azimuth array. The first with the vehicle mast at 4.5 m (15 ft) was done from 05 to 24 (200 m to 3000 m from azimuth transmitter) and the second with the mast at 9.75 m (32 ft) from 24 to link A (3000 m to 2150 m from azimuth transmitter). These recordings enabled an assessment to be made of the difference in levels of multipath and direct signal, but were ambiguous as far as determining which was the greater signal. The recordings also gave some indication as to the coherence of the reflected multipath signal. Relative multipath level plots are given in Fig 11a and 11b, for these two runs, for the 521 building reflection region. It is seen that large fluctuations in multipath level occurred whilst the vehicle traversed the specular reflection region for building 521, and high levels of multipath (almost up to unity) occurred on the 4.6 m (15 ft) run, outside the specular region. Beyond threshold on this run (*ie* at 4.6 m) the multipath level was somewhat indeterminate, since other multipath signals were present, as well as that from 521 building. A study of the photographs of building 521 in Fig 6 shows that the surface was not the flat metal sheet assumed for buildings in many airport simulation studies, but had three gable ends, glass sections and protruding girders. The surface was also of corrugated metal. Thus it is not surprising that variations in reflection level occurred as the reflection zone moved across the building. The multipath levels in excess of unity were deduced from spectral measurements, since AGC variations alone were not sufficient to determine which was the greater signal. The cyclic beat between the direct and multipath signals can be used to check the offset angle $\theta$ of the reflector with respect to the runway centre line, as seen from the receiver. Thus, if $d$ is the distance moved during one cycle, then

$$d = \lambda/(1 - \cos\theta) \quad , \tag{1}$$

where $\lambda$ is the wavelength. Thus for variations on the 4.6 m run, near to the MLS elevation site, a cyclic spacing of 3.48 m was estimated, corresponding to an offset angle $\theta$ of $10.6^{\circ}$. This agrees well with the specular angle measured from the airfield chart of $10.5^{\circ}$. A section of the AGC recording is shown in Fig 12, and illustrates the variation in multipath level.

Although the main azimuth multipath source for the runway region was reflection from building 521, other lower level multipath signals were present, and can be used to illustrate the validity of the multipath assessment techniques. A section of the AGC record in Fig 13 shows the effects of multipath at a distance

144

of approximately 1000 m from the azimuth transmitter. The multipath was present along a region of approximately 100 m of the runway, and unlike that in the 521 building region, the multipath level faded away smoothly on either side of the peak value. The maximum level was -9 dB as deduced from the peak to peak AGC variations. The offset angle from centre line, as seen from the receiver can again be deduced from the periodic spacing of the AGC variations. A linear spacing between maxima of 0.33 m implied an offset angle of $34^{\circ}$, but gave no information on which side of the centre line the reflector was situated. Spectral measurements described later show that it was offset to the north of the runway, at an angle of about $32^{\circ}$. Inspection of the airfield chart identified the reflector as 'BIB centre'. This was a brick building, about 5 m high (H) and 22 m long (W). The building can be seen in the photograph from the azimuth site in Fig 14. The dimensions of the building were such that $H$ and $W \sin \theta$ are of the order of the first Fresnel zone $F$ at that point $\left(F = \sqrt{(\lambda d)}/2 \doteqdot 4 \text{ m}\right)$ and therefore the building should be an effective reflector. Previous measurements of C-band reflections gave a reflection level of -5 dB for a brick surface so that the additional loss can be attributed to path length differences (1.5 dB) and the horn radiation pattern (2.5 dB).

The specular reflection region should extend for 44 m along the runway and the AGC measurements show that this corresponded to multipath levels within about 3 dB of the maximum but with no sharp cut-off beyond these points.

A further low level multipath signal occurred at a distance of 1200 m to 1500 m from the azimuth transmitter. From the periodic spacing of AGC variation, an offset angle from centre line of about $25^{\circ}$ was deduced, and spectral measurements (described later) showed that the reflector was again to the north of the runway and offset about $25^{\circ}$. The airfield plan and the photograph in Fig 14 show that the reflection was due to the airfield boundary fence which ran parallel to the runway. This fence was aboug 3 m high and of wire mesh supported by concrete posts. The multipath level from the fence was about -15 dB. Such a level is insignificant on an azimuth system, but in other situations could be troublesome, *eg* for an elevation system, if giving an 'in beam' multipath.

#### 4.1.3 Vehicle runs recording analyser spectra

The use of a C-band spectrum analyser, with an array scanning set to be continuously bi-directional (*ie* no TDM), and no reference signal radiated, enabled recordings to be made of the received spectra. A section of such a recording is shown in Fig 15. This shows the direct signal spectrum, together with the multipath spectrum from building 521 during the runway run with vehicle 144 mast at 9.75 m (32 ft). The levels of direct and multipath signals can be measured, and also the angle coding offset angle as seen from the transmitter.

Plots of the direct and multipath levels deduced from the spectral recordings are shown in Fig 16a&b for a vehicle run at 9.75 m (32 ft) and 4.6 m (15 ft) respectively, for the 521 building multipath region. There is good agreement with the CW AGC measurements in Fig 11a&b. It should be noted that the spectrum analyser sweep time of 2 s limited the number of samples during a run, so that some of the detailed variations of the CW measurements are inevitably missing. Diffraction 'fringe' effects can be seen in Fig 16a at the edge of the specular reflection region, and a dotted curve shows calculated diffraction variations using Fresnel integrals and Babinet's principle. The agreement is reasonably good. (No account was taken of ground reflection.)

#### 4.1.4 Fixed position pole test, recording analyser spectra

The van and pneumatic mast were positioned at 2650 m from the azimuth transmitter, on the runway centre line, and spectral photographs were taken at a series of heights, from 9.75 m (32 ft) down to 3 m (10 ft), using the vehicle mast (Fig 17). The position chosen was in the centre of the 521 building specular reflection region, and the photographs show that the multipath level was equal to the direct signal at a height of 8.5 m (27ft 9in) and below this height, the multipath level predominated. At the lowest height, both signals were almost down to the analyser noise level.

A continuous UV recording was made at the same location, while the vehicle mast was lowered from 9.75 m (32 ft) to 3 m (10 ft) and the estimated direct and multipath signal levels are shown in Fig 18. A similar recording was made using the pneumatic mast, for a height variation of 21.3 m (70 ft) down to 5.2 m (14 ft), and the results are shown in Fig 19. It is seen that multipath levels only a few dB lower than the direct signal were encountered up to heights of 21.3 m (70 ft), and that below a height of about 8.2 m (27 ft), the multipath signal was predominant. (It should be noted that the CW, and spectrum van runs and the spectral pole tests were done during a normal operational day, thanks to the co-operation of ATC and ground movements.)

#### 4.1.5 Summary of ground-based multipath measurements

These measurements were confined to the azimuth system and mainly to the multipath associated with building 521. The three types of measurement, viz normal guidance signal, CW radiation and spectral measurements, gave consistent results, and showed that multipath levels greater than unity were produced by building 521, below a height of 8.5 m (28 ft) and extending for approximately 200 m along the runway. For a slowly moving vehicle, *eg* a taxiing aircraft, this will give false guidance information. The effect on the guidance of a landing aircraft is discussed in section 4.2. Other lower level multipath signal sources were identified as a small brick building and an airfield boundary fence. These multipath levels and offset coding angles were such that no guidance errors were seen, or would be expected.

The measured multipath levels from 521 building have been plotted in Fig 4 as lines of constant multipath to direct signal ratio.

### 4.2 Airborne multipath measurements

The airborne multipath measurements were confined to AGC recordings of CW radiation from single array elements. Spectral measurements similar to those done as part of the ground-based measurements were not feasible in real time with a conventional analyser because of the relatively slow analyser scan rate and the higher aircraft speed. The airborne recordings of azimuth CW AGC from two $3^{\circ}$ approaches to low overshoot, are shown in Fig 20a&b, where the three traces are:-

(1) the aircraft wheel height taken directly from the radio altimeter output;

(2) the instantaneous AGC level on a fast galvanometer, showing the interference pattern generated between the direct and multipath CW signals;

(3) the envelope of multipath signal amplitude as deduced from the amplitude of the interference pattern.

On both flights, peak multipath levels of near 0 dB were seen with the total significant region covering a distance of 240 m and lasting some 7 s at the approach speed of 115 kn typical for the Andover. The wheel height was around 7 m (23 ft), corresponding to an antenna height of 11.3 m (37 ft) for the region between threshold and link B (2800 m to 2650 m from azimuth transmitter). The antenna height at the start of the concrete was about 16 m (52 ft), and high multipath levels extended beyond this point, even though this was well clear of the specular region of 521 building. Similar variations on signal amplitude to those on the ground CW AGC tests occurred throughout the reflection region. The scalloping (or fading) frequency increased from 10 Hz to 17 Hz through the region.

The effect of such high levels of multipath on the azimuth guidance signal depends on the coding separation angle of the multipath signal. The separation angle was around $10^{\circ}$ or 10 beamwidths for the $1^{\circ}$ ($54\lambda$ aperture) system, but only 144
2.5 beamwidths for the $4^{\circ}$ ($15\lambda$ equivalent aperture) system. It is to be expected

that the resultant errors would increase for the larger beamwidth system, but still be acceptably below the ICAO limits of $0.054^{\circ}$ ($2\sigma$) for a full capability system. If the aircraft flight path was such that the antenna went below 8.5 m (28 ft) in the multipath region, then the multipath level would exceed the direct signal, so that larger errors would result, but the time of exposure to this high level (say 3 s) would be short enough for the receiver to 'ride through' without locking to the multipath signal. Actual flight results on aircraft approaches are discussed in section 5.2.

#### 4.2.1 Airborne multipath measurements on elevation subsystem

Measurements of receiver AGC from a CW signal radiated from a single elevation element were performed during $3^{\circ}$ approaches. No variations were noted which could be attributed to building reflection. This result was to be expected from the site survey (Fig 9), which showed that the only significant building, the airport hotel at $32^{\circ}$R azimuth, subtended an elevation angle below $1^{\circ}$, *ie* well below the normal glide slope angle. This is confirmed in a photograph taken from the elevation site, shown in Fig 21.

## 5 SYSTEM TESTS ON ACCURACY AND COVERAGE

The previous section has described multipath measurements made at the airfield, particularly for the azimuth subsystem; this section describes measurements made on the ground and in the air, of the system accuracy and the coverage achieved. The accuracy limits against which the measured values were assessed are those defined by ICAO Working Group A, and are shown in Table 1 for a Full Capability System and Table 2 for a Reduced Capability System. The limits in azimuth at threshold for the full capability system (for a 14000 ft or 4870 m runway) are $0.054^{\circ}$ ($2\sigma$) for noise and for bias. The corresponding limit for elevation is $0.07^{\circ}$ ($2\sigma$) for noise and for bias. These limits are as good as those for a Category III ILS localiser, and better than those for a Category III glide path system.

### 5.1 Ground measurements

#### 5.1.1 Vehicle runway runs - guidance accuracy

The multipath aspects of runway runs recording receiver angle have already been described in section 4. These runs showed that with an antenna height of 4.6 m (15 ft), false azimuth guidance, originating from building 521, was obtained by a slowly moving vehicle, in the threshold region. Relatively large variations in guidance angle also occurred ($0.3^{\circ}$ peak to peak) for the $27\lambda$ transmissions, when not locked to the false guidance signal. Once clear of the multipath region from building 521, both $54\lambda$ and $27\lambda$ azimuth signals gave angle noise of $<0.02^{\circ}$ peak to peak. Plots of receiver azimuth angle during three runway runs are shown in Fig 22a-c. Two runs done with the transmitter radiating in a $54\lambda$ mode showed a mean bias of $0.05^\circ$ left of runway centre line at 2400 m from the transmitter, reducing to zero at about 400 m from the transmitter. This is consistent with an angular misalignment of $0.05^\circ$ and an offset of approximately 0.3 m (1 ft) left (see Fig 22c). The photograph in Fig 5, taken from the array centre line shows a metal post to which the array was aligned. This post was to the right of the lighting pattern, and probably also of the runway white line. These measurements are with respect to the runway white line which was followed by the vehicle to an accuracy of approximately 0.3 m (1 ft). Thus any deviations of the white line from a straight line would show up as a weave on the receiver output trace. There was a deviation of about $0.05^\circ$ right at 1150 m from the transmitter on each of the $54\lambda$ runs which could be caused by a 1 m deviation of the white line. However, the deviation did not show on the $27\lambda$ run so that another explanation is needed. The deviation occurred in the region where there are low level (-15 dB) reflections from the airfield boundary fence, but receiver processor error curves show that it is unlikely that such a level of multipath at an offset angle of $25^\circ$ could cause these errors. In terms of the equivalent physical displacement error of 1 m on the Manchester runway, the error is of course negligible. The cause of the weave remains uncertain.

The $27\lambda$ vehicle run showed a mean angular misalignment of $0.09^\circ$ left of the white line. The difference between the misalignments at $54\lambda$ and $27\lambda$ ($0.04^\circ$) is attributed to the phase distribution of the elements across the array, *ie* the mean phase front across the short section of the array was different from that across the whole array.

5.1.2 Vehicle runs - signal level measurement

Fig 10a-c shows signal level measurements during vehicle runs along the Manchester runway with an antenna height of 4.6 m (15 ft). The measurements were taken with a small horn aerial with an estimated gain of 10 dB and using a 9.1 m (30 ft) cable with a loss of 10 dB. Thus the overall unity gain of the installation is similar to an installation in a large aircraft, using low loss cable and an 'omni' antenna. The signal level fell rapidly beyond the runway hump and was estimated to be approximately -93 dBm in the region beyond the 24 threshold. This level was some 10 dB above the receiver threshold. The ICAO requirement is for azimuth guidance down to a height of 1 m and while measurements were not done at this height, it is doubtful if useful signals would be received, even in the absence of the multipath signal from building 521. The Lincoln Laboratory report[7] 144 on Multipath Parameter Computations uses a paper by Wait and Conda[8] in order to estimate shadowing by runway humps. The method effectively gives a correction term to be added to classical knife edge diffraction theory attenuation. The correction term is dependent on the radius of the hump; the larger the radius of curvature, the greater the divergence from the knife edge case, and the greater the attenuation for a constant diffraction angle $\theta$ . The ratio of the diffracted wave to free-space signal is given as

$$\frac{E_D}{E_0} = \left[\frac{\exp j\pi/4}{\sqrt{2}}\left(F(\infty) - F\left(\frac{\sqrt{2}}{\pi}\alpha\right)\right) - \frac{G(X)}{U}\exp - j\alpha^2\right] \quad (2)$$

where $X = (ka/2)^{1/3}\theta$

$\alpha = \frac{\theta}{2}\left\{2kS_1S_2/(S_1 + S_2)\right\}^{\frac{1}{2}}$

$a$ = radius of curvature

$\theta$ = diffraction angle

$k = 2\pi/\lambda$

$S_1$ , $S_2$ = tangential distance from transmitter and receiver to hump, and

$F(x)$ = a Fresnel integral.

The first two terms are the knife edge attenuation and the third term is the hump radius correction term.

For the Manchester runway with the transmitter at a height of 1.5 m (5 ft) and a receiver height of 4.6 m (15 ft) at a range of 3000 m, the diffraction angle $\theta = 0.31^\circ$ or 5.4 mrad. The radius of curvature of the hump was estimated to be 25000 m. Values have been calculated for the hump shadowing loss using equation (2) and are plotted in Fig 10a. It is seen that there is very good agreement with the measured values for the 4.6 m (15 ft) runway run. Also shown are calculated attenuation values for 3 m height at 2600 m and for 9 m and 12 m at 3000 m. In all cases the theoretical signal level is at least 8 dB above the receiver acquisition level and therefore should be adequate, if no multipath signal were present. Because the position of the hump is closer to the 24 threshold than to the 06 threshold, diffraction angles would be greater for an installation giving guidance for approaches to 06 threshold. Theoretical attenuation values for such an installation are given in Fig 23. For a height of 4.6 m (15 ft) above the runway, a maximum attenuation of 31 dB is predicted at a range of 2600 m, and this reaches 36 dB for a receiving antenna height of

3 m (10 ft). This latter value would give a signal level of -102 dBm for a receiving installation of similar overall gain to that in the test vehicle, and would be at the limit of receiver operation. Such conditions might arise in the case of an executive jet at or close to touch-down in the flare region. Roll out guidance could also be effected after an early touch-down.

Another aspect of the large attenuation of the azimuth signal by the runway hump, is that it occurred at the same time as high signal levels from the elevation transmitter. This is illustrated in Fig 24 which shows a plot of azimuth and elevation signal level during an approach to land. Shortly after threshold there was a 30 dB difference between the two signals, which rose to 39 dB close to the elevation transmitter. This dynamic range requirement caused no problems to the DMLS receiver, since each subsystem signal was handled separately by a fast acting AGC loop. There is a danger, however, if a common AGC was used for azimuth and elevation, that the gain could be depressed so that the azimuth signal fell below the receiver acquisition level.

5.1.3 Pole tests on elevation subsystem

Accuracy flights tracked by the CAA telecroscope gave no measure of the absolute accuracy of the elevation system as no absolute bias term was available. Pole tests were therefore done at distances of 75.9 m (249 ft) and 401 m (1316 ft) in front of the elevation transmitter, and plots of the error angle between the DMLS receiver angle and the theodolite measured angle are given in Fig 25a-d for $54\lambda$ and $27\lambda$. The measurements at $54\lambda$ show a bias error of $-0.04^{\circ}$ at 401 m (1316 ft) and $-0.03^{\circ}$ at 75.9 m (249 ft). The separation angle between the direct and ground reflected signal (assuming flat ground) is marked on the scale and also the corresponding side lobe angles. A receiver processor error curve for $54\lambda$ elevation with a -3 dB multipath is given in Fig 26 and the slowly varying error for $54\lambda$ at 401 m (1316 ft) (Fig 25c) is consistent with the error distribution in Fig 26, and implies a (ground reflected) multipath in the region of -3 dB. The measurements at $27\lambda$ show a positive bias of $0.035^{\circ}$, and this difference in bias between the $54\lambda$ and $27\lambda$ configurations ($0.07^{\circ}$) was probably due to the difference in phase distribution across the two arrays. (The $27\lambda$ array used the centre portion of the $54\lambda$ array.) The $27\lambda$ curves in Fig 25b and 25d are again consistent with a ground reflected multipath in the region of -3 dB (see Fig 27), except for an error of $+0.5^{\circ}$ at 16.5 m (54 ft) on the 401 m (1316 ft) curve, and for two large negative errors at 7.8 m (25.6 ft) and 8.1 m (26.5 ft) on the 75.9 m (249 ft) curve. Some form of abnormal operation is suspected for these points. When relating the error curves from static pole tests to the performance in flight, 144 the aircraft elevation angle can be taken to be half the separation angle. Thus, as far as the specular ground-reflected signal is concerned, the 54λ configuration should give acceptable performance at elevation angles down to about $1^{\circ}$. In the case of the 27λ configuration, unacceptably large errors (greater than $0.1^{\circ}$) occurred at elevation angles in excess of $3^{\circ}$, which is a standard aircraft approach angle. It will be seen later that flight tests show that specular ground reflections are probably not the sole limiting factor, but a combination of this with scattered signals from other objects, giving effectively 'in beam' multipath.

## 5.2 Approach accuracy flight tests

### 5.2.1 Azimuth

Accuracy flight tests were performed in the RAE Andover, and for centre line approaches, the aircraft was tracked by the telecroscope operated by CAA personnel. The flight recording system and tracker operation are described in a separate report[4]. As stated earlier, the telecroscope was not used to measure system bias, so that the mean bias error was set nominally to zero for each run. It was not possible to mount the telecroscope at the phase centre of either array, and in the case of the azimuth system it was offset by 2.7 m to the side of the array. Consequently there was an increasing bias difference between the DMLS angle and the telecroscope angle as the array was approached. This bias value has been calculated and is plotted on the error plot in curves (b) below, together with the ICAO limits of $\pm 0.054^{\circ}$ for $2\sigma$ noise.

Two plots are shown for each approach:-

(a) the raw DMLS receiver output with no smoothing;

(b) the error trace (raw DMLS minus telecroscope tracker angle) with major telecroscope drop-outs censored by hand.

An example is given in Fig 28 of the telecroscope tracker angle, and the untouched error trace, in addition to (a) and (b) above, so that the type of hand censoring can be seen.

Tracked azimuth approaches with the system operating with apertures of 54λ and 27λ are shown in Figs 28 and 29. The system performance is well inside the ICAO Full Capability System noise limits for the longest runway. There is only a very small effect due to the high level multipath signal just inside threshold.

At Manchester some flights were made with the receiver modified to use only the 20λ or 15λ centre position of the 27λ ground system. This was easily done due
144 to the sequential nature of the ground radiated signal thus enabling a quick evaluation of the performance of very small apertures on a long humped-runway site.

Results are shown in Figs 30 and 31. At 20λ aperture (1.2 m wide) there was a general increase in short term noise, although it was still very small. There was also some evidence of a long period bend during the last mile of the approach. Overall performance lies just inside the ICAO Full Capability System noise limits. At 15λ aperture (only 0.9 m) the short term noise was still well inside the ICAO specifications but overall noise including the bend in the last mile was just outside. Considering the runway hump and length this was a very good result from such a short aperture.

There was an increase in the angular noise due to the high level multipath from building 521, just inside threshold, being a maximum of $0.07^{\circ}$ peak to peak at 20λ and $0.16^{\circ}$ at 15λ *. The latter would be outside limits for a Full Capability System on a maximum length runway, but it is unlikely that such a small aperture system would be used for such operations, on a long runway.

The long period bend during the last mile of the approach is attributed to scattering from the 06 approach lighting in front of the azimuth array. Due to the misalignment of the array with respect to the lights (see Fig 5), energy scattered from the lights was coded slightly differently from that going directly to the aircraft.

A combination of signals scattered from a number of the lights could give rise to the errors seen, if one assumes a total scattering level of approximately -15 dB. This is a surprisingly high level when it is realised that there is a separation in the vertical plane of approximately $1.8^{\circ}$, which should result in a relative attenuation of some 7 dB of the scattered signal, due to the vertical aperture of the azimuth antenna. It is possible that the antenna was not realising the full ground cut off potential during the tests. However, the errors produced are within the ICAO tolerance for a full capability system except for the 15λ aperture, which is unlikely to be used for such category landings.

### 5.2.2 Elevation

A series of approaches was made to runway 24 with the telecroscope tracker positioned for tracking in elevation. It was sited close to the runway edge, so as to give mainly planar movement of the tracker head in the vertical plane, with the aircraft in as close as threshold. The fore and aft position of the tracker was changed for the different elevation angles of approach. Two plots are given for each approach, as for the azimuth tracked runs, and bias curves on the error

---

* For a 15λ aperture ($4^{\circ}$ beamwidth) the 521 building, coded at $10^{\circ}$ puts high energy into the first side lobe of the multipath response curve.

plots (b) show the effect of the offset position of the tracker with respect to the array phase centre. The ICAO limits of $\pm 0.07^{o}$ for $2\sigma$ noise are shown relative to the telecroscope bias curve. Additional plots are given in Fig 32 in order to illustrate the hand censoring applied to the error plots.

Tracked elevation approaches with a system aperture of $54\lambda$ are shown in Figs 32, 33 and 34 for approach angles of $4^{o}$, $3^{o}$ and $2^{o}$ respectively. There was an increase in the noise on the error plot for the $2^{o}$ approach, but it was still well within the ICAO $2\sigma$ limits. The increase in noise was probably due to signals scattered from objects subtending an elevation angle above the horizontal relative to the array phase centre and hence giving coding angles within the main error lobe of the receiver error curve (approximately $2.1^{o}$), as seen in the error plot of Fig 26. The effects of decreasing the system aperture are shown in Figs 35, 36 and 37 which show $3^{o}$ approaches for apertures of $39\lambda$, $30\lambda$ and $27\lambda$ respectively. For the $39\lambda$ aperture, with a main error lobe of approximately $2.9^{o}$, scattering objects have coding angles outside this lobe and there was only a small increase in angular noise. However, for the $30\lambda$ aperture (main error lobe $3.8^{o}$) and the $27\lambda$ aperture (main error lobe $4.2^{o}$), scattering objects had coding angles inside the main error lobe and relatively large errors resulted. The effects of specular ground reflection can also be seen as longer period weaves. Both these array apertures gave errors which were outside the ICAO noise limits for a full capability system, but would be just inside the reduced capability limits of $0.1^{o}$ ($2\sigma$), especially with the additional smoothing inherent in an aircraft autopilot system*. It is estimated that multipath levels of the order of -18 dB would be necessary to give the angular noise experienced. This could be made up of scattered signals from many objects situated close to the approach direction. A photograph taken from the elevation site, and looking along the approach (Fig 38) shows that the skyline on centre line is composed of house roofs at about $+0.3^{o}$ elevation, with trees at about $0.5^{o}$ elevation within $10^{o}$ in azimuth of centre line (see Fig 9). It is thus a 'clean' site, with no isolated multipath sources affecting centre line approaches and the results can be taken as typical of those to be expected for an uncluttered elevation site.

### 5.3 Coverage radials

The design limits of angular coverage for the DMLS system used at Manchester were $\pm 40^{o}$ in azimuth and $1^{o}$ to $30^{o}$ in elevation. No azimuth system information was available beyond the $\pm 40^{o}$ limit because of a receiver flag set to operate at

---

* A bandwidth of 2.5 Hz is estimated for the DMLS angle processor output.

this point. Elevation system information extended to $\pm 90^\circ$, although in practice it would not be used beyond $\pm 40^\circ$.

Untracked coverage radials were flown inbound from 32 n mile at azimuth angles of $0^\circ$, $\pm 20^\circ$ and $\pm 39^\circ$ with respect to the azimuth site and at a height of 3500 ft, with array apertures of $54\lambda$. The centre line radial was repeated with an azimuth system array aperture of $27\lambda$, and one approach was made from 100 n mile at 10000 ft on centre line. The results from these flights are given in Figs 39 to 50. The digital data was not recovered from the $39^\circ$ right radial, and hence no plots are given. Coarse scale plots, from $0^\circ$ to $30^\circ$ in elevation, show the coverage limits in range and elevation angle of the elevation system. The flag marker trace shows the operation of the digital flag which responds to individual missing function identities and would only be accompanied by the overall system (analogue) flag, if the function identity code was missing or erroneous for a period of 1 s. Expanded scale plots of elevation angle are given for some radial flights, by using a crude pseudo tracker angle derived from range and height information. The untracked azimuth radials are given as plots to a scale of $0.05^\circ$ per cm. The coverage obtained is summarised in Table 3.

A comparison with the skyline elevation angles, in Figs 8 and 9, shows that the range was not limited by blockage in the case of the elevation system, except for the $39^\circ$L radial where trees limited the range to 26 n mile. In the case of the azimuth system, the elevation angle was almost coincident with the surveyed skyline on acquisition. The angular noise on the two systems at range was quite different. For example, on UT36/14 (Figs 45 and 46), the angular noise on elevation at 20 n mile was $0.1^\circ$ peak to peak, whereas at the same range, the azimuth angular noise was about $0.025^\circ$ peak to peak. This is due to the fact that the elevation system is susceptible to scattered ground signals coming from a wide range of azimuth angles, whereas the azimuth system is only susceptible to the scattered ground signals within an azimuth code range of $\pm 2^\circ$ (for a $54\lambda$ system). Thus Fig 46 shows that the elevation noise became negligible at ranges less than 14 n mile when the elevation angle was above $2.25^\circ$, or $1.85^\circ$ above the local skyline. This then put scattered ground signals outside the main error lobe of the receiver characteristic. Measurements of received signal level show that acquisition took place on each system at a signal level of -106 dBm.

The coverage achieved at 3500 ft on the radials which were checked, was thus in excess of the ICAO requirement of 20 n mile, and on most of the radials, it approached the ICAO recommendation of 32 n mile. The lower limit of coverage in the ICAO requirement is the obstacle clearance line of a 1 in 50 slope, giving 144 an elevation angle of $1.14^{\circ}$ and the measured coverage for the elevation system went below this angle except on the $39^{\circ}$L radial. The low angle coverage on the azimuth system was limited to $1.2^{\circ}$ by the skyline, except on centre line where coverage went down to $0.9^{\circ}$. The long range radial at 10000 ft gave coverage down to elevation angles of $1.5^{\circ}$ and $1.2^{\circ}$ for the aazimuth and elevation systems respectively.

5.4 Coverage orbits

Semi-orbits were flown to assess the coverage of the system at 20 n mile range and at heights of 3000 ft and 6000 ft using the $54\lambda$ aperture for azimuth and elevation. The 6000 ft orbit was repeated with the $27\lambda$ aperture for azimuth. The results are given in Figs 51 to 56, with the following plots for each orbit.

(a) Azimuth coarse scale plot ($\pm 60^{\circ}$).

(b) Azimuth control motion filtered plot, $0.05^{\circ}$ per cm.

(c) Elevation raw angle plot, $2.5^{\circ}$ per cm.

(d) Elevation control motion filtered plot, $0.05^{\circ}$ per cm.

Flag data is also plotted, and the azimuth flag was pre-set in the receiver to operate at $\pm 40^{\circ}$, so that no azimuth data is presented for angles beyond this limit. In most cases the azimuth transmissions continued to give successful function identity decoding beyond these angles, and the angle information was used to operate the overall system flag whenthe measured angle exceeded $40^{\circ}$ from centre line. No false course information occurred on the azimuth system (this would have been indicated by a good flag outside the $\pm 40^{\circ}$ sector), even though the OCI (out of coverage indication) antennas were not being used.

The limits of successful function identity decoding are summarised in Table 4 for the coverage orbits.

The 3000 ft orbit gave elevation angles of just over $1^{\circ}$ which was very close to the skyline in azimuth, and blockage took place for obstacles such as the brickworks chimney and radar tower and dish, and part of the tree skyline. The errors close to the chimney and radar tower were of the order of $0.25^{\circ}$ peak to peak. The coverage of the azimuth system for this orbit was therefore not satisfactory because of high noise and loss of signal caused by the airfield environment. The elevation system gave a noisy (greater than $0.1^{\circ}$ peak to peak) angular guidance signal for most of the orbit, with a clearance above the elevation skyline of about $1^{\circ}$. At about $20^{\circ}$ left of centre line, the elevation angle fell to
144 about $1^{\circ}$ and thus dropped below the tops of some of the trees close to the airfield.

A large positive angle spike of $0.5^{\circ}$ coincided with the position, $28^{\circ}$ left, of an isolated tree which is shown in Fig 57. An angle scale was photographed in front of the tree, such that 1 ft represents $1^{\circ}$, and it is seen that the top of the tree is at $1.6^{\circ}$ above horizontal, with the $1^{\circ}$ elevation angle of the aircraft path passing behind a substantial part of the tree. At the time of the measurements, the tree was in full leaf, and the apparent effect was that the aircraft receiver 'read' the angle of the top of the tree because of the signal diffracted over the tree, and the loss of the direct signal. The effect of other trees can be seen further round in the orbit, before the aircraft dropped too far below the skyline to be able to receive a usable signal. The elevation system was thus barely usable for most of this orbit, and gave large errors when the line of sight was partly obscured by trees.

The orbit at 6000 ft and 20 n mile in Figs 53 and 54 is for the $54\lambda$ aperture azimuth system. The coarse-scale azimuth plot in Fig 53a shows no flag operation within the $\pm 40^{\circ}$ coverage, and the control motion filtered plot in Fig 53b shows acceptable noise of less than $0.05^{\circ}$ peak to peak, except for angles close to the limits of coverage. At the left hand end, the brickworks' chimney intercepted the line of sight and large errors of up to $0.3^{\circ}$ resulted. Near the right hand end of the orbit there was an increase of noise to $0.13^{\circ}$ peak to peak, which may be associated with the radar tower at $36^{\circ}$ right, even though this was $1^{\circ}$ below the flight path. The elevation system plots in Fig 54 show acceptable noise over $\pm 40^{\circ}$, but near $55^{\circ}$ left, there is another example of diffraction over trees giving errors of $+0.3^{\circ}$. The trees subtended an elevation angle of about $2.8^{\circ}$, and the flight path was at an elevation of $2.4^{\circ}$ at that point. The shape of the top of the tree can be seen on the angle plot, even to the extent of the double tree formation. A similar effect is seen in the second orbit at 6000 ft in Fig 56, but in this case the flight path was at $2.3^{\circ}$, and loss of signal was experienced behind the highest point of the tree, at a diffraction angle of $0.5^{\circ}$. A photograph of the skyline showing the trees is given in Fig 58.

Fig 55 shows the results from the 6000 ft orbit using the $27\lambda$ azimuth system. There was a general increase in noise, compared with the $54\lambda$ system plot in Fig 53 and the brickworks' chimney gave $0.35^{\circ}$ peak-to-peak noise. The ICAO limits for the full capability system are shown on Fig 55 and it is seen that because of the degradation in accuracy allowed for range and azimuth angle, the noise limits were still met. (This was of course after the application of the control motion filter, so that bias terms were not included.)

5.4.1 Summary of coverage measurements

The radial and orbital coverage flights show that the DMLS installation at Manchester on runway 24 did not quite meet the ICAO noise requirement for low angle coverage down to a 1 in 50 slope. The failure to do so was due to the local airfield environment of buildings and trees which subtended elevation angles above $1.14^{o}$ and affected both the azimuth and elevation system. In clear line of sight conditions, such as occurred within $\pm 12^{o}$ of centre line, both systems met the requirement, including a $27\lambda$ aperture azimuth system. Obstruction of the line of sight for the elevation system gave errors up to $+0.5^{o}$, *ie* in a fly down sense. The azimuth and elevation angles at which this effect occurred, mean that the errors are probably not operationally significant. A brick chimney which obscured the line of sight, caused large errors in the azimuth systems. The performance of the system is totally consistent with the operating frequency of 5 GHz and the results obtained reflect the behaviour that would be expected from any type of 5 GHz MLS having similar system apertures and multipath rejection techniques.

The coverage of the system can be largely predicted from the following criteria:

(1) azimuth coverage down to skyline angle over trees;

(2) azimuth guidance disturbed by obstacles (*eg* masts, chimneys) $0.5^{o}$ below the flight path;

(3) elevation coverage down to $1^{o}$ above skyline, to a minimum elevation angle of $1.4^{o}$ ($1^{o}$ beamwidth system).

The resultant predicted coverage at Manchester, for a $1^{o}$ beamwidth system, is shown in Table 5. A similar technique could be used at other airfields.

5.5 Autoland flights

Four autoland flights were performed at Manchester, with a total of 17 landings, 15 using MLS guidance from the $54\lambda$ aperture antennas, and 2 using the standard ILS transmissions. The automatic landing trials using DMLS guidance was conducted by Operational Systems Division, Flight Systems Department RAE Bedford using a HS 748 aircraft. The autopilot installed in the aircraft was a SEP 6 certificated for Category II operations. Experimental glide path extension and flare modifications gave a full automatic landing capability; the glide path extension commenced at 150 ft and flare, using radio altimeter guidance, at 45 ft. A vertical acceleration term was included in the vertical guidance control, which had not been used in the first DMLS autolands at Gatwick. The autolands were
144
included with normal airfield traffic, resulting in a large variation in starting

heights and distances from threshold, and necessitating some low drag configuration approaches. All the autolands on DMLS signals (which were used without additional smoothing), gave consistent touch-down performance, with no noticeable effects due to the runway hump shadowing or the high azimuth multipath in the flare region. Recordings were made of the MLS and ILS guidance signals, indicated airspeed, pitch attitude, roll attitude and radio altimeter height and a selection of such recordings is shown in Figs 59 to 63. The scaling on the guidance signals is $\pm 150$ μA which is equivalent to $\pm 0.67^{\circ}$ for elevation (ICAO $2\sigma$ limit $\pm 0.07^{\circ}$) and $\pm 2.2^{\circ}$ for azimuth (ICAO $2\sigma$ limit $\pm 0.054^{\circ}$). Thus, only coarse effects can be seen, two of which are immediately apparent:-

(1) propeller modulation effects on ILS glide path;

(2) aircraft overfly effects on ILS localiser.

The ILS glide path and MLS antennas were both sited in the nose of the aircraft, but the MLS guidance showed none of the propeller modulation effects seen on the ILS. The propeller effects on the ILS glide path were very variable from run to run, and depended on aircraft attitude and propeller speed and possibly propeller pitch.

The effects due to aircraft overflight of the ILS localiser were as large as $\pm 0.4^{\circ}$, whereas they were only just discernible on the DMLS trace, occurring approximately 8 s earlier, with an estimated magnitude of $\pm 0.05^{\circ}$. The reason for the earlier occurrence of the effects on DMLS is that this is probably a shadowing effect, just after the interfering aircraft leaves the runway, whereas the ILS effect is mainly a reflection effect as the aircraft passes overhead of the localiser.

It is also apparent from these recordings that the DMLS elevation system gave usable guidance at heights below 9 m (30 ft), whereas the ILS glide path guidance became very noisy below about 21.3 m (70 ft).

The final recording in Fig 64 shows the DMLS azimuth locked to the multipath signal during a take-off by the Bedford HS 748 from runway 24. It should be noted that the MLS azimuth and ILS localiser recordings were in opposite sense.

## 6 CONCLUSIONS

The tests at Manchester were done on a medium sized airport with a single runway. The notable feature of the airport is the humped runway, which gave severe attenuation of the MLS azimuth signals at threshold, and was also associated with a large hangar giving azimuth system multipath reflections in the flare region. This multipath, together with the shadowing by buildings within 144 the $\pm 40^{\circ}$ sector, meant that Manchester was a difficult site for azimuth system operation.

The tests demonstrated the ease of installation of DMLS equipment during normal airfield operations, although very wet weather did cause some delays. The DMLS equipment caused no interference to the existing Category II ILS installation and was positioned to give the same crossing height as the ILS, for a $3^{\circ}$ approach, so that the two systems were compatible and gave simultaneous operation.

Autoland tests using a simplex autoland system gave satisfactory performance using the DMLS signals and radio altimeter, and showed no adverse effects due to the shadowing of azimuth signals by the hump, or due to the azimuth multipath in the flare region. Effects seen on the ILS localiser guidance due to overflying aircraft and propeller modulation on the ILS glide path were not present on the MLS guidance.

Multipath investigations at the airport showed that the combination of shadowing of the direct azimuth signal by the runway hump, together with reflections from a large hangar, gave multipath signals greater than the direct signal at heights below 8.5 m (28 ft) over a region extending 200 m along the centre line in the flare region. This would give false guidance for a taxiing aircraft (*eg* on take-off), but the receiver design and the short duration would mean that this would not happen during a landing. This region (*ie* antenna height below 28 ft) was not entered during the autoland or accuracy flight tests. At greater heights, high levels of azimuth multipath were still encountered, but the performance of the system was such that an effective azimuth antenna aperture of $20\lambda$ was still adequate to support Category III operations.

The accuracy tests on the elevation system were done in an uncluttered site with no isolated multipath sources. ICAO Full Capability System performance (equivalent to ILS Category III) was achieved using a $54\lambda$ aperture down to a $2^{\circ}$ glide slope and using a $39\lambda$ aperture down to a $3^{\circ}$ glide slope. Apertures of $30\lambda$ and $27\lambda$ gave performances outside the full capability system requirement due to ground reflection, and other scattered signals.

The coverage of the DMLS installation was better than the ICAO requirement in terms of range (20 n mile) and azimuth angle ($\pm 40^{\circ}$ from centre line), once clear of shadowing by features near the airfield. Low angle coverage down to a 1 in 50 slope from threshold at 20 n mile range, was only achieved within $\pm 12^{\circ}$ of centre line for the azimuth system, because of shadowing losses. The elevation system had clearer line of sight and gave a (noisy) guidance signal from $-30^{\circ}$ to $+86^{\circ}$ in azimuth. Shadowing of the elevation system behind trees gave a positive fly down error as large as $0.5^{\circ}$. Since the aircraft was already at an elevation angle of $1^{\circ}$, it is unlikely that such an elevation angle would be demanded and the fly down guidance followed. However, it does mean that in shadowing conditions large fly down errors can be produced, and this will also apply to other microwave landing systems using this frequency band.

The coverage measurements showed that the ICAO requirement of guidance down to a 1 in 50 slope from threshold, over $\pm 40^{\circ}$ is unlikely to be met at typical airports such as Manchester and will certainly not be met at hilly or mountainous sites. A visual inspection at an airfield can be quite misleading in this respect, and it is recommended that skyline surveys should be made at proposed MLS azimuth and elevation sites, if low angle coverage is in question.

In all aspects the total system behaved in a logical and consistent manner, with no equipment failures and the objectives of the trials were fully met.

Table 1

ERROR SPECIFICATION, FULL CAPABILITY SYSTEM

| | Bias ($2\sigma$) | | Noise ($2\sigma$) | | Guidance error ($2\sigma$) | | Distance to error window | Total error allowable degradation (1) | | |
|---|---|---|---|---|---|---|---|---|---|---|
| | ft (3) | deg | ft (3) | deg | ft (3) | deg | | W/distance (2) | With Az angle | With El angle |
| Azimuth | 14 | 0.054 | 14 | 0.054 | 20 | 0.076 | 15000 ft | Linearly to $0.15^{\circ}$ at 20 n mile along CL | 1.5:1 in angle from CL error at $\pm 40^{\circ}$ Az | 2:1 in angle from $9^{\circ}$ to $15^{\circ}$ elevation |
| Elevation | 1.4 | 0.07 | 1.4 | 0.07 | 2.0 | 0.10 | 1145 ft | None | None | Bias - proportional to angle above $4^{\circ}$. Noise - none |
| DME | - | - | - | - | 40 | - | 15000 ft | 10:1 at 20 n mile | None | None |
| Flare (5) | 1.4 | | 1.4 | | 2.0 (4) | | | Not specified | None | |
| Missed approach azimuth | 0.11 | | | 0.11 | | 0.15 | | None | None | None |

(1) Degradation varies linearly between the limited indicated. Proportionality between bias and path following noise shall be maintained.

(2) R = slant range. Range is measured from elevation reference datum.

(3) Measured at error window; azimuth figures hold through the roll-out zone.

(4) The linear errors hold throughout the touch-down zone.

(5) The flare errors include contributions of all equipments necessary to compute height.

Table 2

ERROR SPECIFICATION, REDUCED CAPABILITY SYSTEM

| | Bias (2) | | Noise (2) | | Guidance error (2) | | Distance to error window | Error allowable degradation (1) | | |
|---|---|---|---|---|---|---|---|---|---|---|
| | ft | deg | ft | deg | ft | deg | | With distance | With Az angle | With El angle |
| Azimuth | 28 | 0.16 | 28 | 0.16 | 40 | 0.23 | 10000 ft | Linearly to $0.5^{o}$ at 10 n mile | 2:1 angle from CL error at $\pm 20^{o}$ azimuth | None |
| Elevation | 7 | 0.10 | 7 | 0.10 | 10 | 0.14 | 4000 ft | None | None | None |
| DME | - | - | - | - | 600 (2) | - | 10000 ft | None | None | None |

(1) Degradations vary linearly between the limits indicated.

(2) This accuracy allows decision height determination only for a $2.5^{o}$ glide path.

Table 3

SUMMARY OF DMLS COVERAGE ON RADIAL FLIGHTS

| Radial | Azimuth system | | | Elevation system | | | |
|---|---|---|---|---|---|---|---|
| | n mile | Elevation angle deg | Angle above skyline deg | n mile | Elevation angle deg | Angle above skyline deg | High angle coverage deg |
| CL 3500 ft | 28 | 0.9 | 0.4 | 28 | 1.01 | 0.7 | 24 |
| $20^{o}$L 3500 ft | 23 | 1.2 | 0.1 | 29 | 0.9 | 0.5 | 23.5 |
| $39^{o}$L 3500 ft | 24 | 1.2 | 0.1 | 26 | 1.3 | 0 | 23 |
| $20^{o}$R 3500 ft | 23 | 1.2 | 0 | >30 | 0.8 | 0.4 | 22.5 |
| $39^{o}$R 3500 ft | 23 | 1.2 | 0 | 30 | 0.8 | 0.4 | - |
| CL 3000 ft (27λ) | 25 | 0.9 | 0.4 | - | - | - | - |
| CL 10000 ft | 48 | 1.5 | 1.0 | 56 | 1.2 | 0.9 | 22.5 |

Table 4

LIMITS OF SUCCESSFUL FUNCTION IDENTITY DECODING DURING COVERAGE ORBITS

| Semi-orbit (20 n mile) | Azimuth system | | | | Elevation system | | | |
|---|---|---|---|---|---|---|---|---|
| | El angle deg | Az angle deg | | | El angle deg | Az angle deg | | |
| | | Start | 99% decode | Finish | | Start | 99% decode | Finish |
| 3000 ft CCW | 1.0 to 1.4 | -58 | -11 to +12 | +82 | 1.05 to 1.5 | -50 | -29 to +41 | +90 |
| 6000 ft CW | 2.3 to 2.6 | +81 | +65 to -68 | -77 | 2.4 to 2.7 | +88 | +76 to -81 | -86 |
| 6000 ft CCW | 2.2 to 3.0 | -75 | -37 to +58 | +75 | 2.3 to 3.1 | -85 | -58 to +58 | +85 |

Table 5

PREDICTED MLS COVERAGE AT MANCHESTER INTERNATIONAL AIRPORT, RUNWAY 24

| Azimuth system | | | | | | Elevation system (54λ) | | | | | |
|---|---|---|---|---|---|---|---|---|---|---|---|
| Azimuth sector deg | El angle deg (skyline) | Height m (ft) at | | | | Azimuth sector deg | El angle deg (skyline + $1^{o}$) | Height m (ft) at | | | |
| | | 5 n mile | 10 n mile | 15 n mile | 20 n mile | | | 5 n mile | 10 n mile | 15 n mile | 20 n mile |
| ±12 | 0.5 | 82 (270) | 189 (620) | 305 (1000) | 433 (1420) | +60R to -27L | 1.5 | 244 (800) | 512 (1680) | 792 (2600) | 1067 (3500) |
| +15R (Control tower) | 1.4 | 232 (760) | 485 (1590) | 731 (2400) | 1006 (3300) | -27L to -55L | 2.5 | 405 (1330) | 838 (2750) | 1280 (4200) | 1737 (5700) |
| +20R to +40R -20L to -40L | 1.5 | 244 (800) | 512 (1680) | 792 (2600) | 1067 (3500) | -56L (trees) | 3.75 | 606 (1990) | 1243 (4080) | 1881 (6170) | 2530 (8300) |
| -37L (Chimneys) | 3.9 | 631 (2070) | 1295 (4250) | 1951 (6400) | 2621 (8600) | -60L to -80L | 2.5 | 405 (1330) | 838 (2750) | 1280 (4200) | 1737 (5700) |

Heights (QFE) and elevation angles above which guidance should be satisfactory.
(Local terrain and flight procedures ignored, *ie* lowest heights may not be usable.)

## REFERENCES


| No. | Author | Title, etc |
|---|---|---|
| 1 | J.M. Jones | MLS trials at Brussels National Airport, June 1977 and January 1978.<br>RAE Technical Report (to be published) |
| 2 | P.L. Gibson | Trials of the Doppler Microwave Landing System at London (Gatwick) airport.<br>RAE Technical Report 78124 (1978) |
| 3 | R. Matthews | Microwave landing system trials at Kristiansand, Norway, 1977, 1978.<br>RAE Technical Report (to be published) |
| 4 | R. Matthews | Performance assessment trials of the Doppler Microwave Landing System at Berne airport.<br>RAE Technical Report (to be published) |
| 5 | P.L. Gibson<br>D. Walker | Comparative trials of the Doppler Microwave Landing System and the Time Reference Scanning Beam microwave landing system at the John F. Kennedy International airport, New York.<br>RAE Technical Report (to be published) |
| 6 | J.M. Jones | Contributions to the UK microwave landing system research and development programme 1974-1978.<br>RAE Technical Report (to be published) |
| 7 | J. Capon | Multipath parameter computations for the MLS simulation computer programmes.<br>Lincoln Laboratory MIT Project Report ATC-68<br>FAA Report No.FAA-RD-76-55 |
| 8 | J.R. Wait<br>A.M. Conda | Diffraction of electromagnetic waves by smooth obstacles.<br>*Jour. Res*. NBS 63D No.2, 181-197 (September-October 1959) |

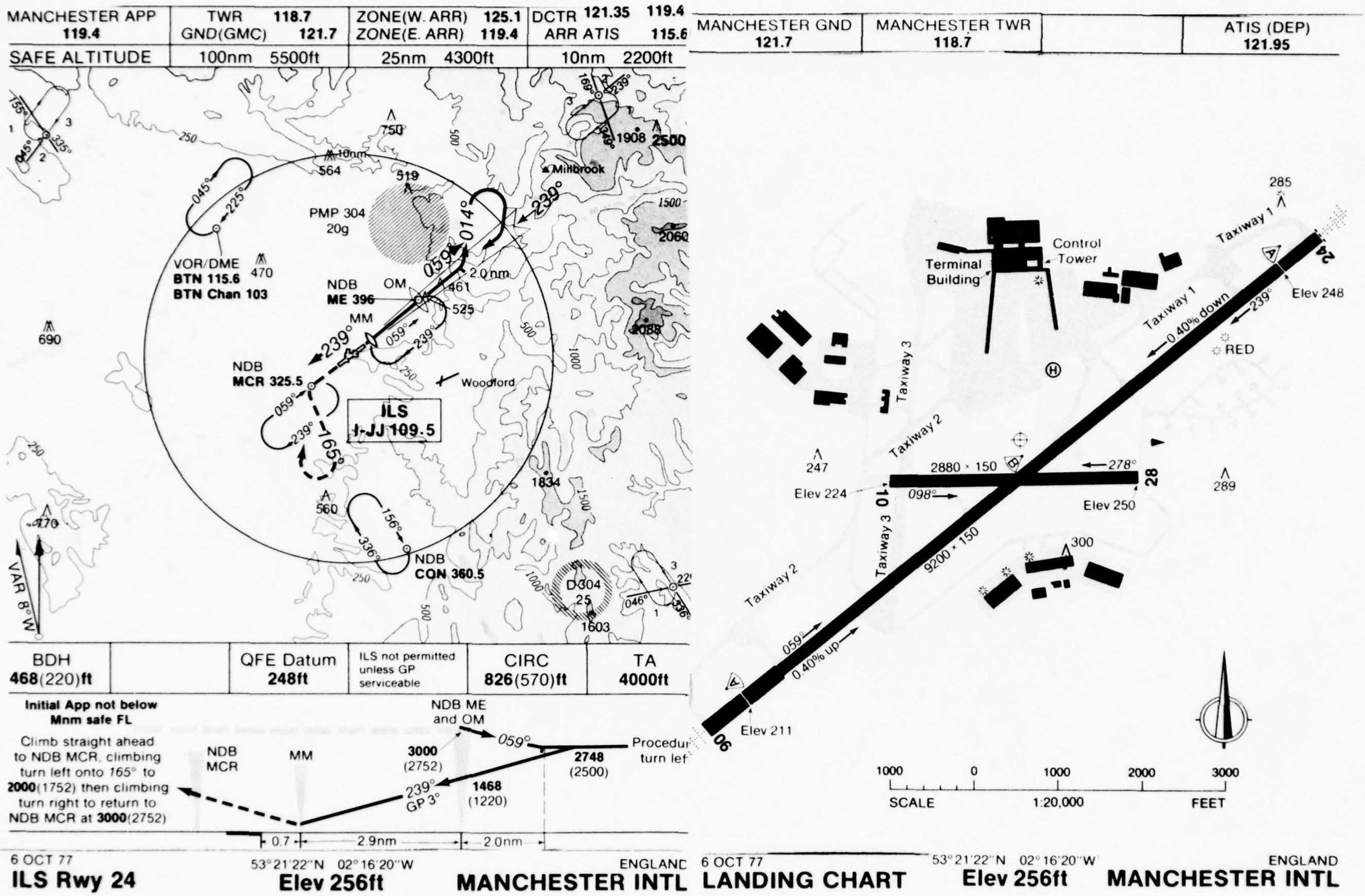


Fig 1 Manchester International Airport, runway 24, approach and landing charts

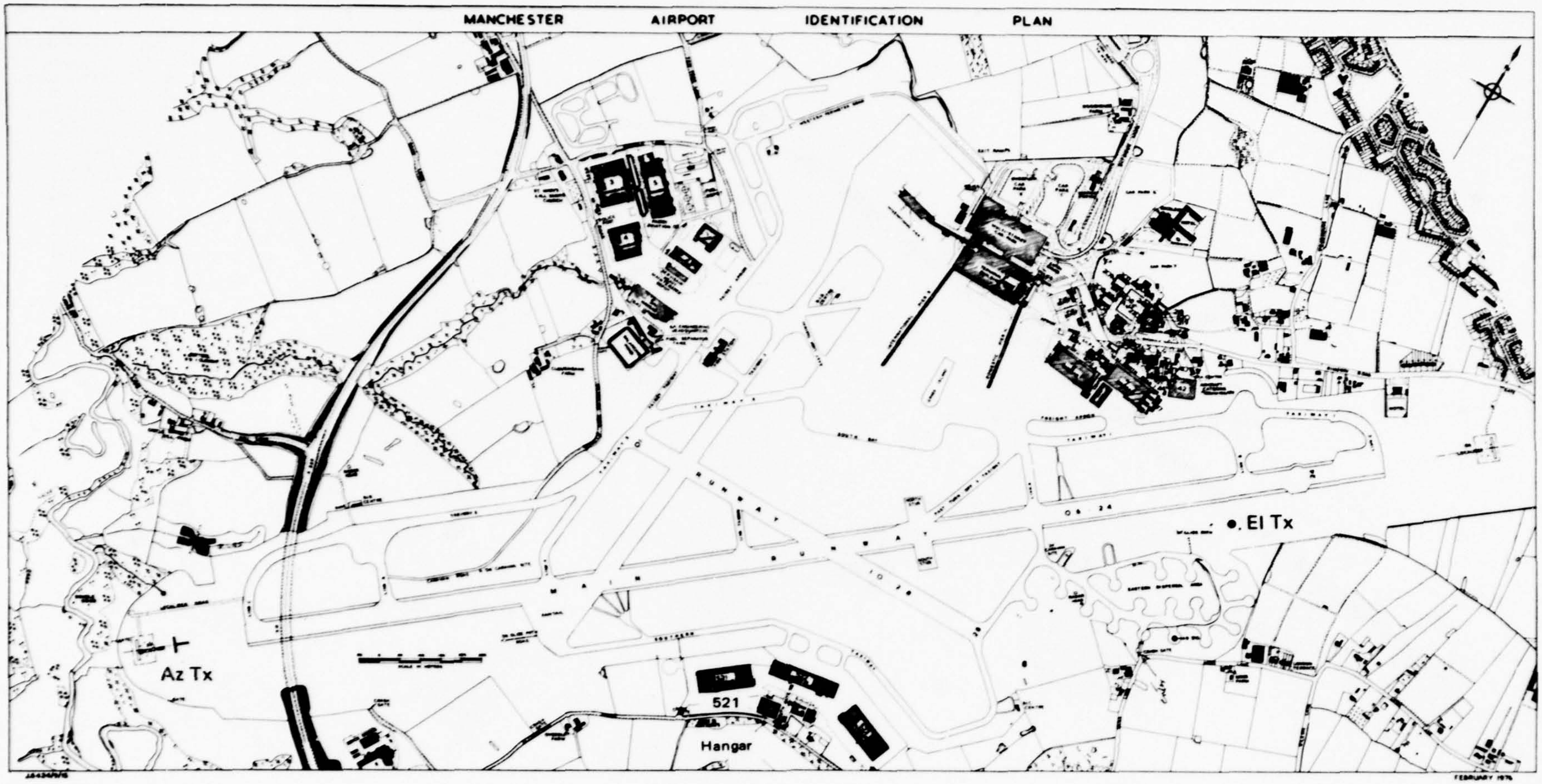


Fig 2 Manchester International Airport plan showing location of DMLS transmitters

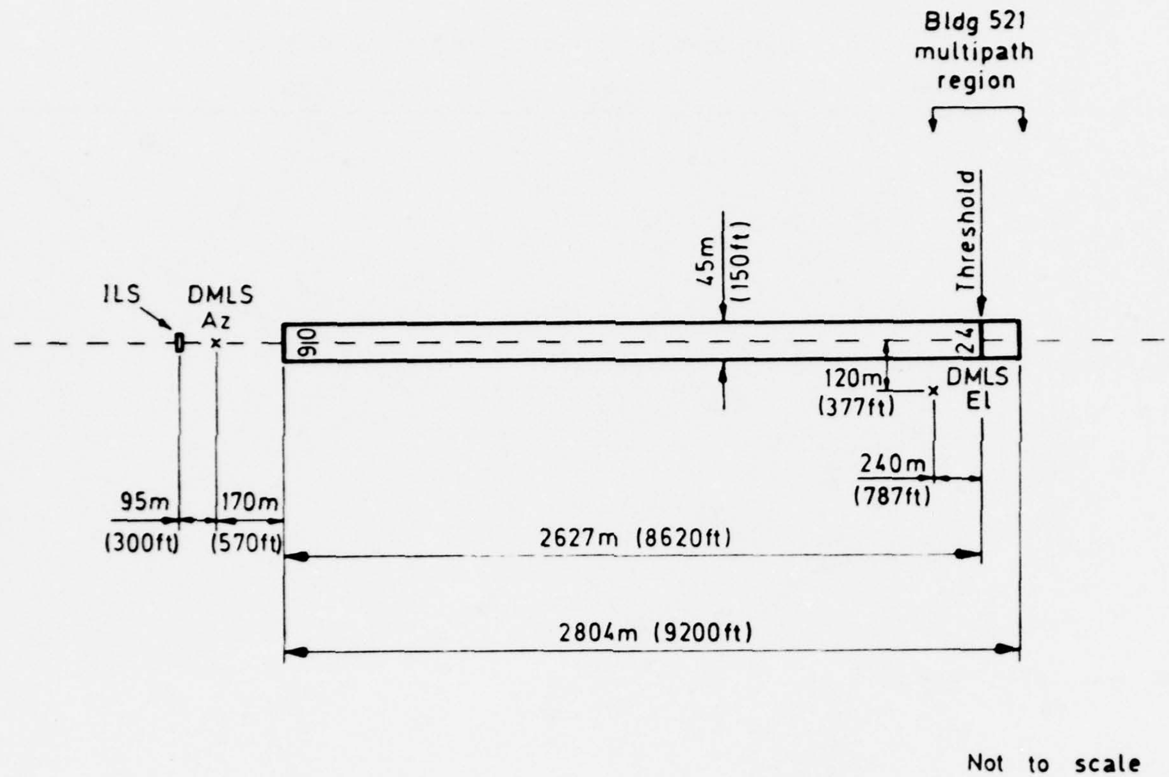


Fig 3 Manchester Airport site details

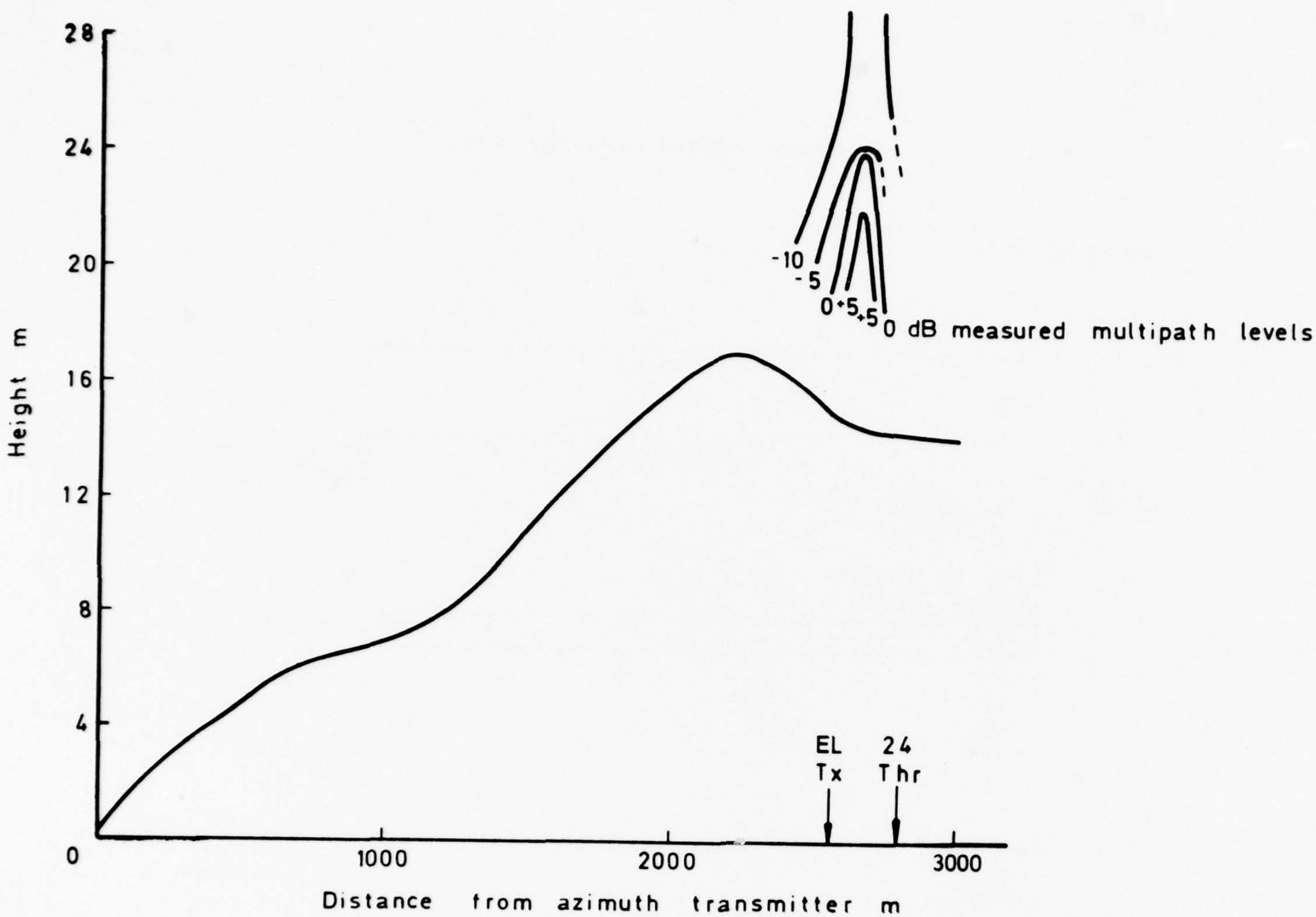


Fig 4 Manchester runway profile

Fig 5 View from azimuth transmitter along centre line

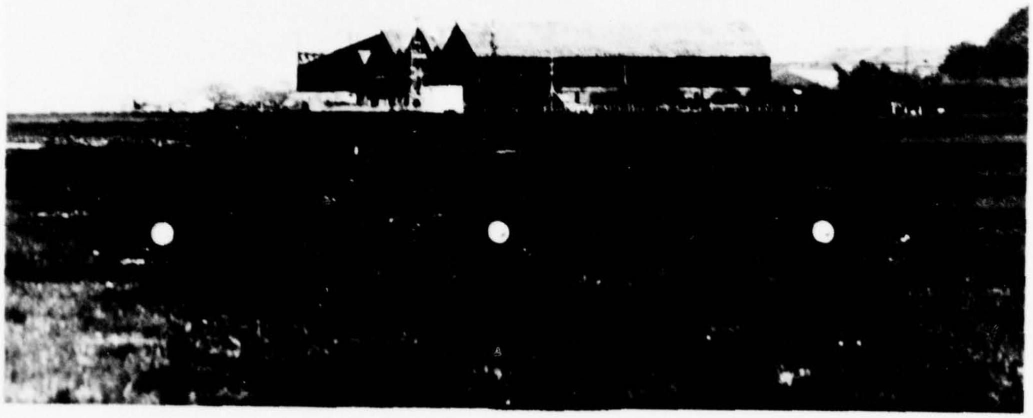

a

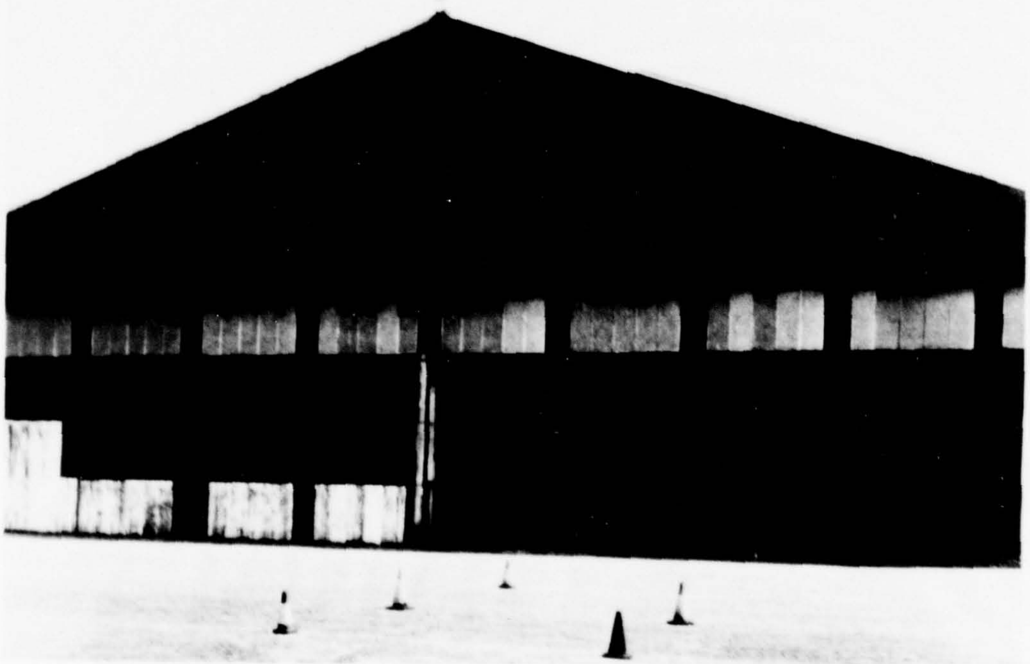

b

Fig 6a&b 521 Building

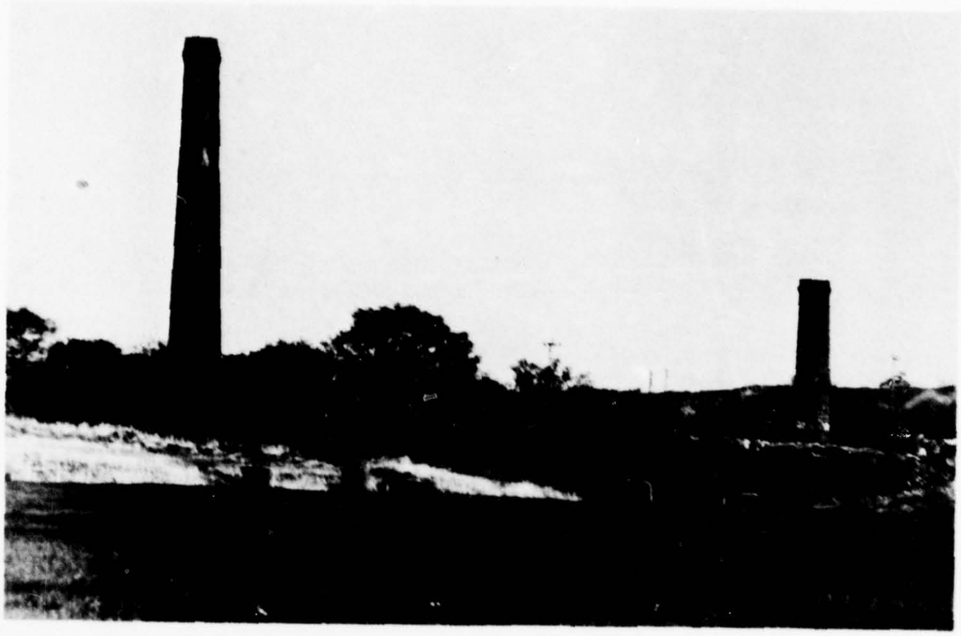

a Brickworks chimneys

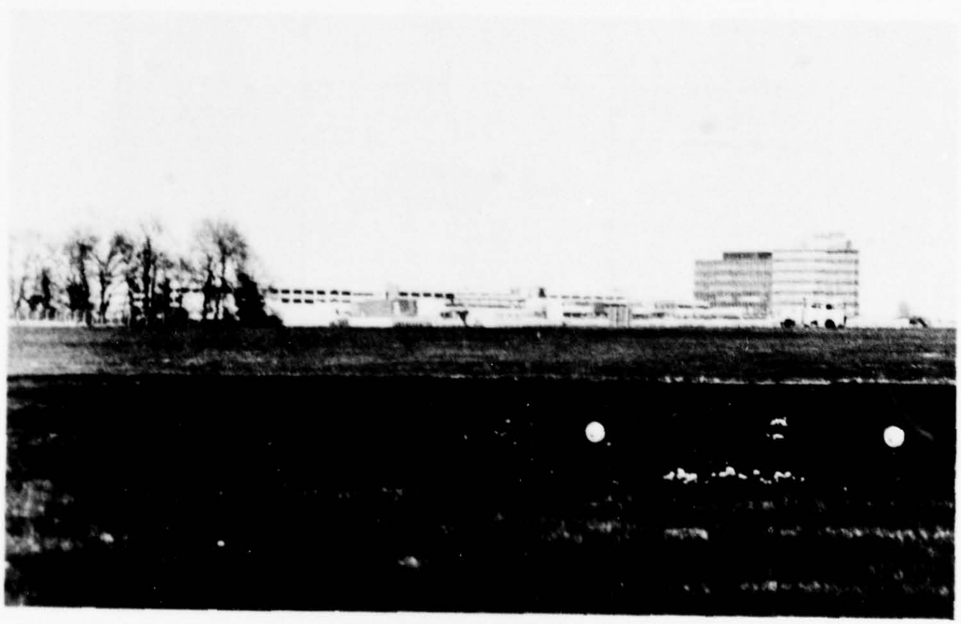

b Control tower and tree line

**Fig 7a&b Azimuth skyline features**

TR 78144 C15304

Fig 17

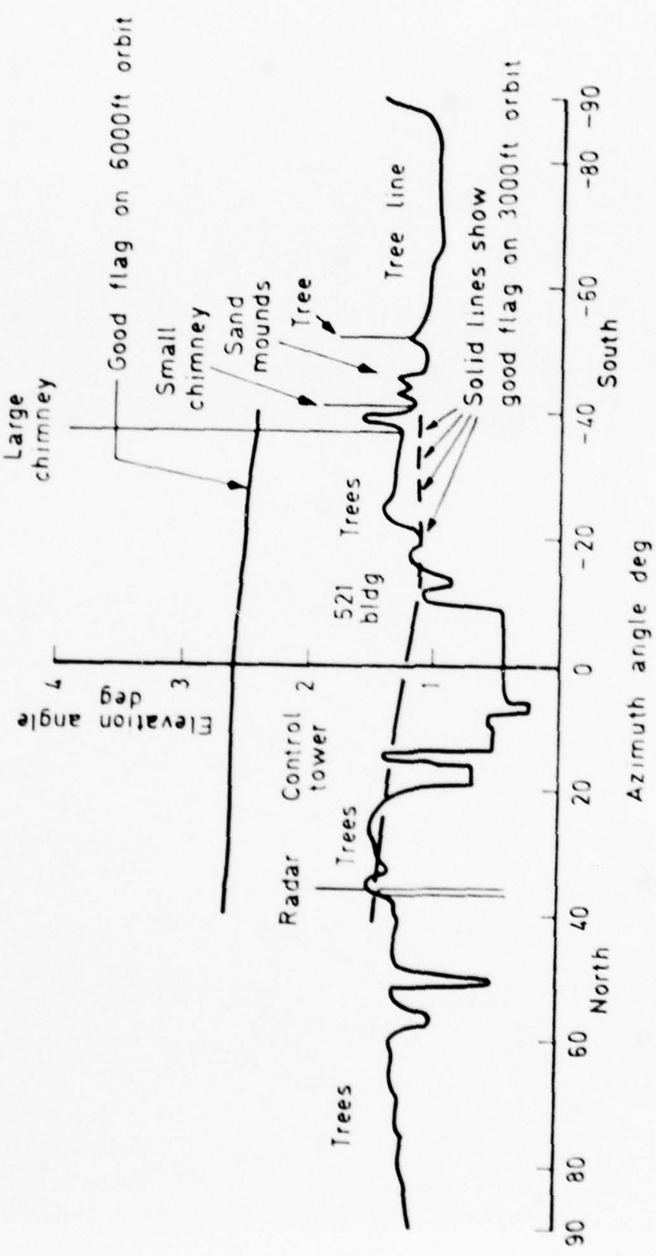


Fig 8 Azimuth site skyline survey

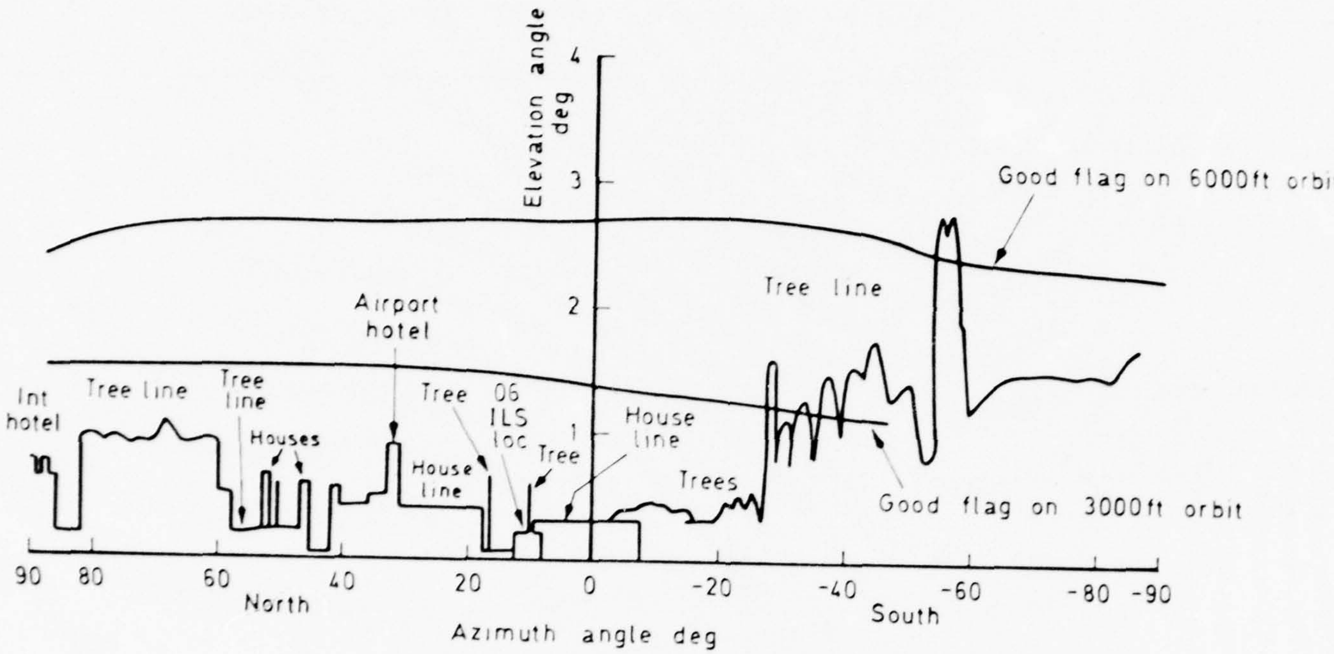


Fig 9 Elevation site skyline survey

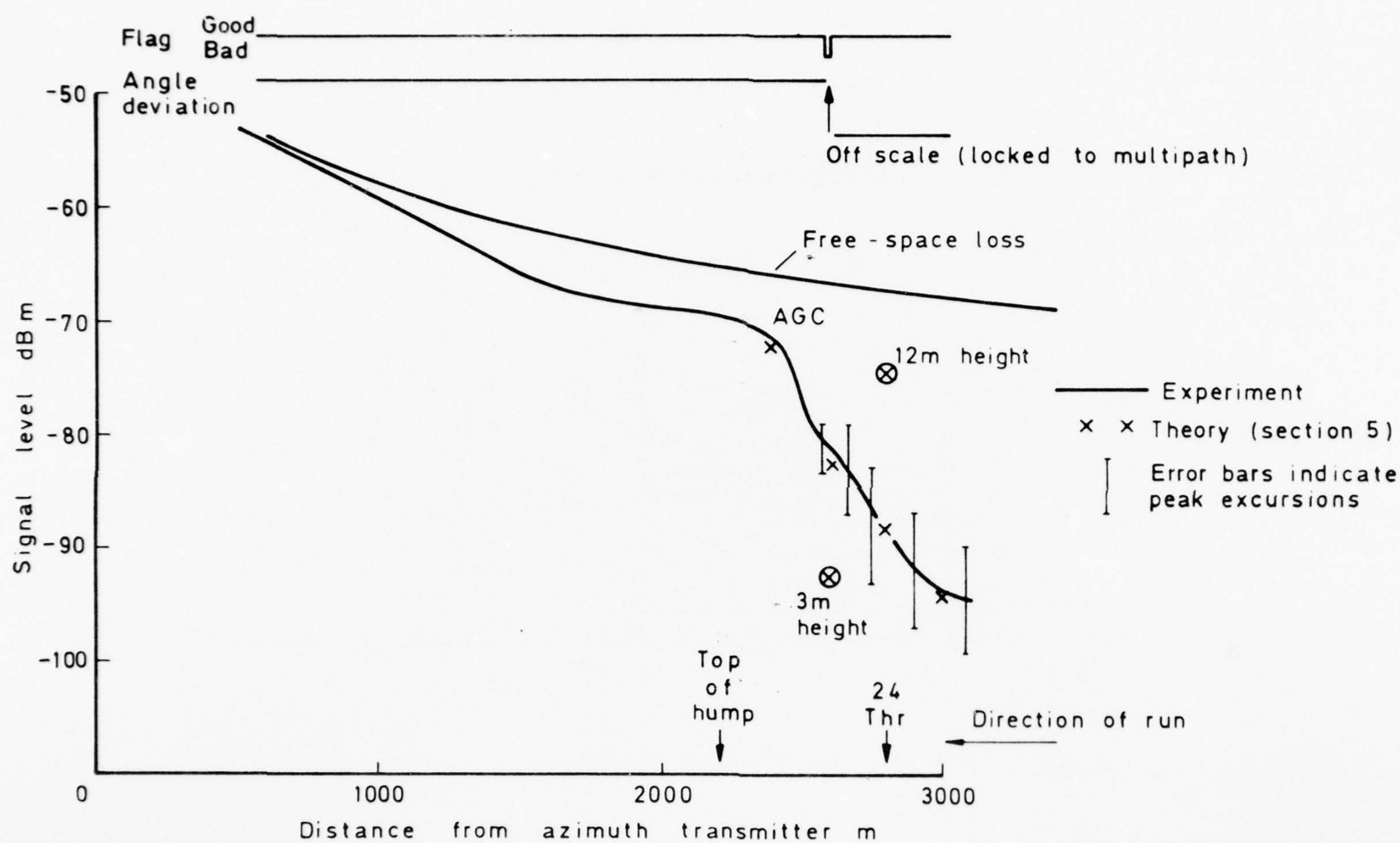


Fig 10a Receiver vehicle run 1, mast height 4.6 m (15 ft), 54 λ azimuth, runway 24

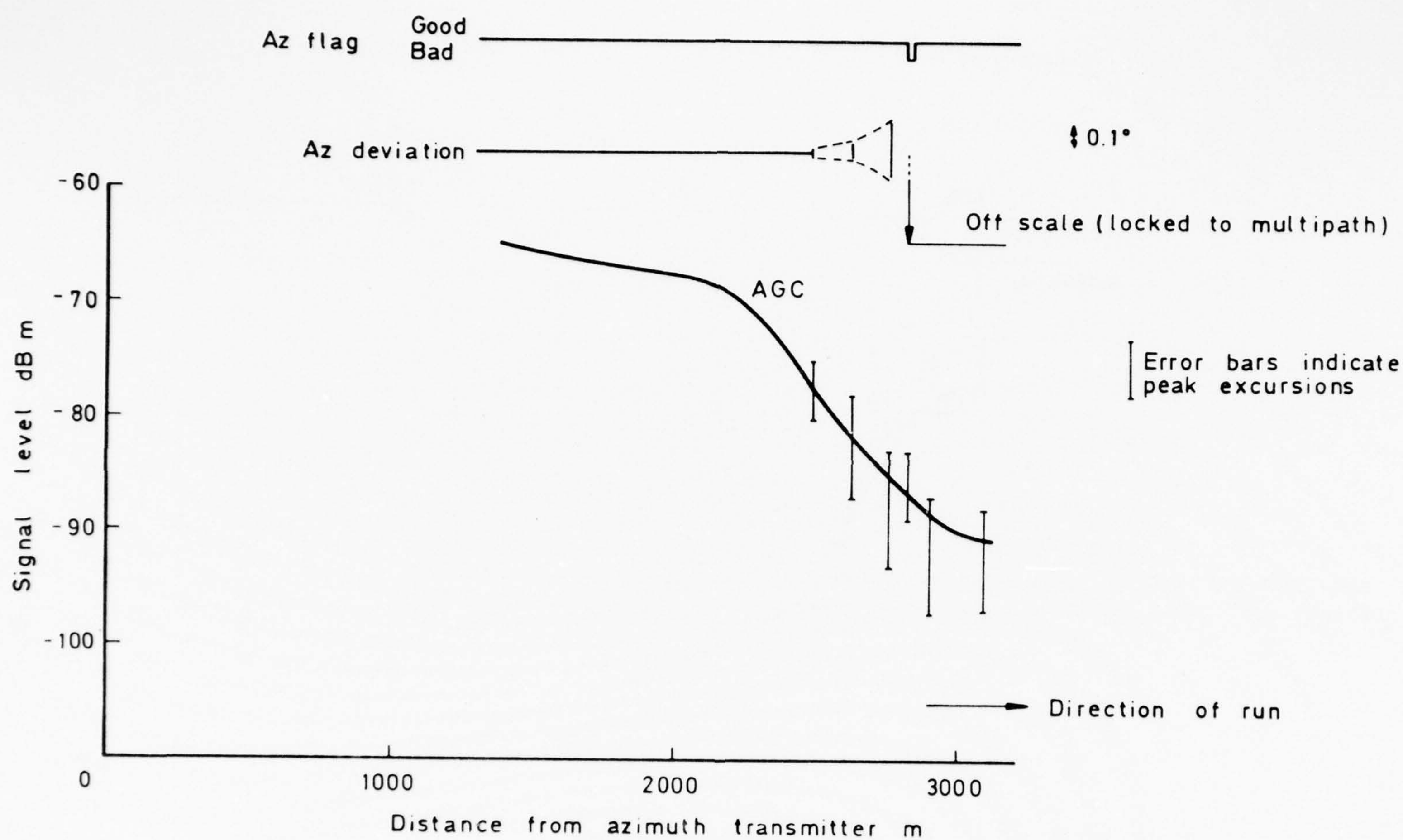


Fig 10b Receiver vehicle run 2, mast height 4.6 m (15 ft), 27 λ azimuth

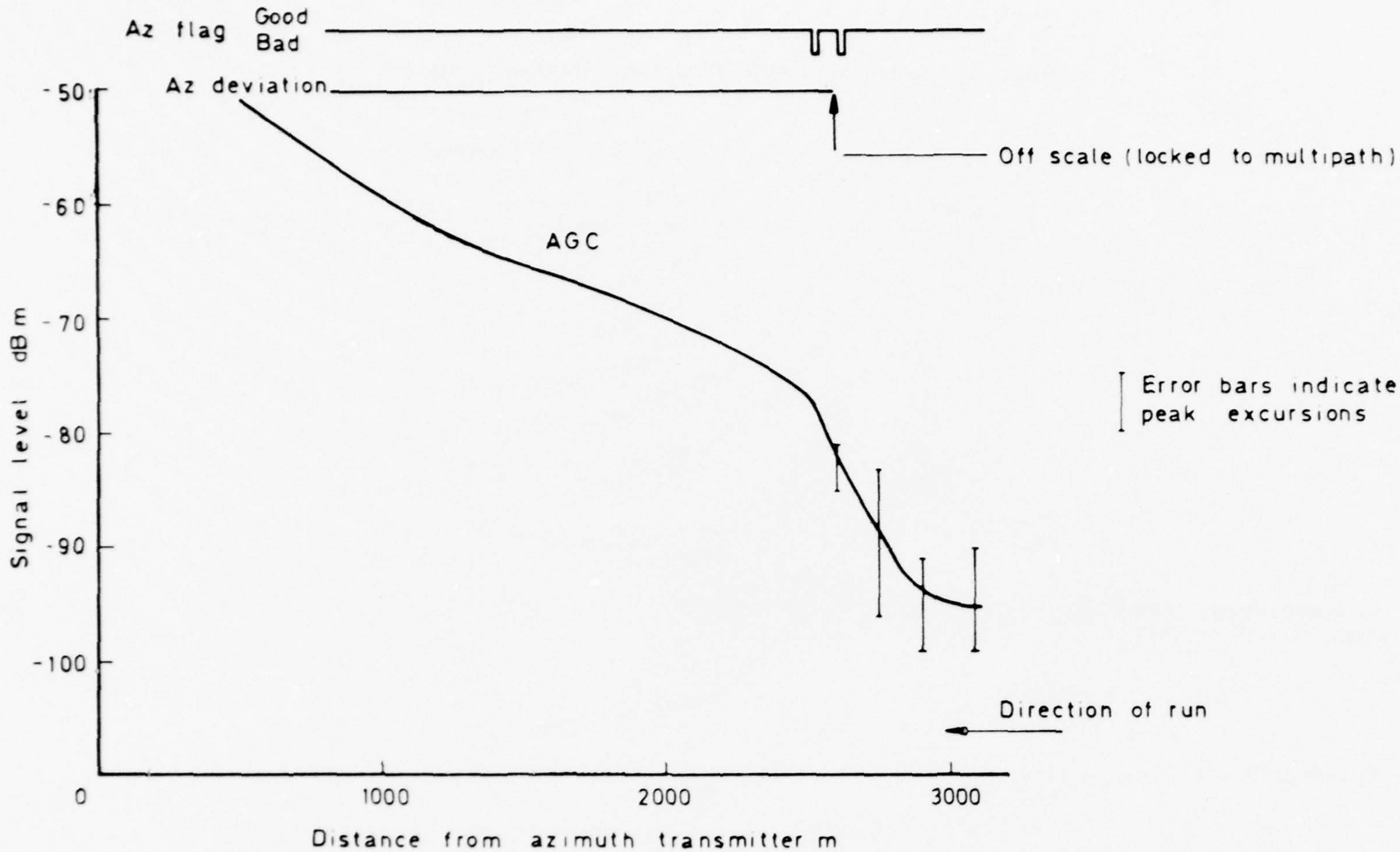


Fig 10c Receiver vehicle run 3, mast height 4.6 m (15 ft), 54 λ azimuth

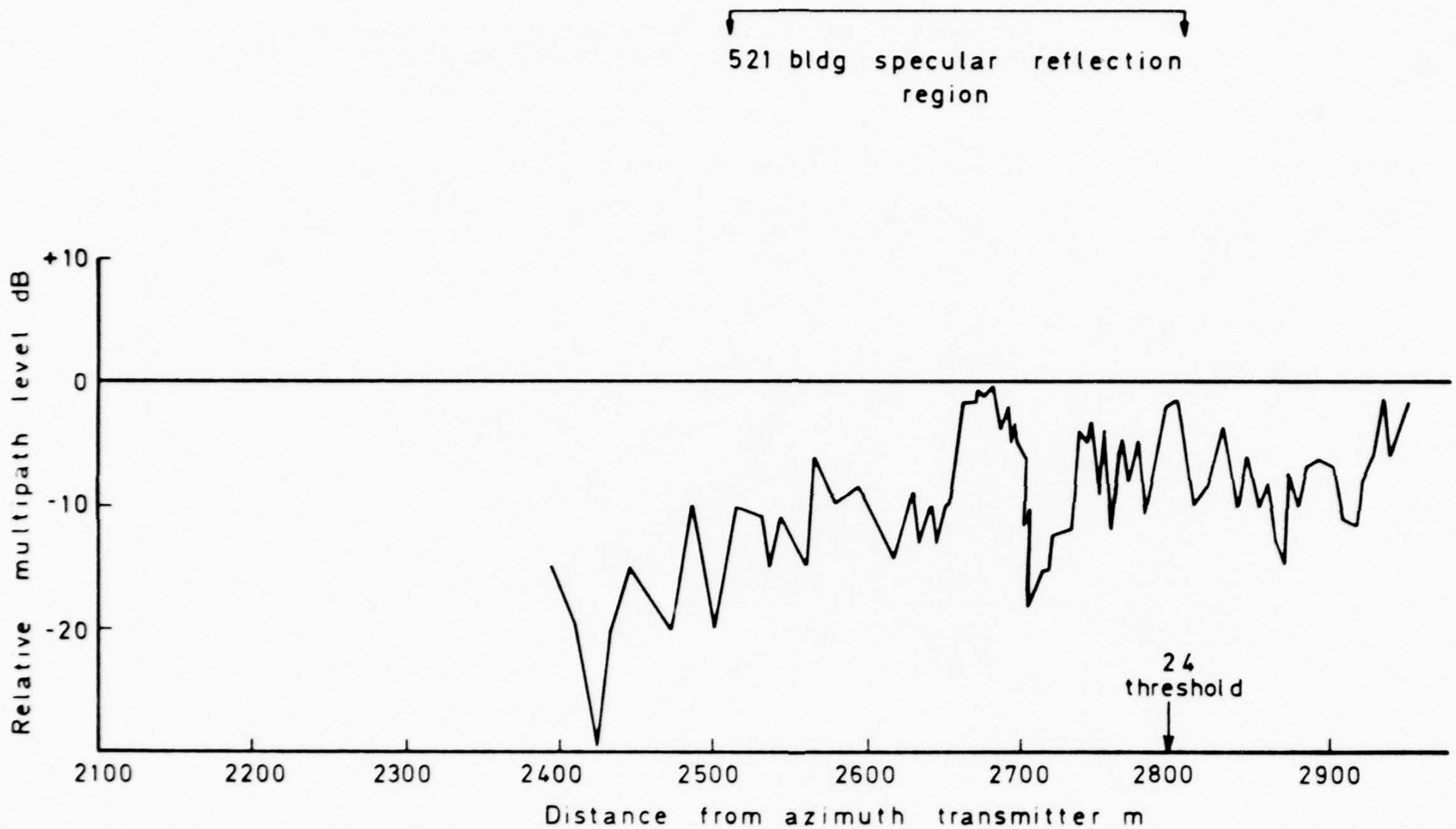


Fig 11a Relative azimuth multipath level from C-W transmission at Manchester International Airport 8 November 1977, runway run, mast height 9.75 m (32 ft)

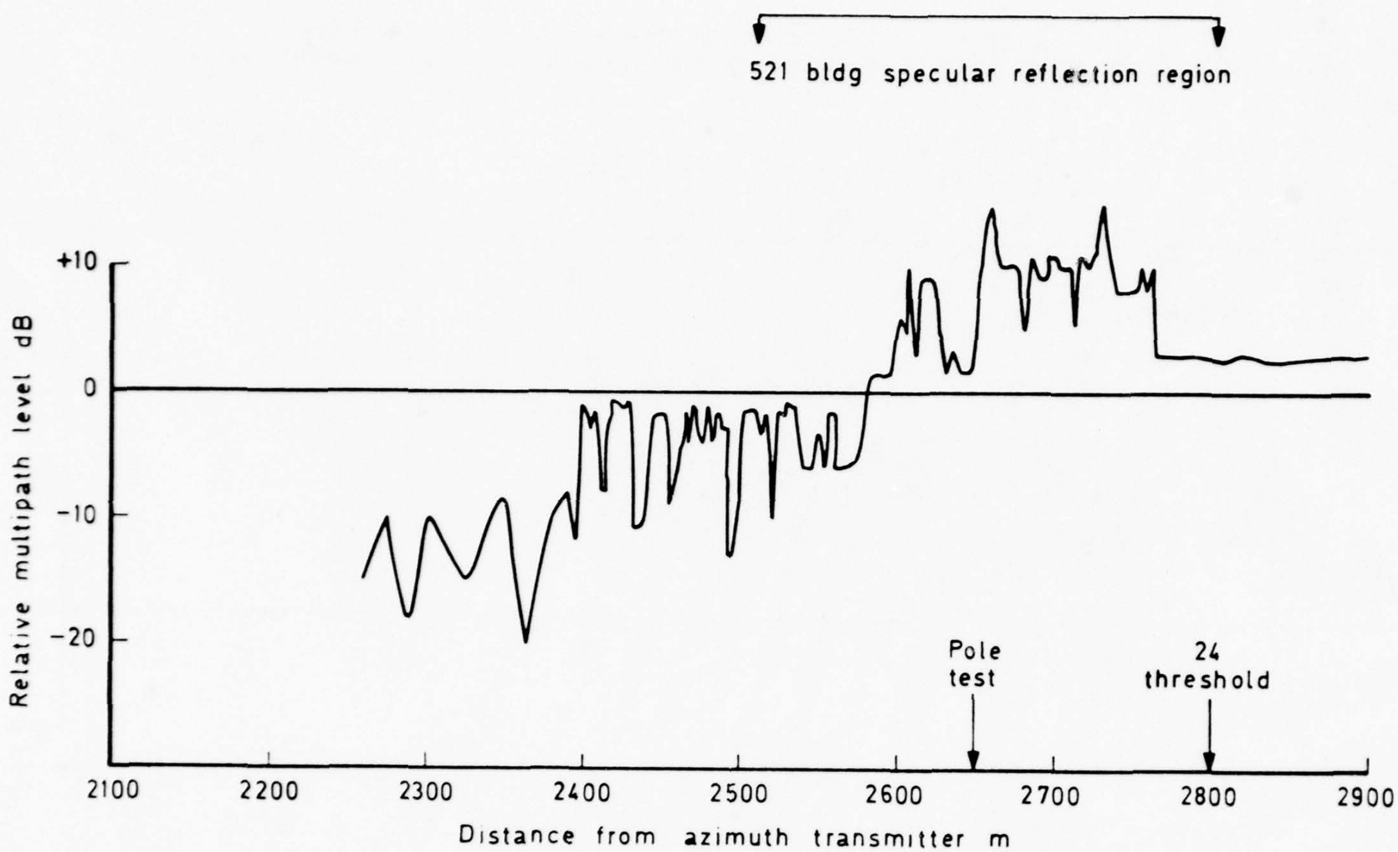


Fig 11b Relative azimuth multipath level from C-W transmission at Manchester International Airport 8 November 1977, runway run, mast height 4.6 m (15 ft)

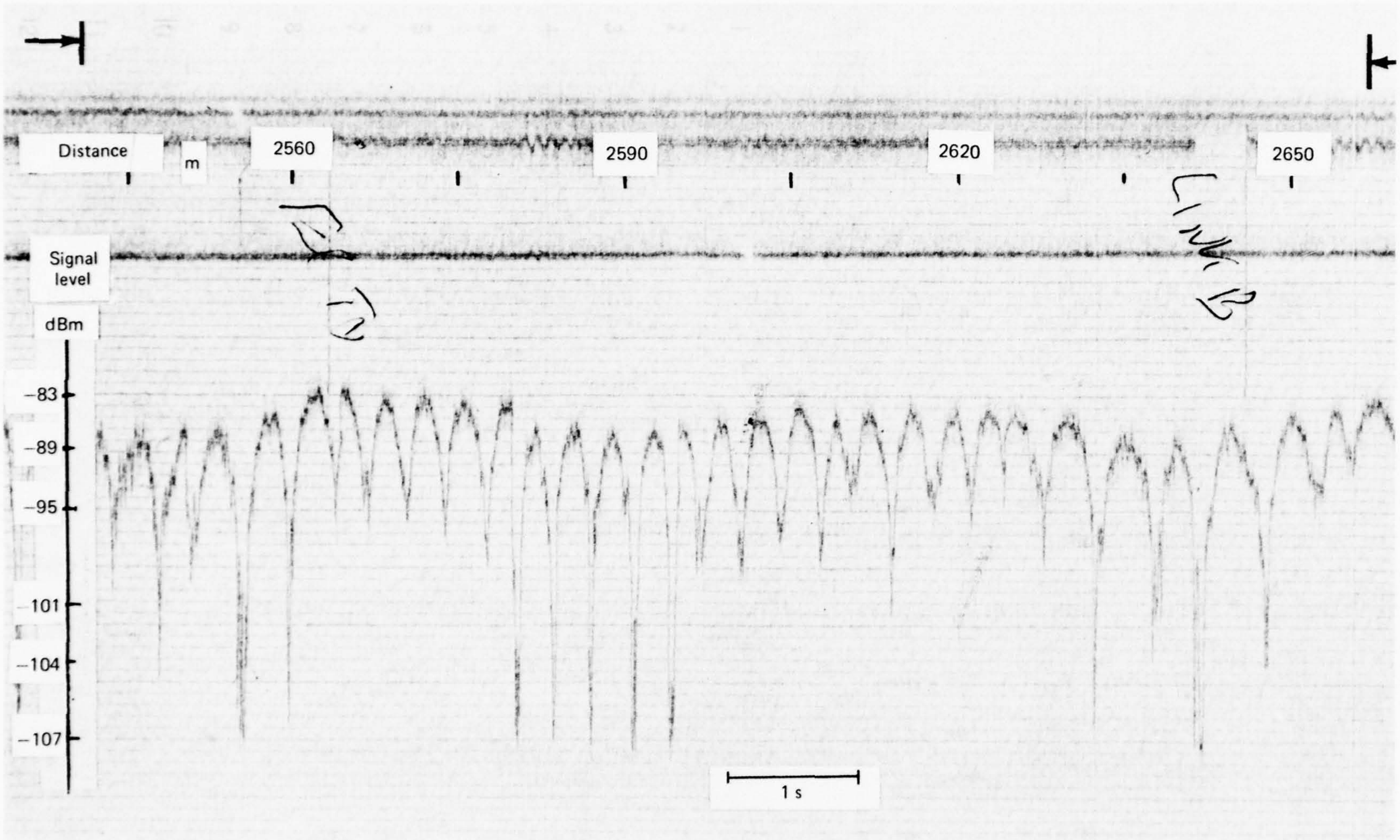


Fig 12 Azimuth C-W AGC during runway run, mast height 4.5 m, 8.11.77

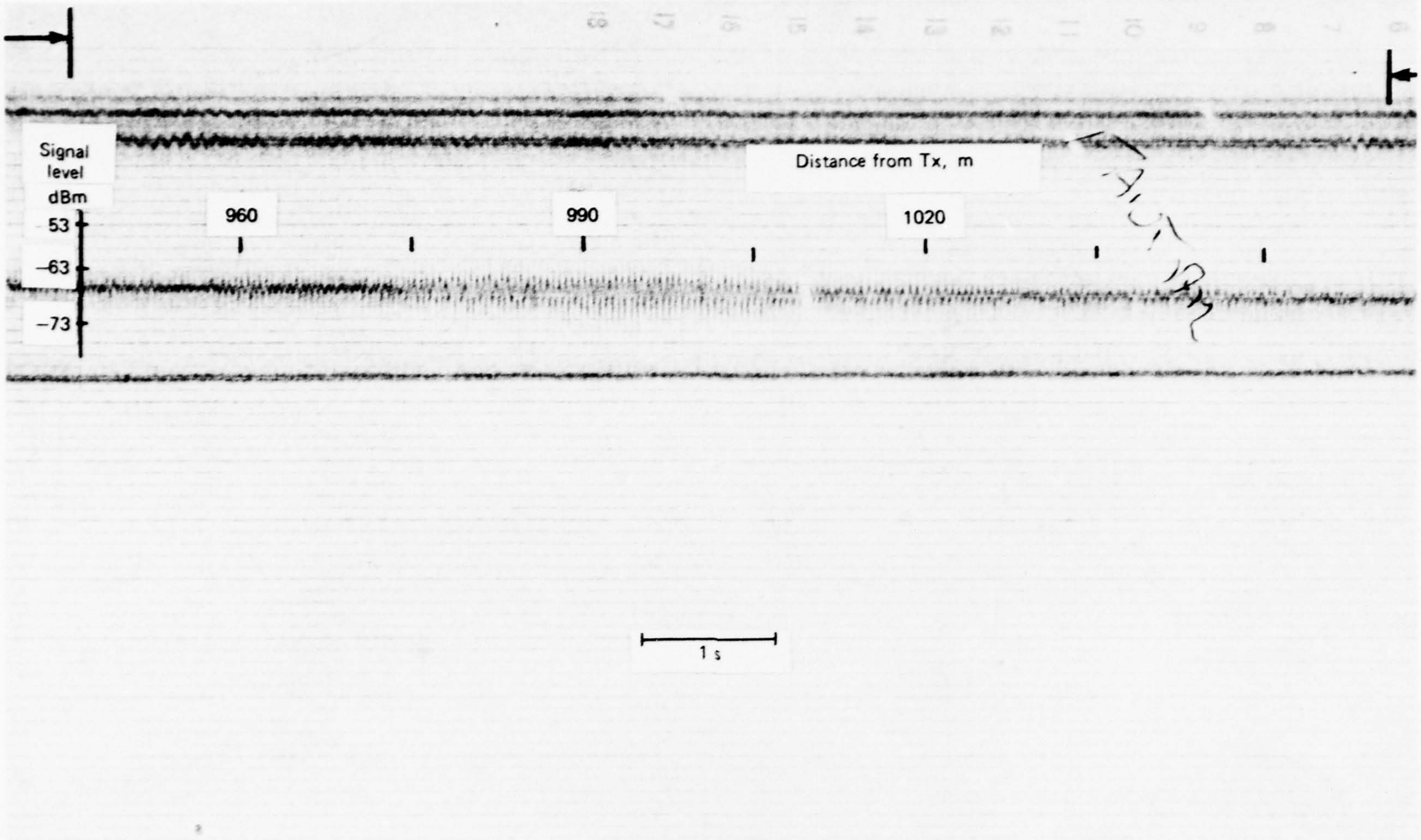


Fig 13 Azimuth C-W AGC record during runway run showing reflections from BIB centre


Fig 14 Photograph from azimuth site showing BIB centre etc

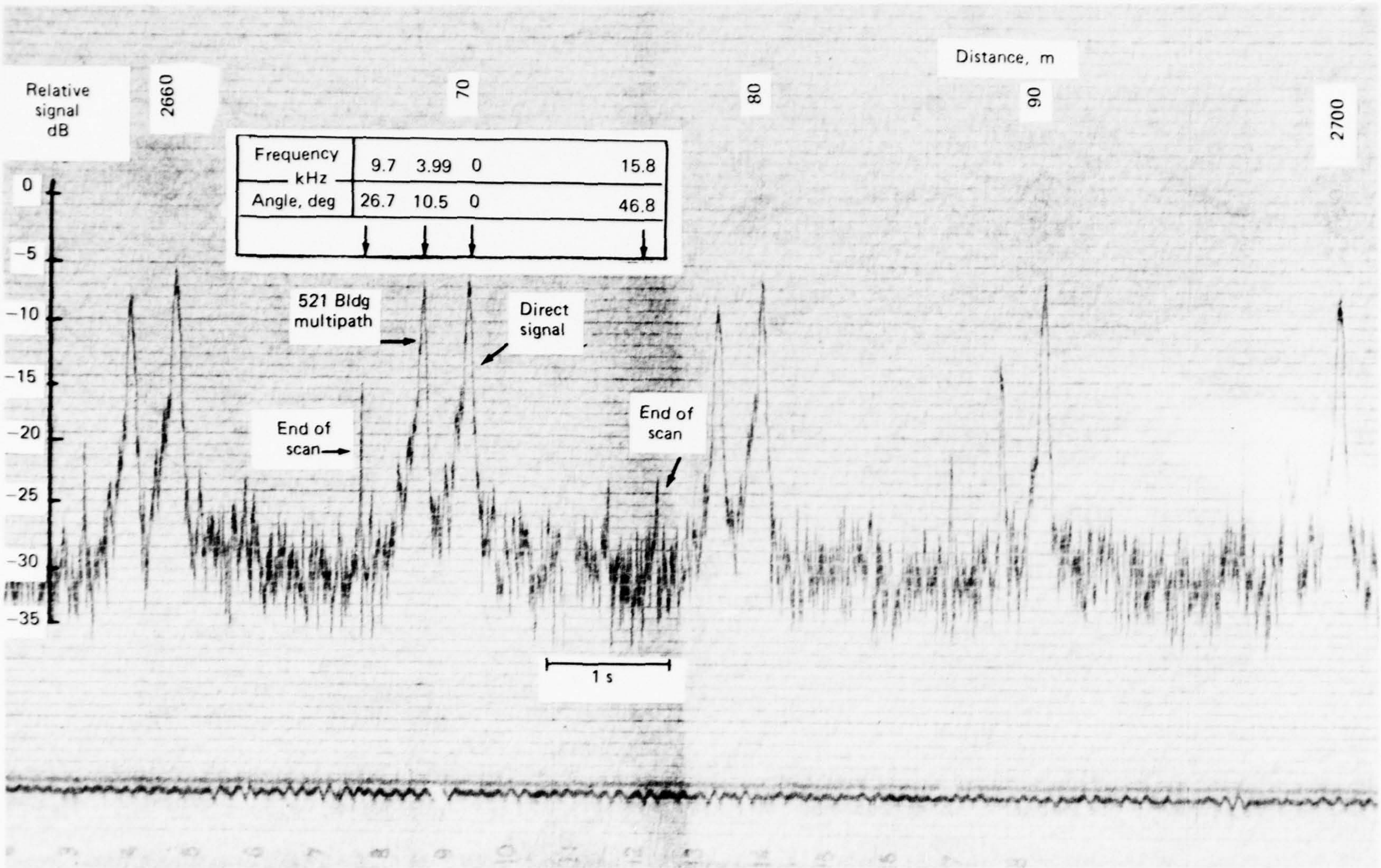


Fig 15 Spectral recording during runway run, mast height 9.75 m

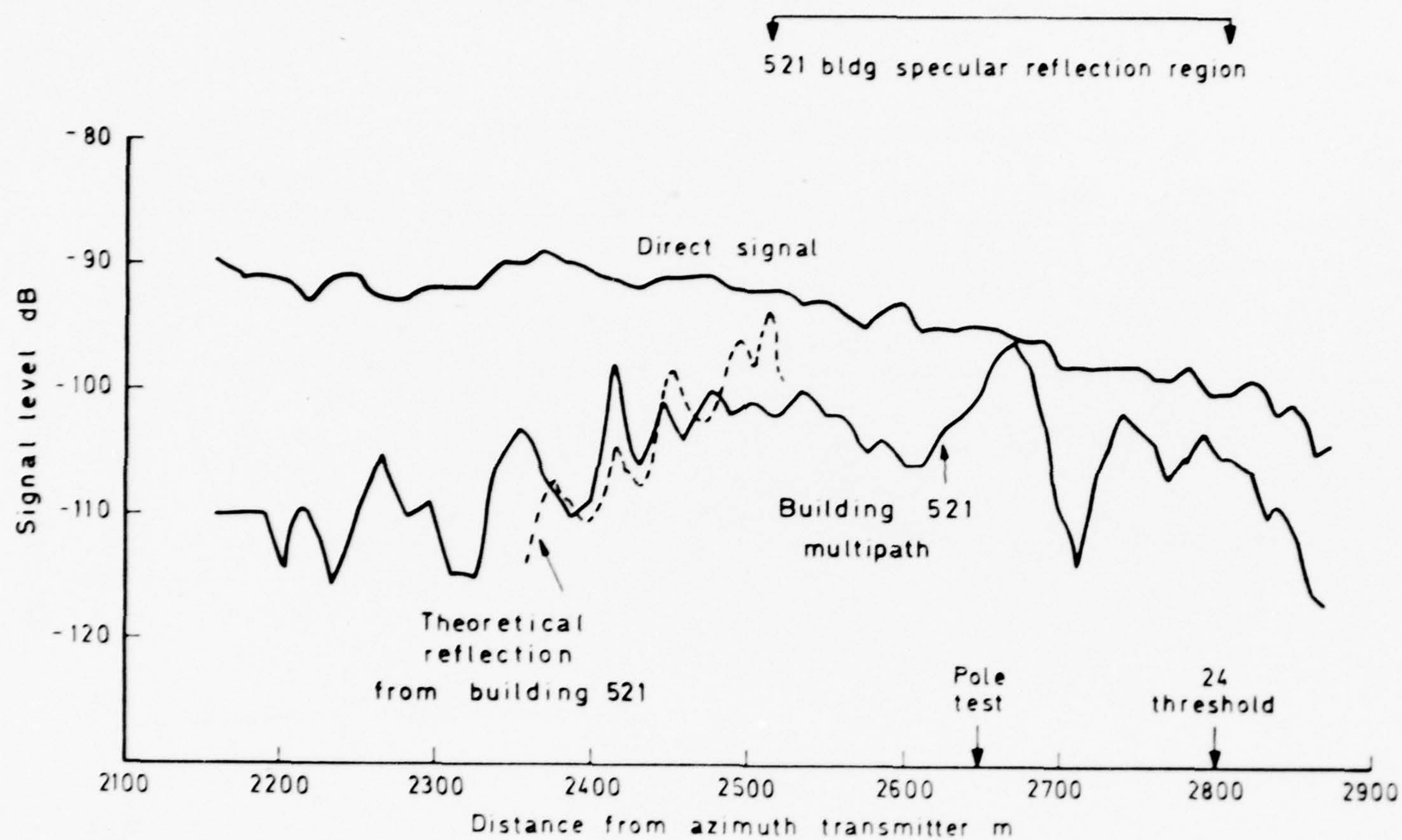


Fig 16a Direct and multipath signals from spectral recordings at Manchester International Airport 8 November 1977, runway run, mast height 9.75 m (32 ft)

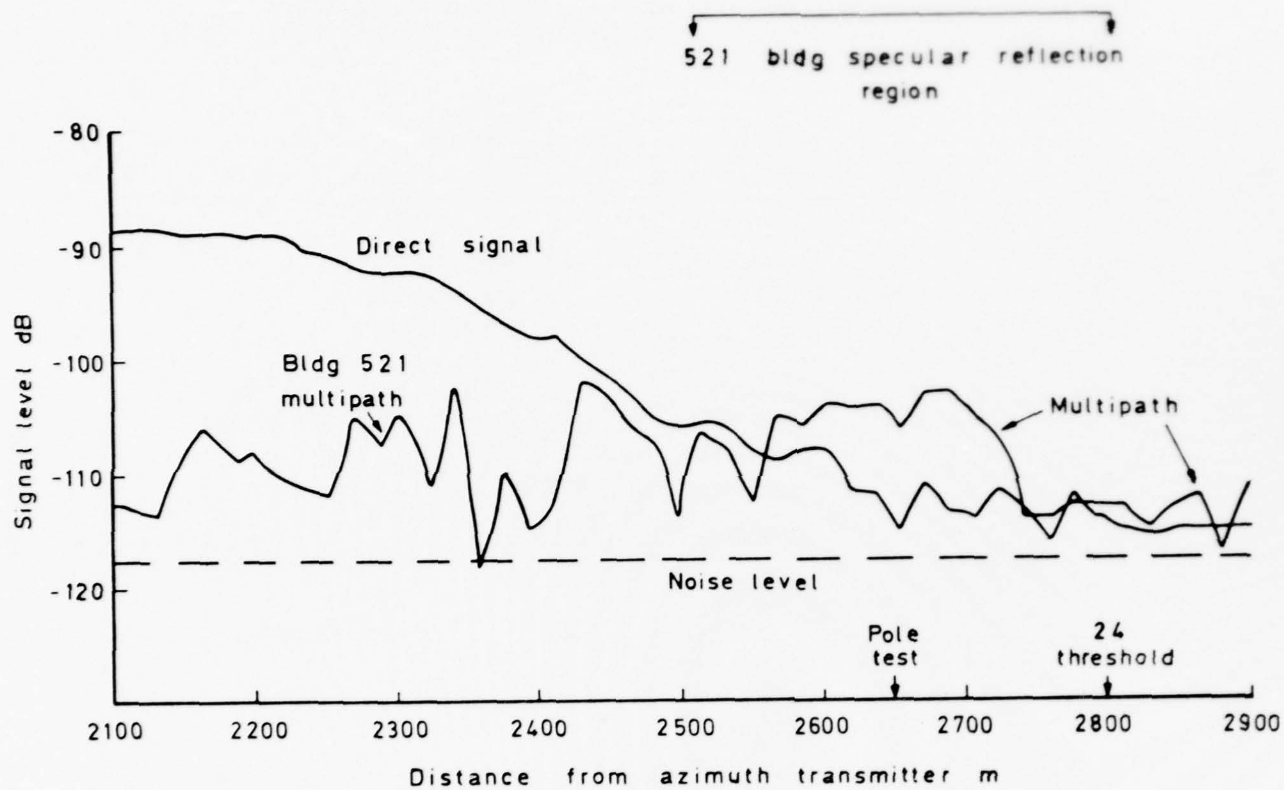


Fig 16b Direct and multipath signals from spectral recordings at Manchester International Airport 8 November 1977, runway run, height 4.6 m (15 ft)

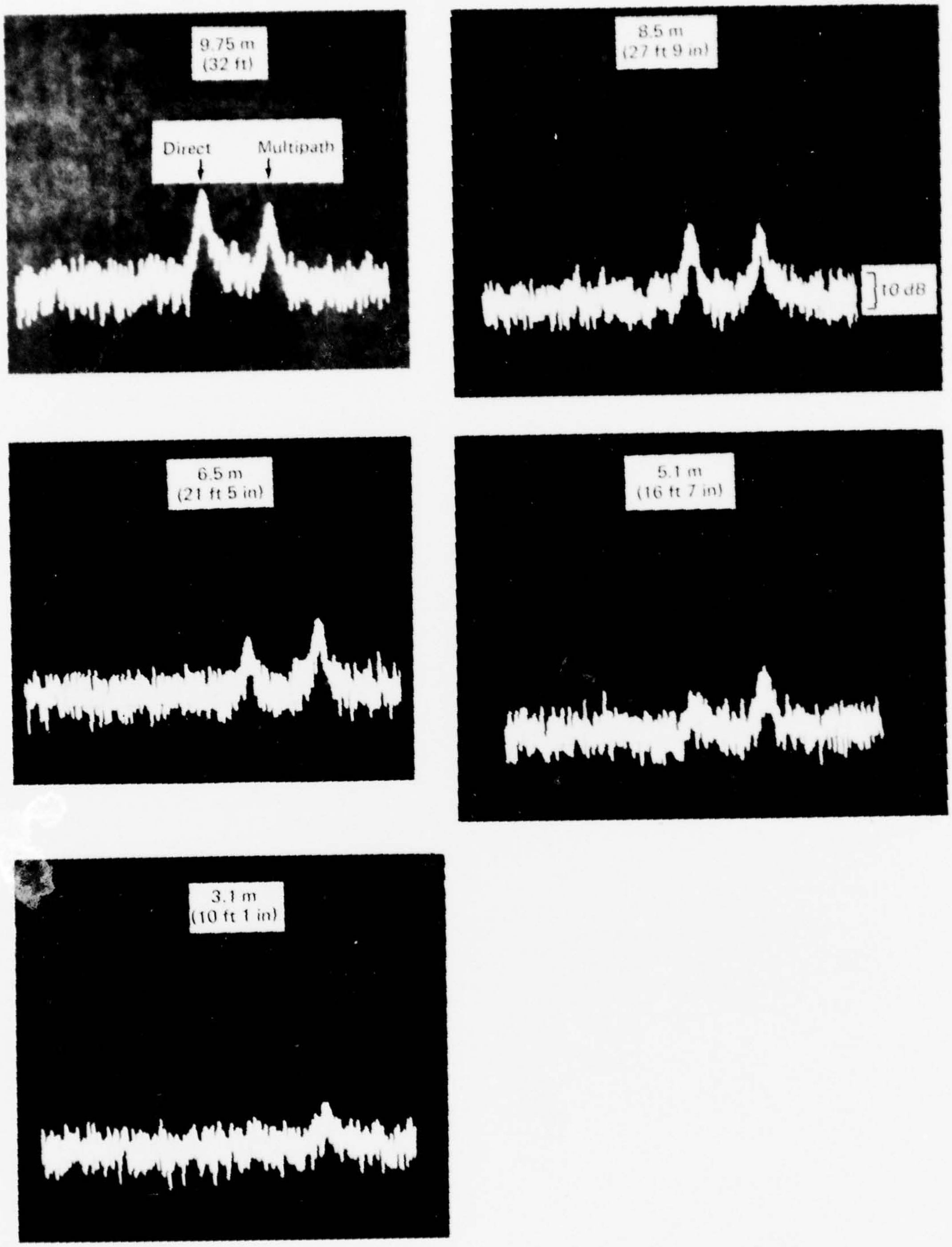


Fig 17 Azimuth system spectral photographs at 2650 m

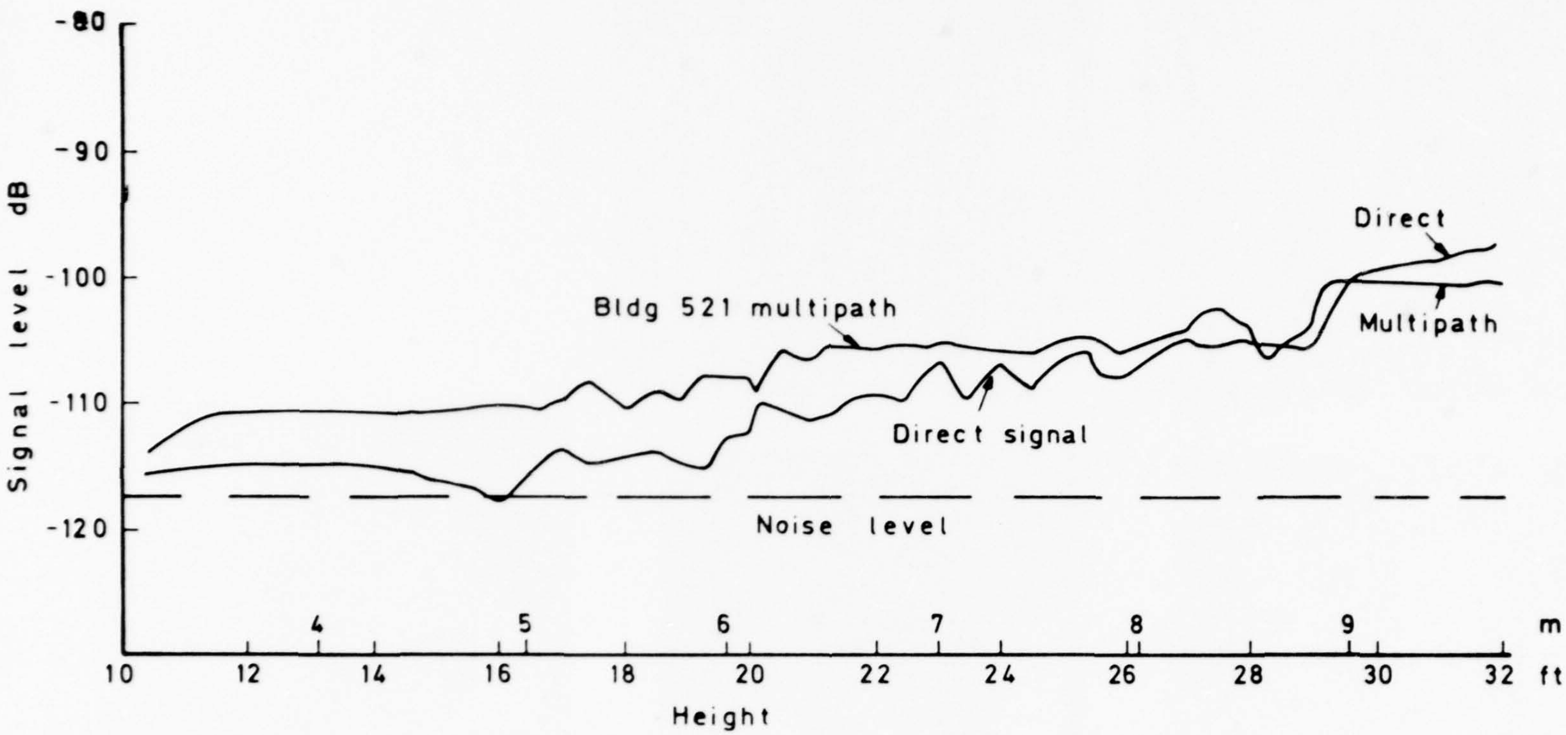


Fig 18 Variation of direct signal and multipath with height at 2650 m from azimuth transmitter, from spectral recordings

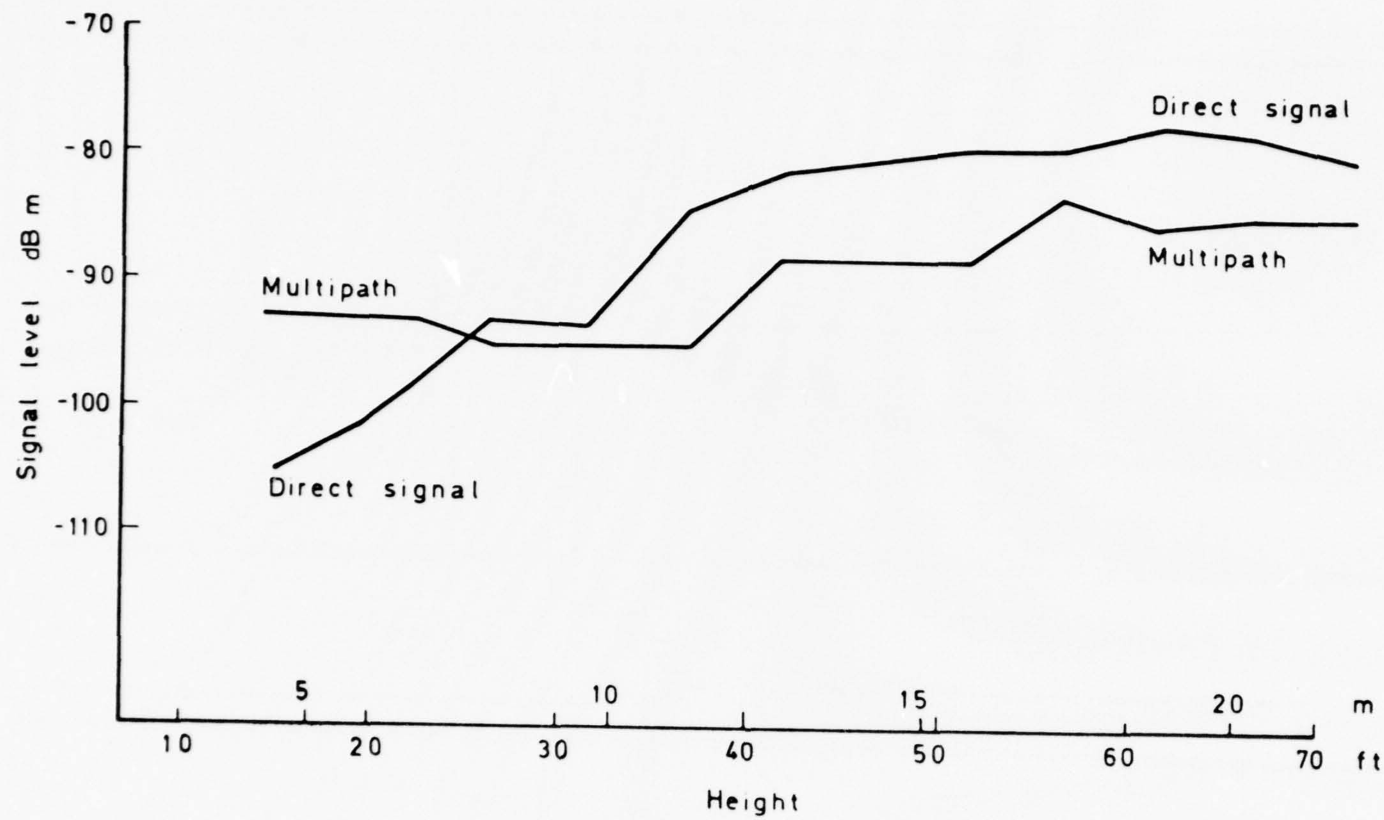


Fig 19 Variation of direct signal and multipath with height at 2650 m from azimuth transmitter, from spectral recordings

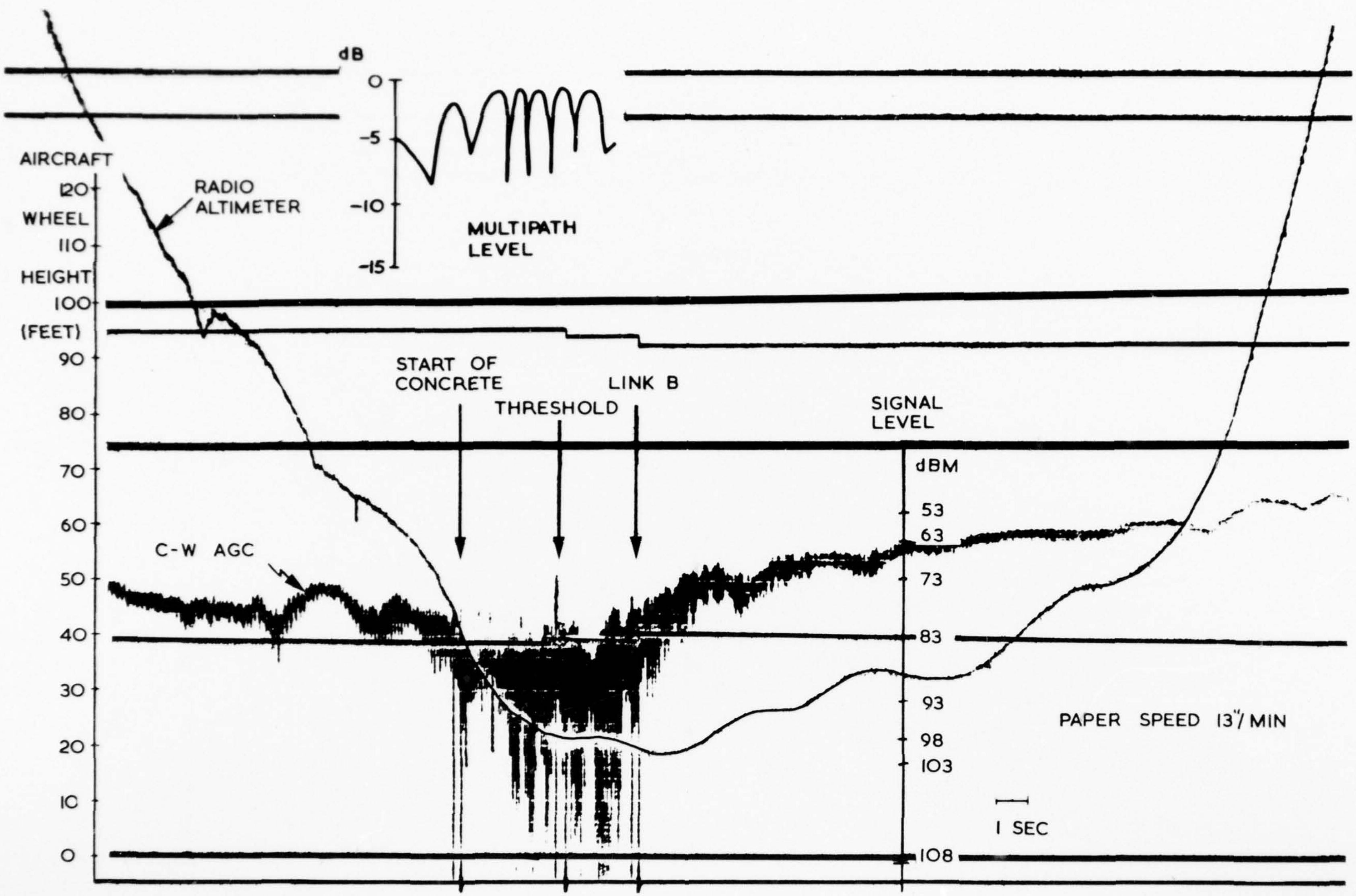


Fig 20a Flight recording of C-W AGC during low approach, UT 37/9 4.11.77

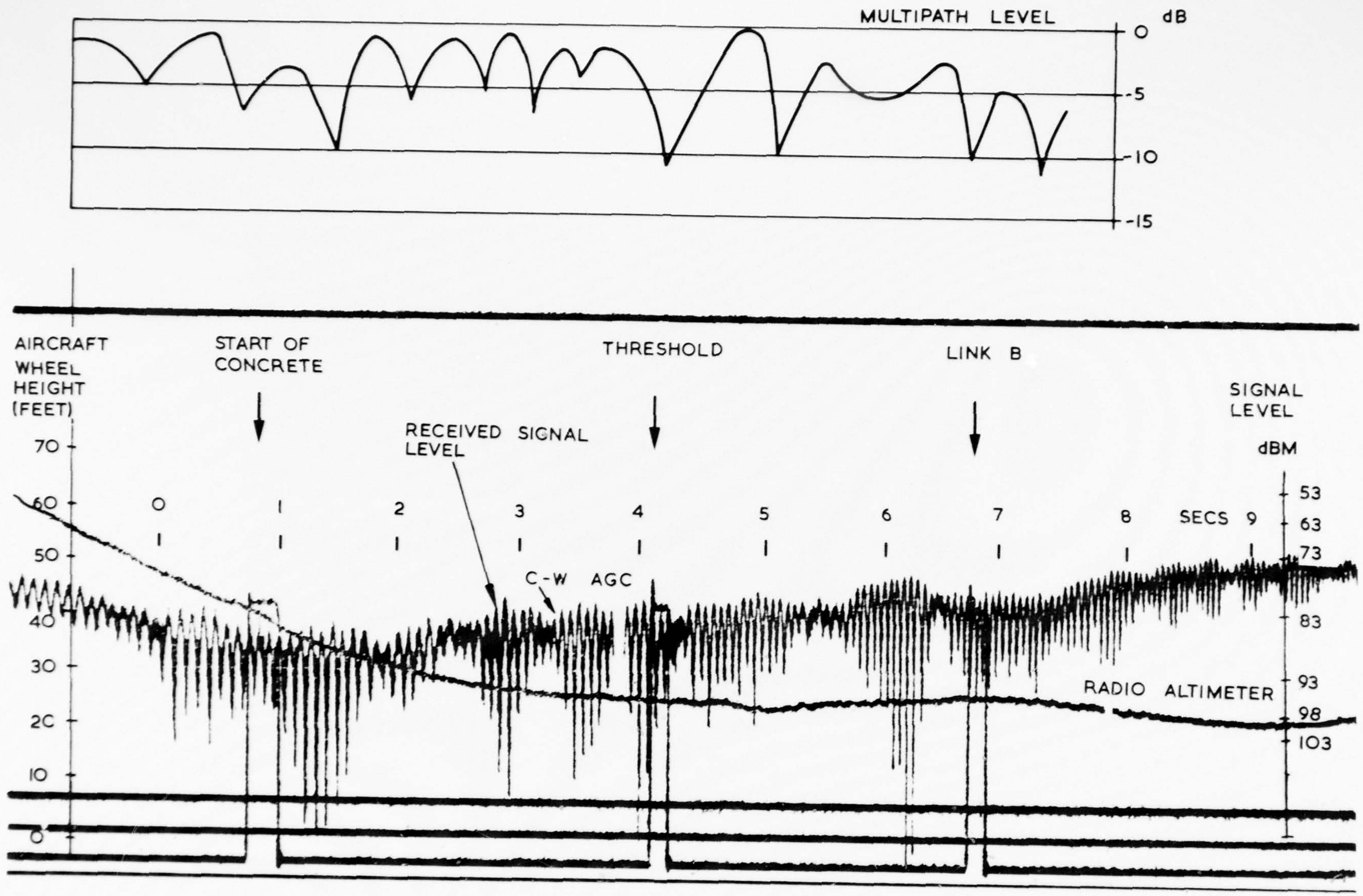


Fig 20b Flight recording of C-W AGC during low approach, UT 37/10 4.11.77


Fig 21 Photograph of Airfield Hotel from elevation site

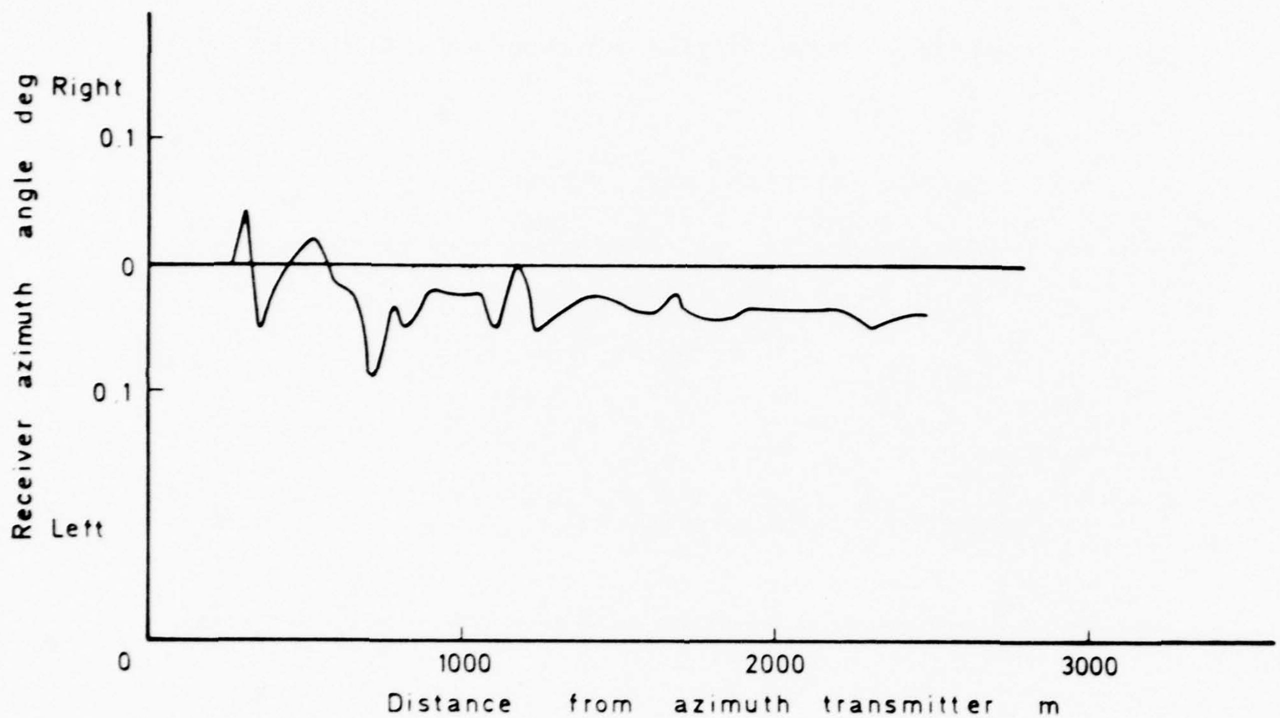


Fig 22a Azimuth receiver angle during runway centre line run 1, mast height 4.6 m (15 ft), 54 λ aperture

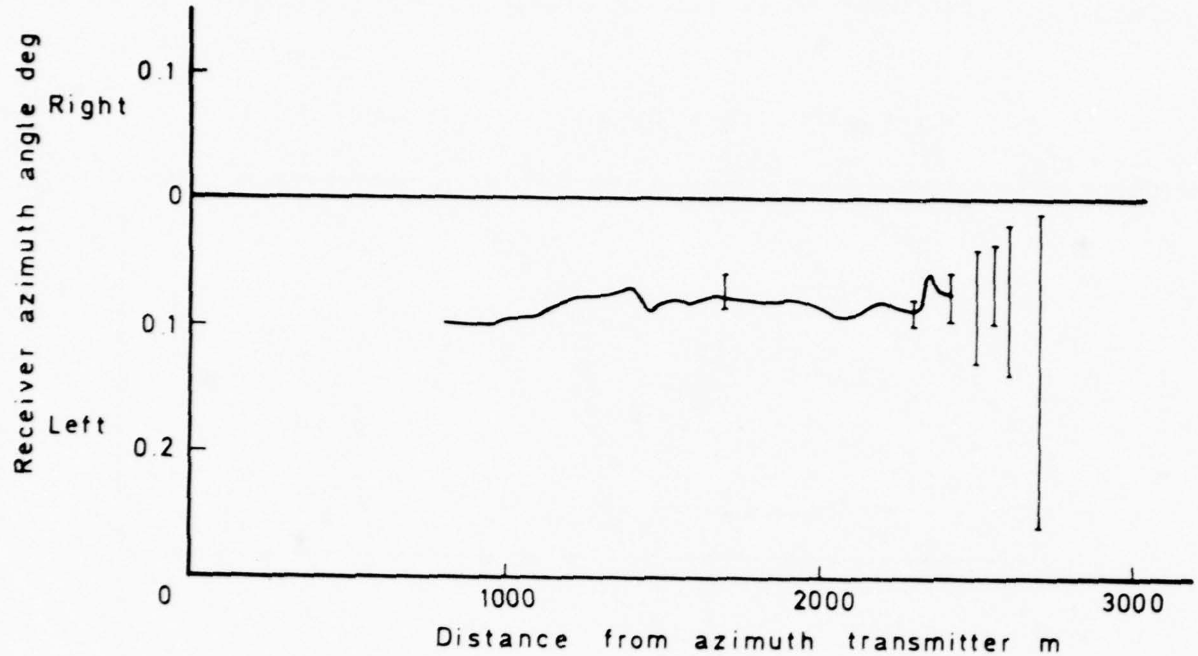


Fig 22b Azimuth receiver angle during runway centre line run 2, mast height 4.6 m (15 ft), 27 λ aperture

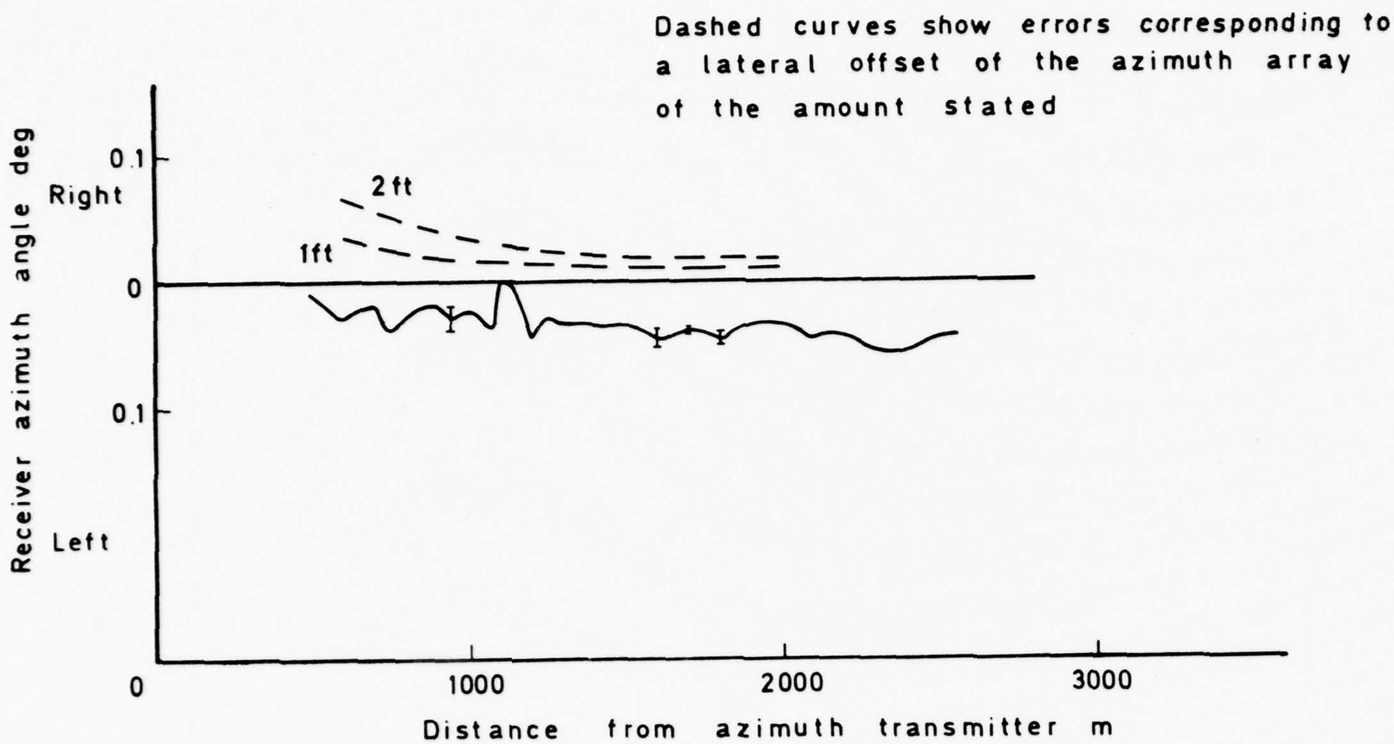


Fig 22c Azimuth receiver angle during runway centre line run 3, mast height 4.6 m (15 ft), 54 $\lambda$ aperture

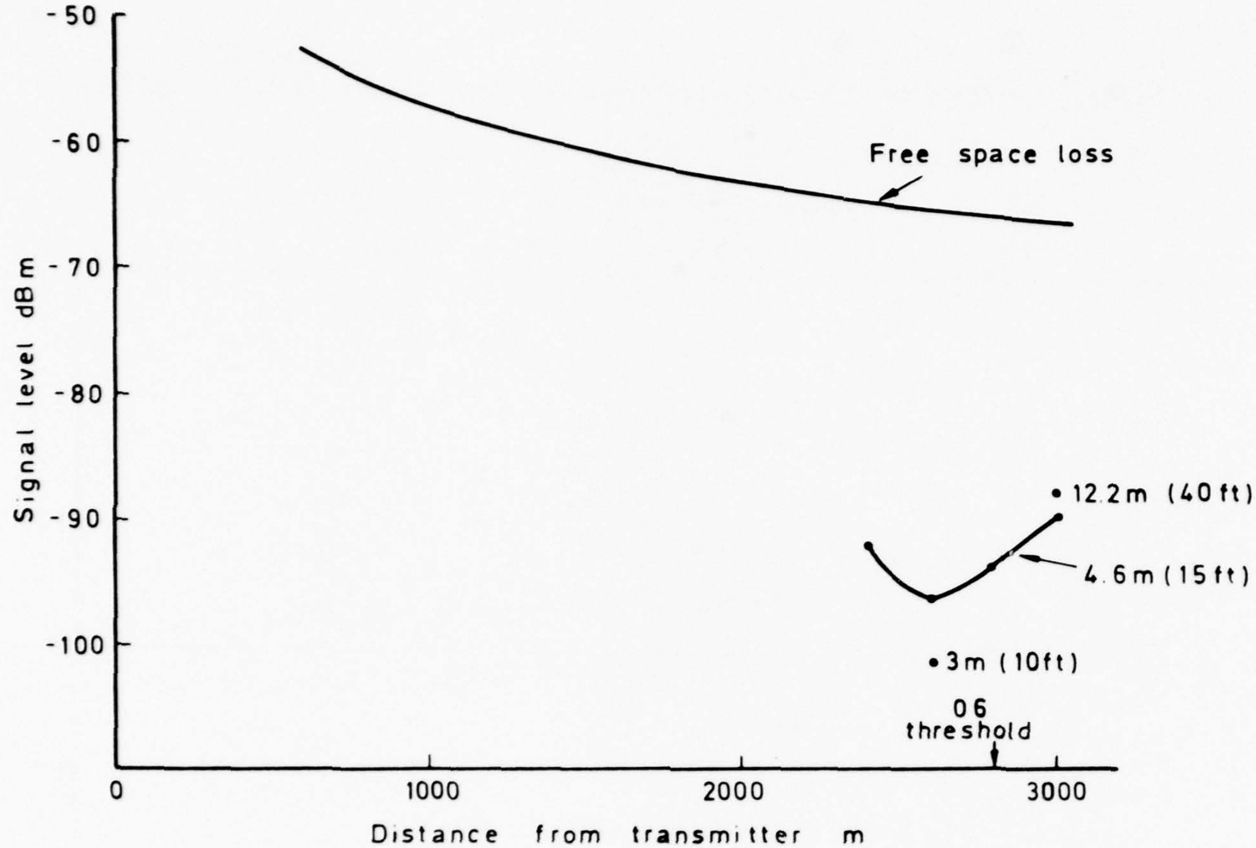


Fig 23 Theoretical shadowing loss for Manchester runway 06

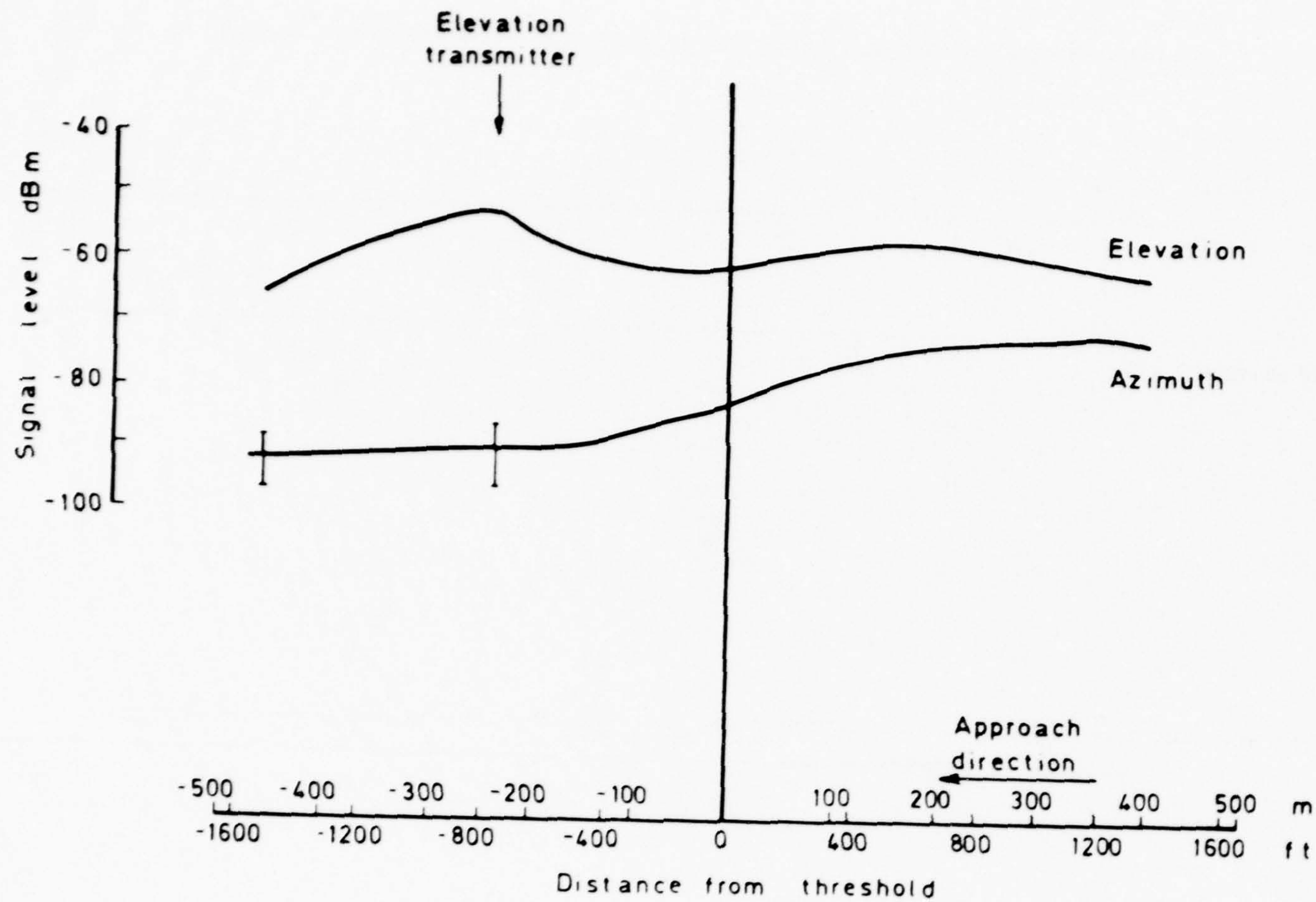


Fig 24 Azimuth and elevation system signal levels during a 3° approach to land

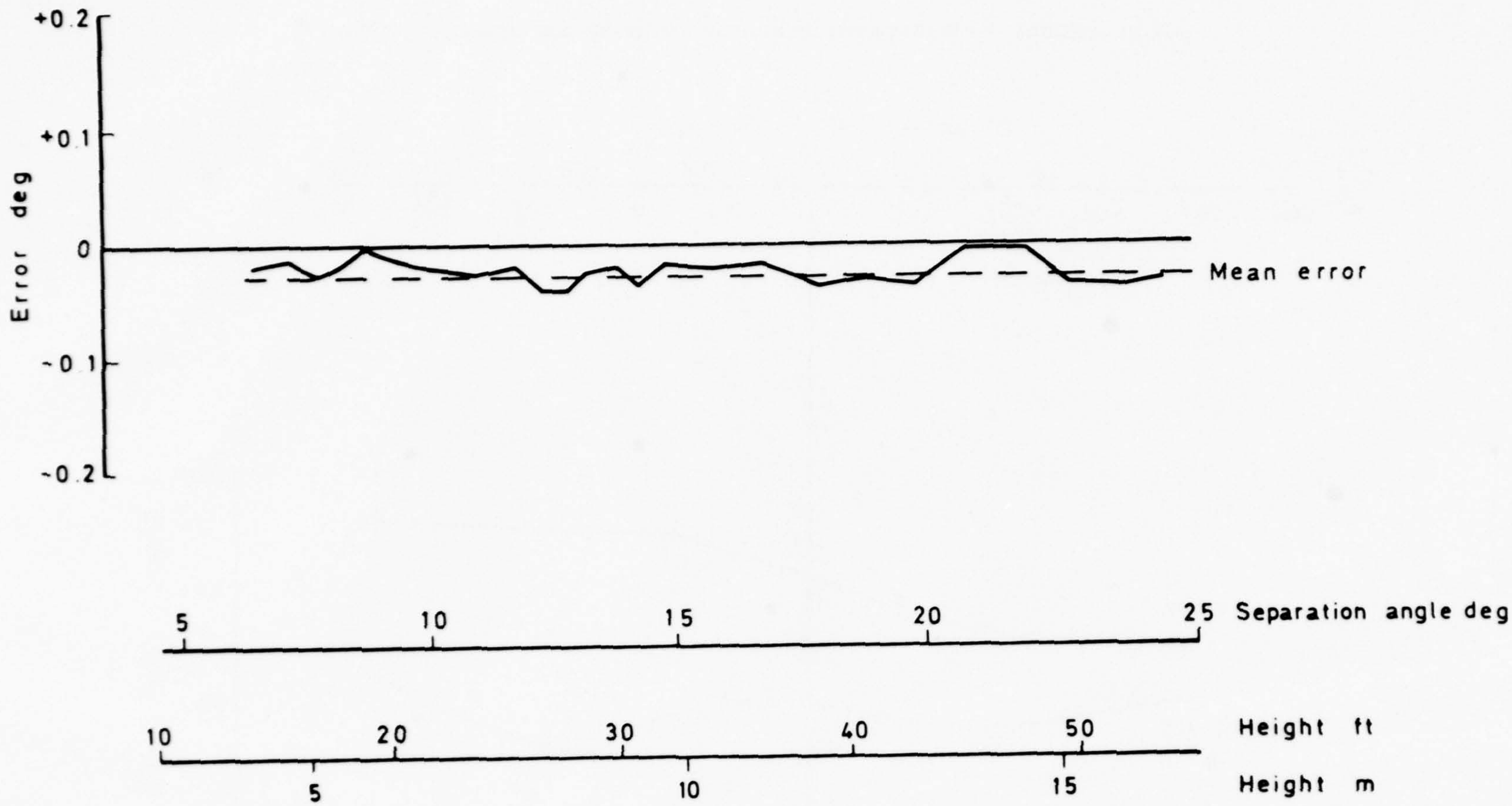


Fig 25a Elevation system pole test at 76 m (250 ft), 28.5° azimuth, 54 λ aperture

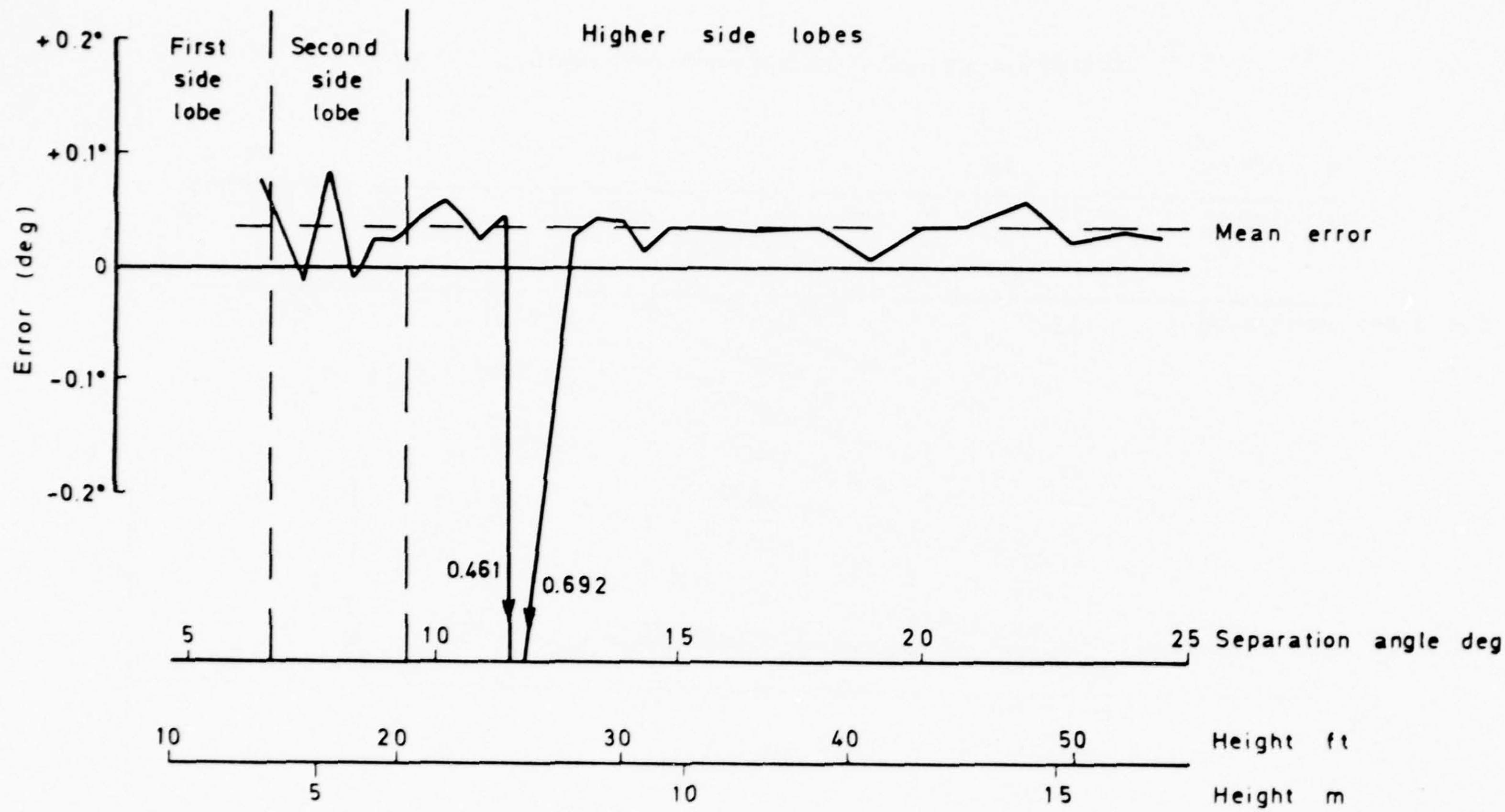


Fig 25b Elevation system pole test at 76 m (250 ft), 28.5° azimuth, 27 λ aperture



Fig 31b

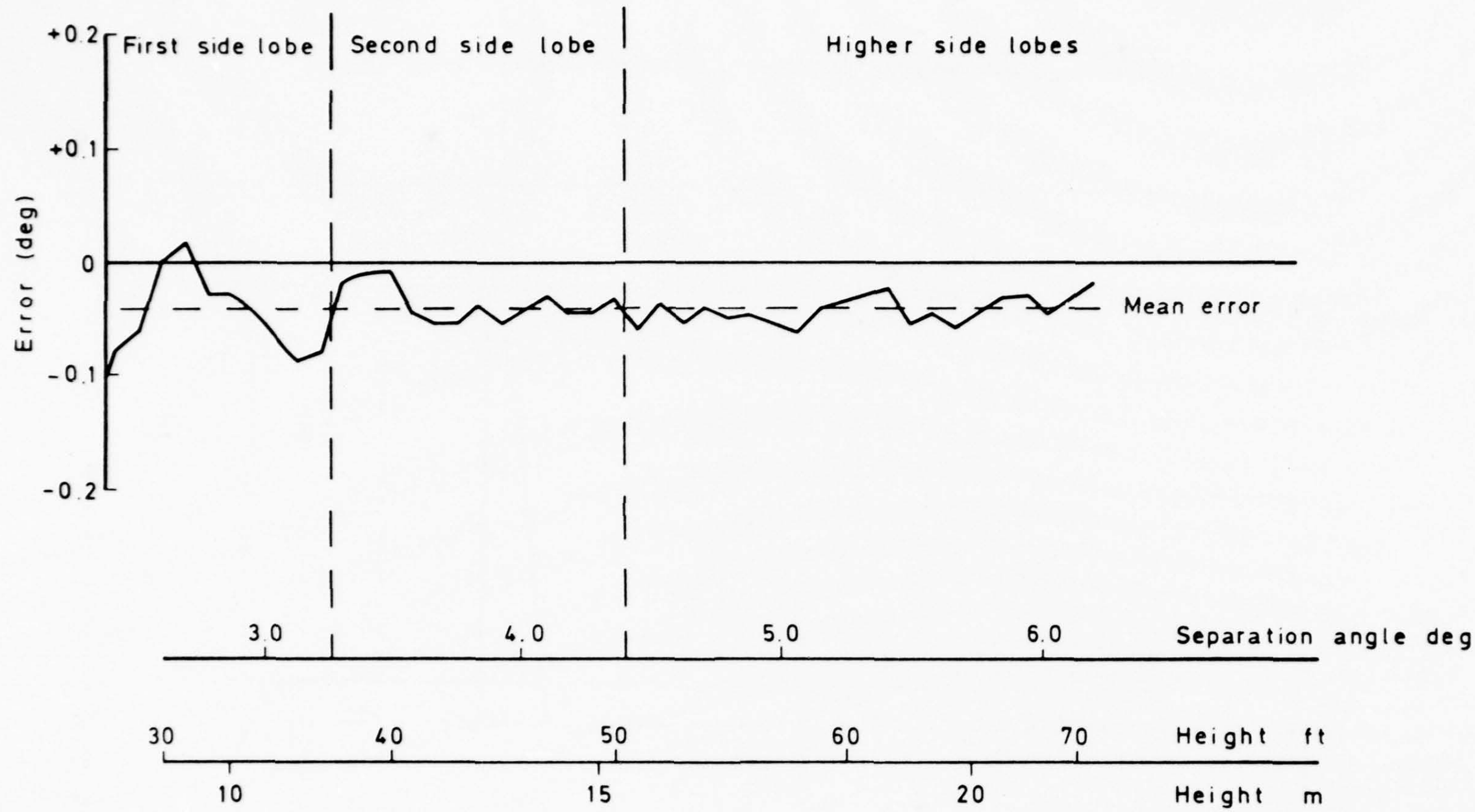


Fig 25c Elevation system pole test at 401 m (1316 ft), 54 λ aperture

TR 78144

Fig 32a

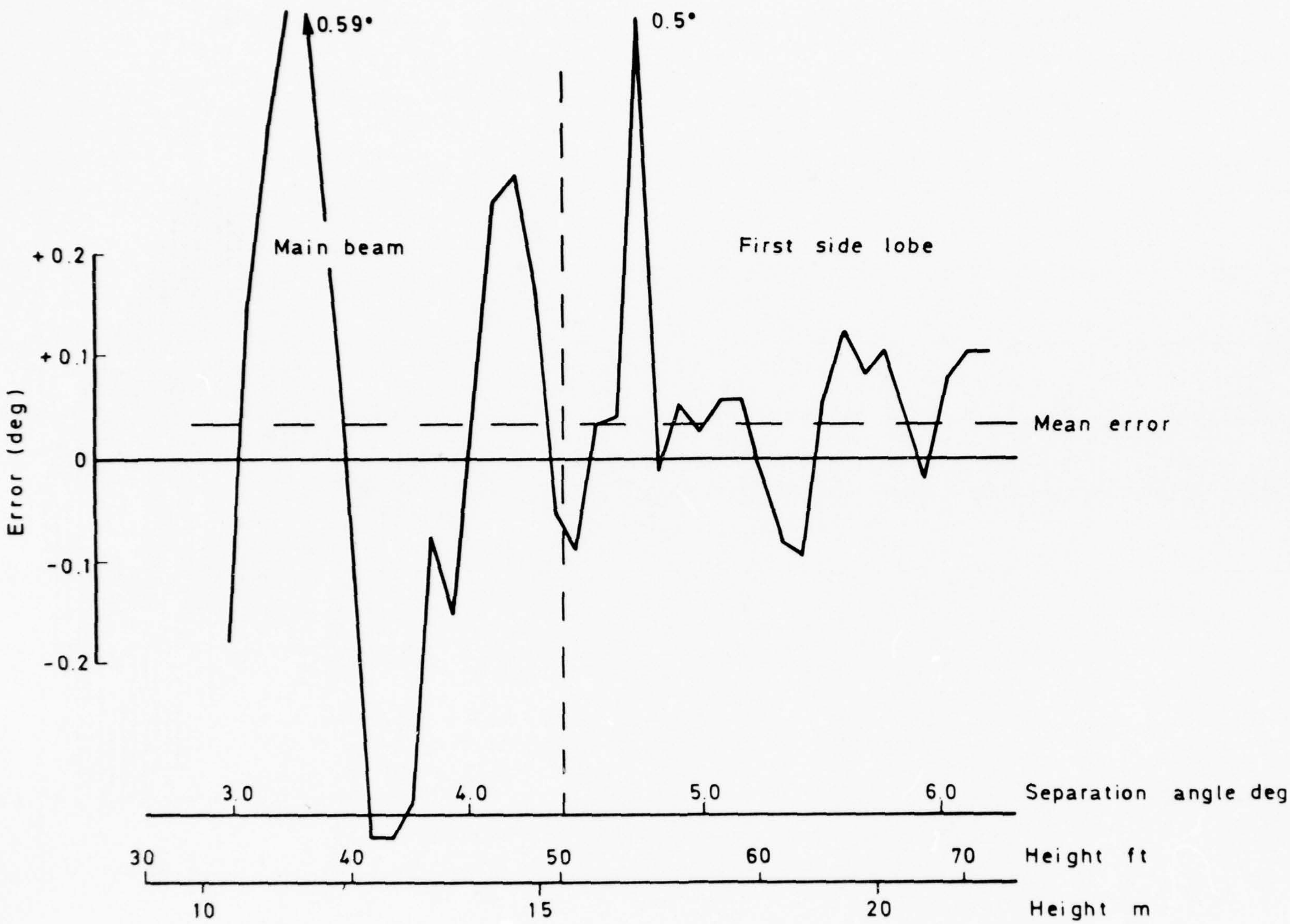


Fig 25d Elevation system pole test at 401 m (1316 ft), 27 λ aperture

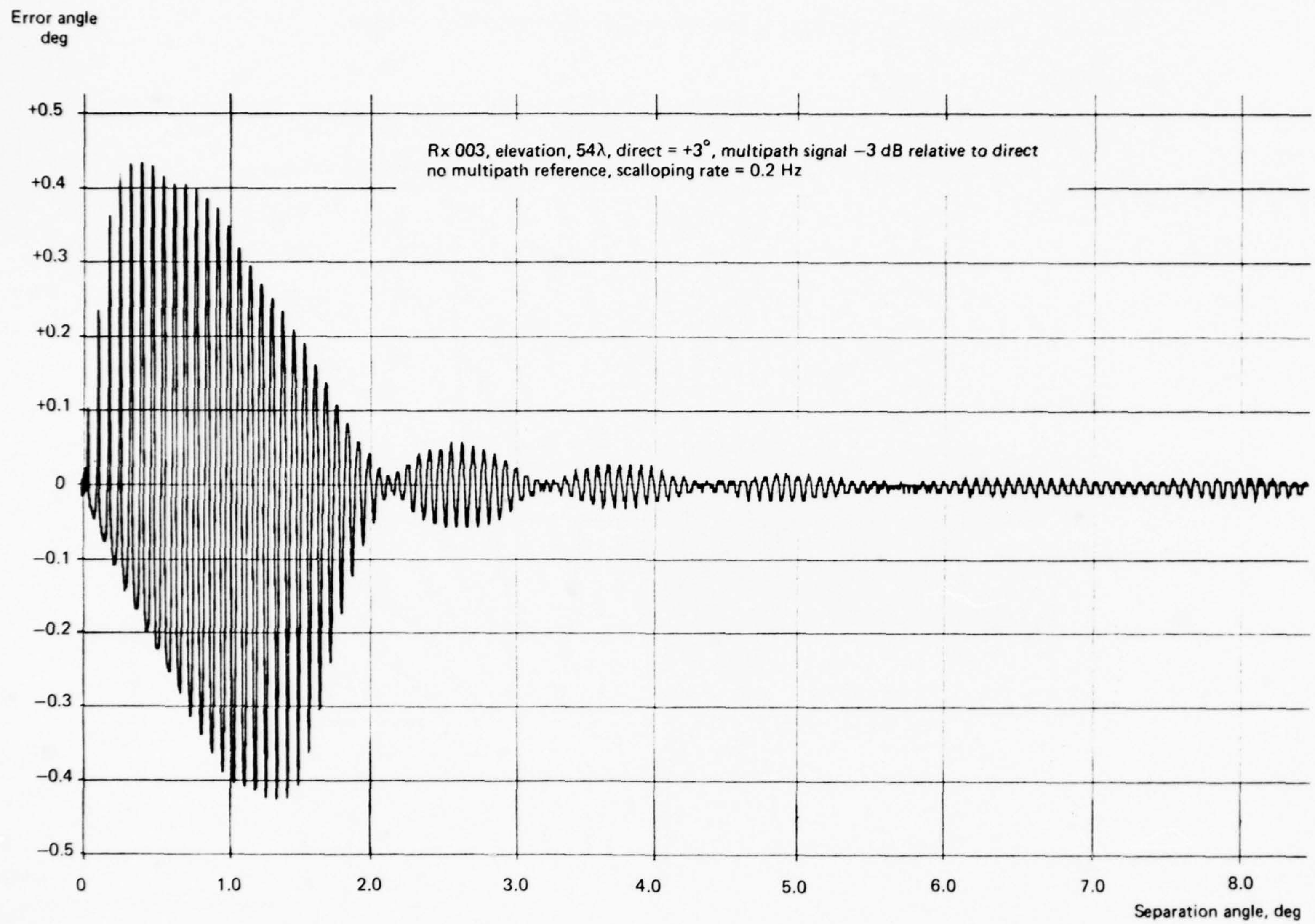


**Fig 26 Receiver error v separation angle – three frequency processor, 54λ elevation array**

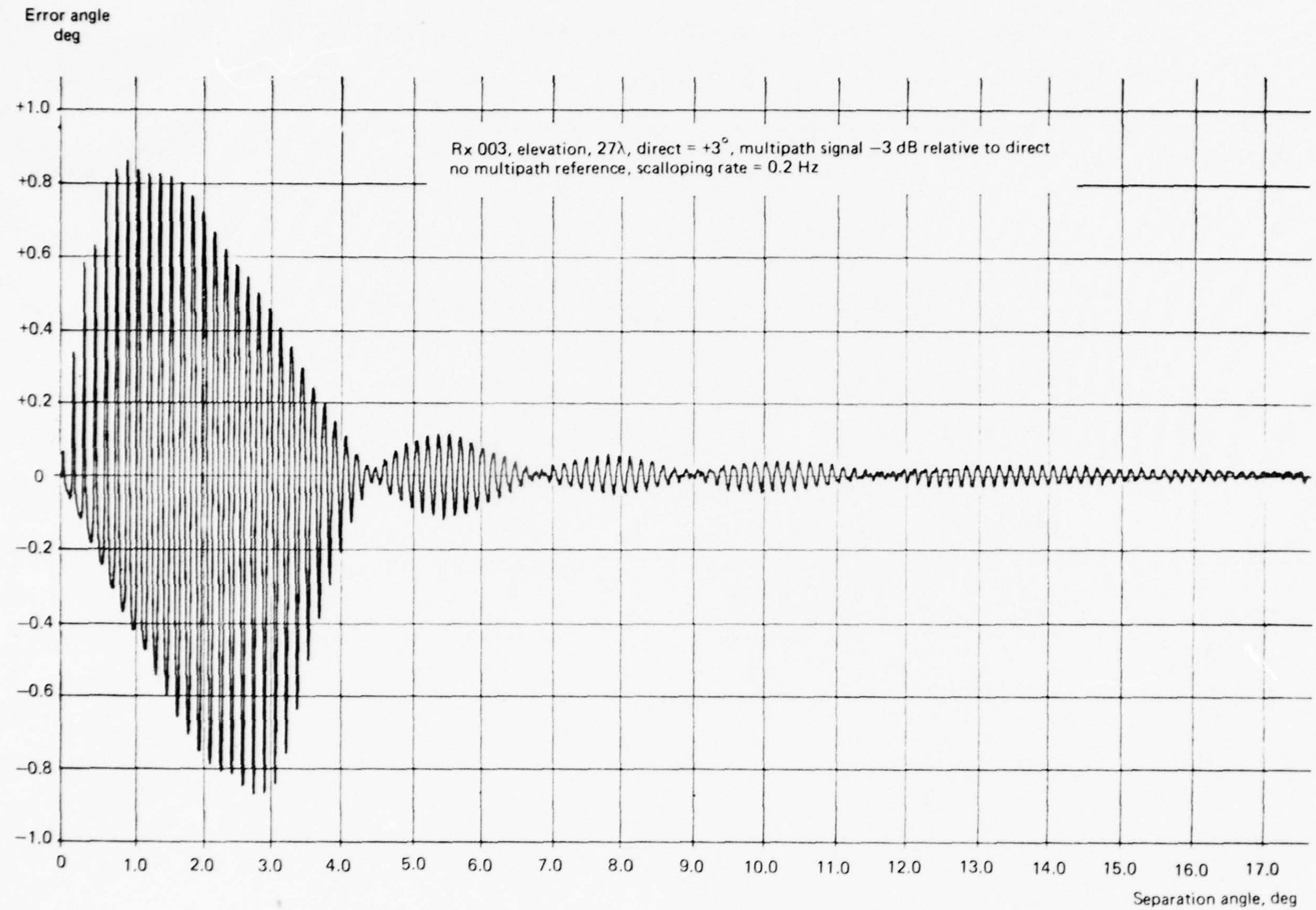


Fig 27 Receiver error v separation angle – three frequency processor, 27λ elevation array

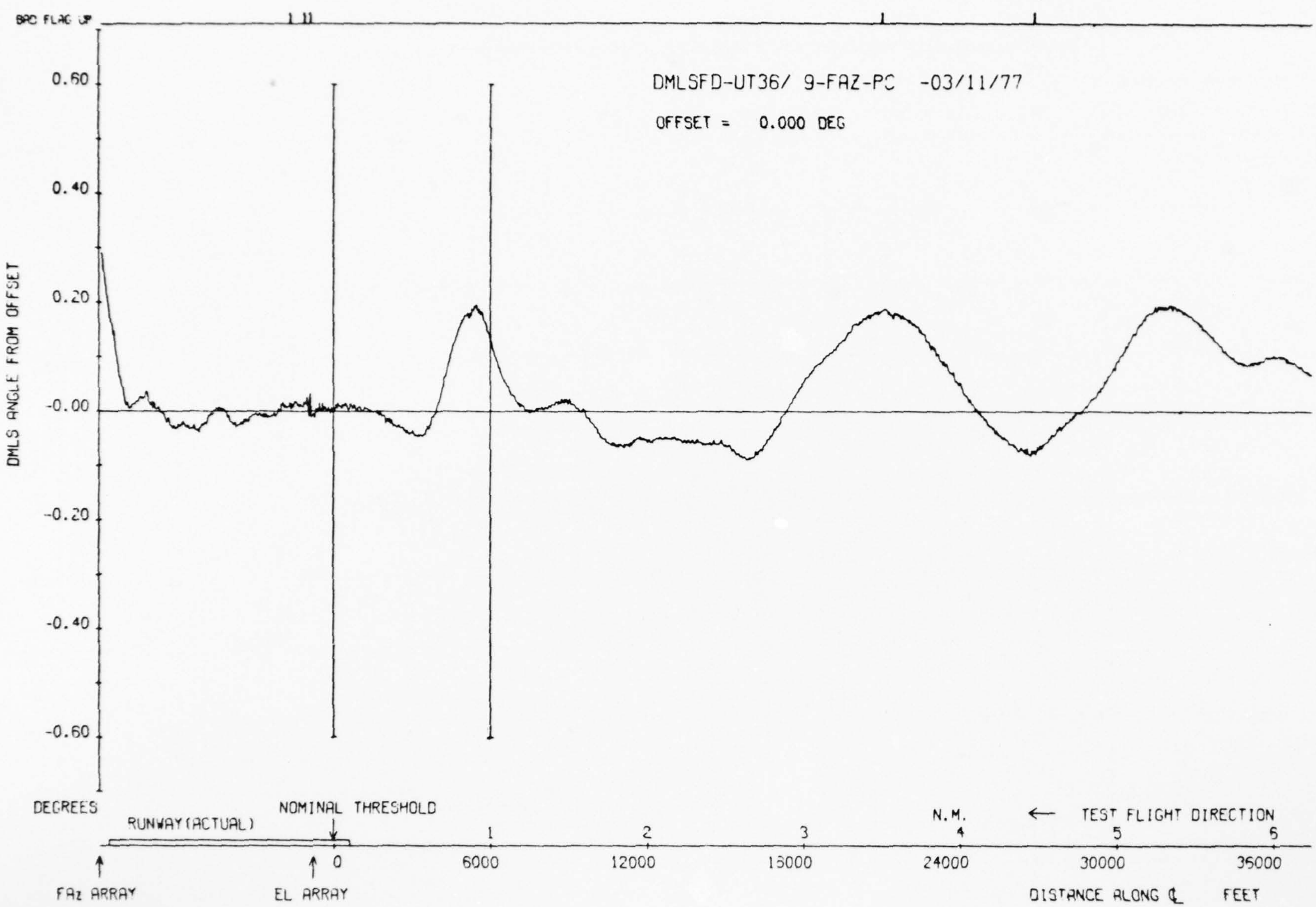


Fig 28a Manchester International Airport – azimuth centre line approach, 54λ aperture

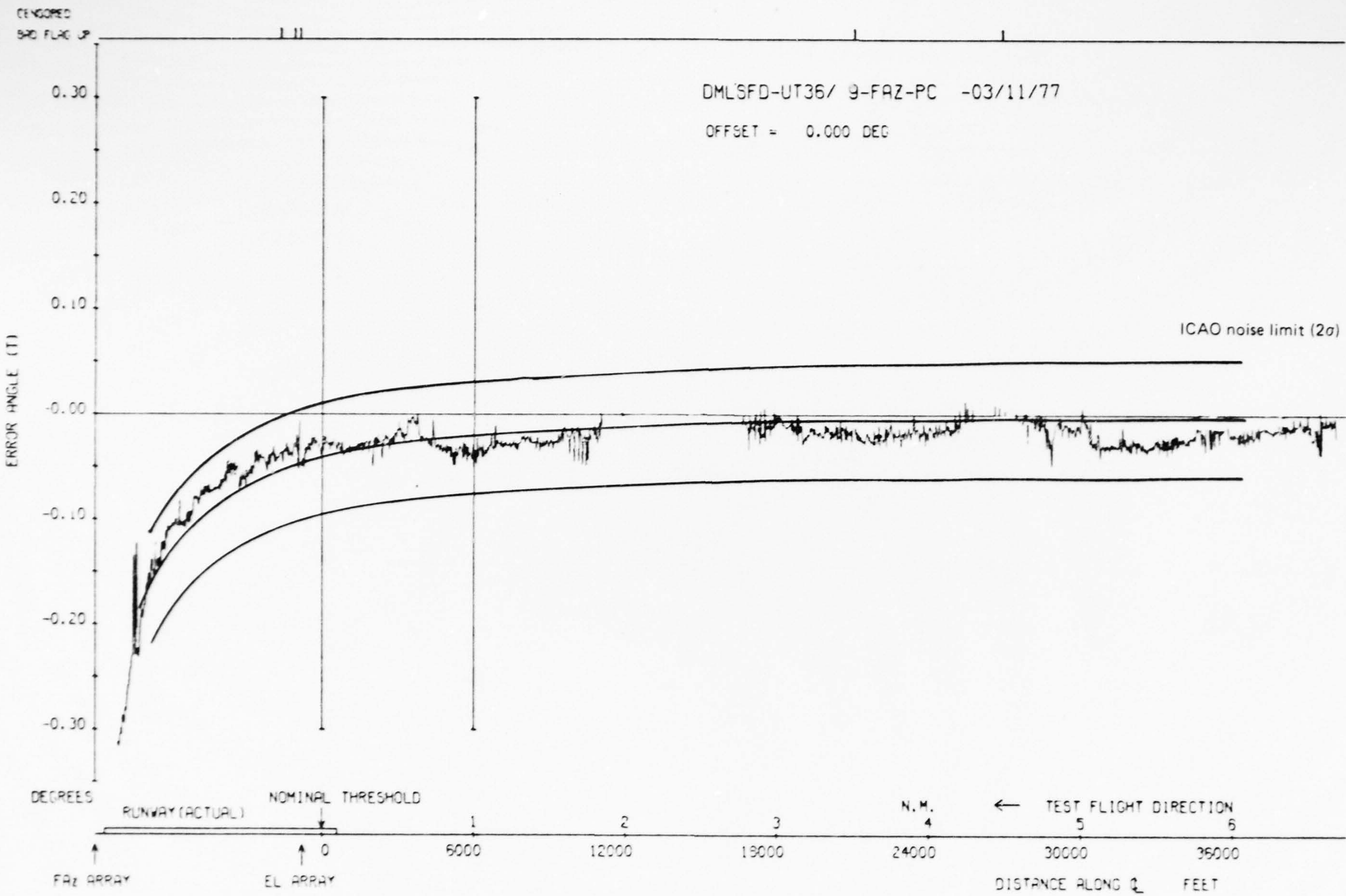


Fig 28b Manchester International Airport – azimuth centre line approach, 54λ aperture. Telecroscope induced errors censored by hand

Fig 28b

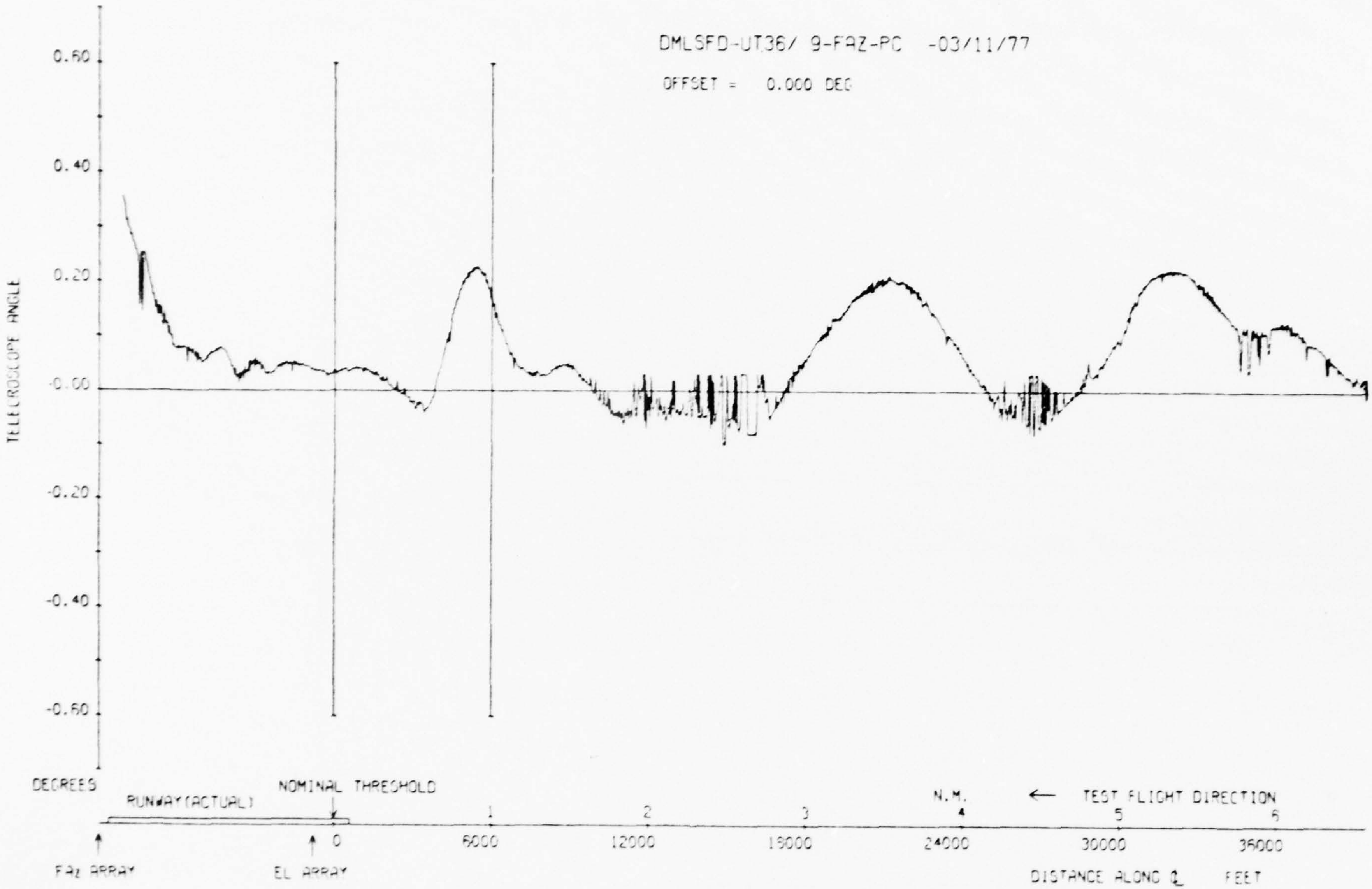


Fig 28c Manchester International Airport – azimuth centre line approach, 54λ aperture

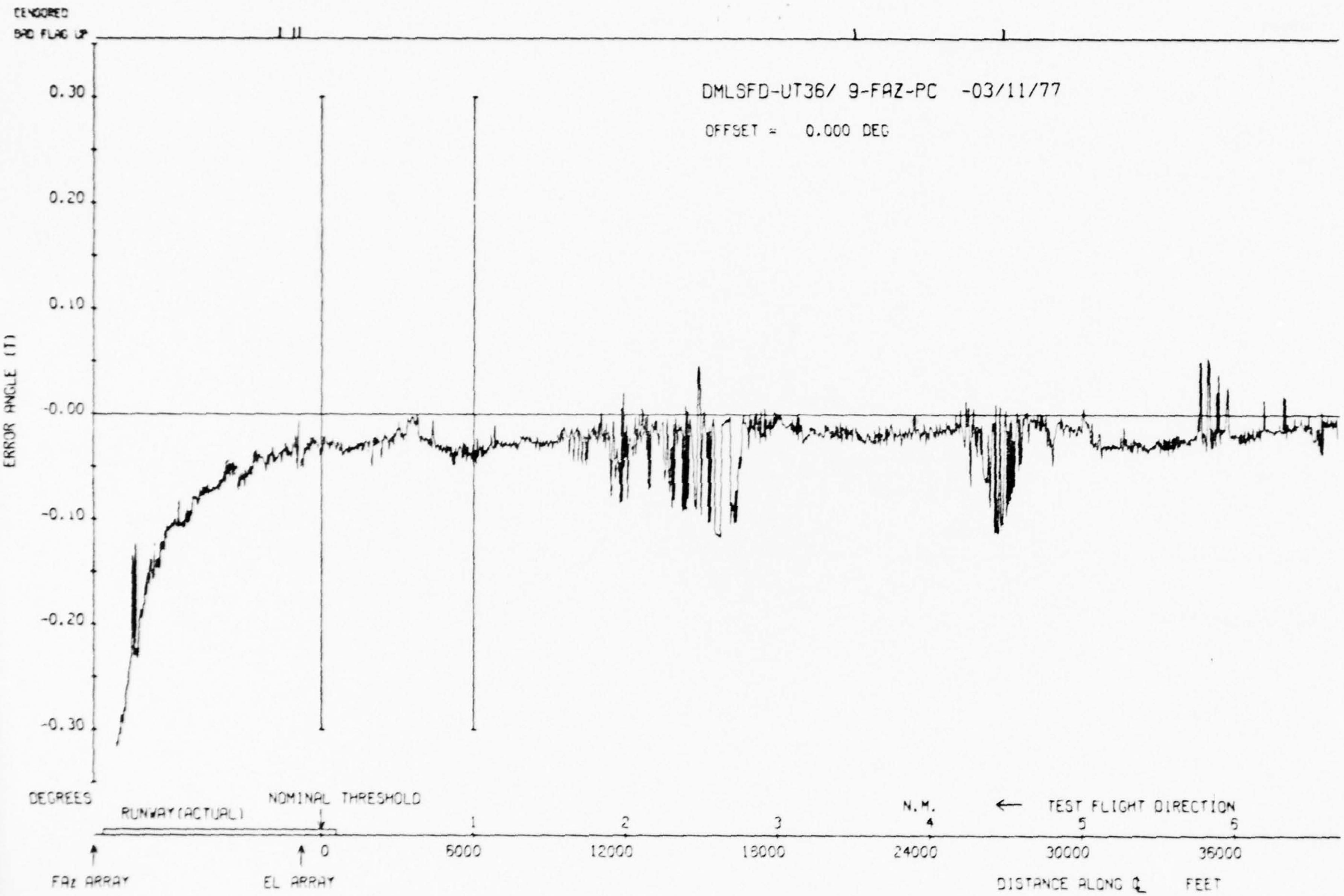


Fig 28d Manchester International Airport – azimuth centre line approach, 54λ aperture. Telecroscope induced errors uncensored

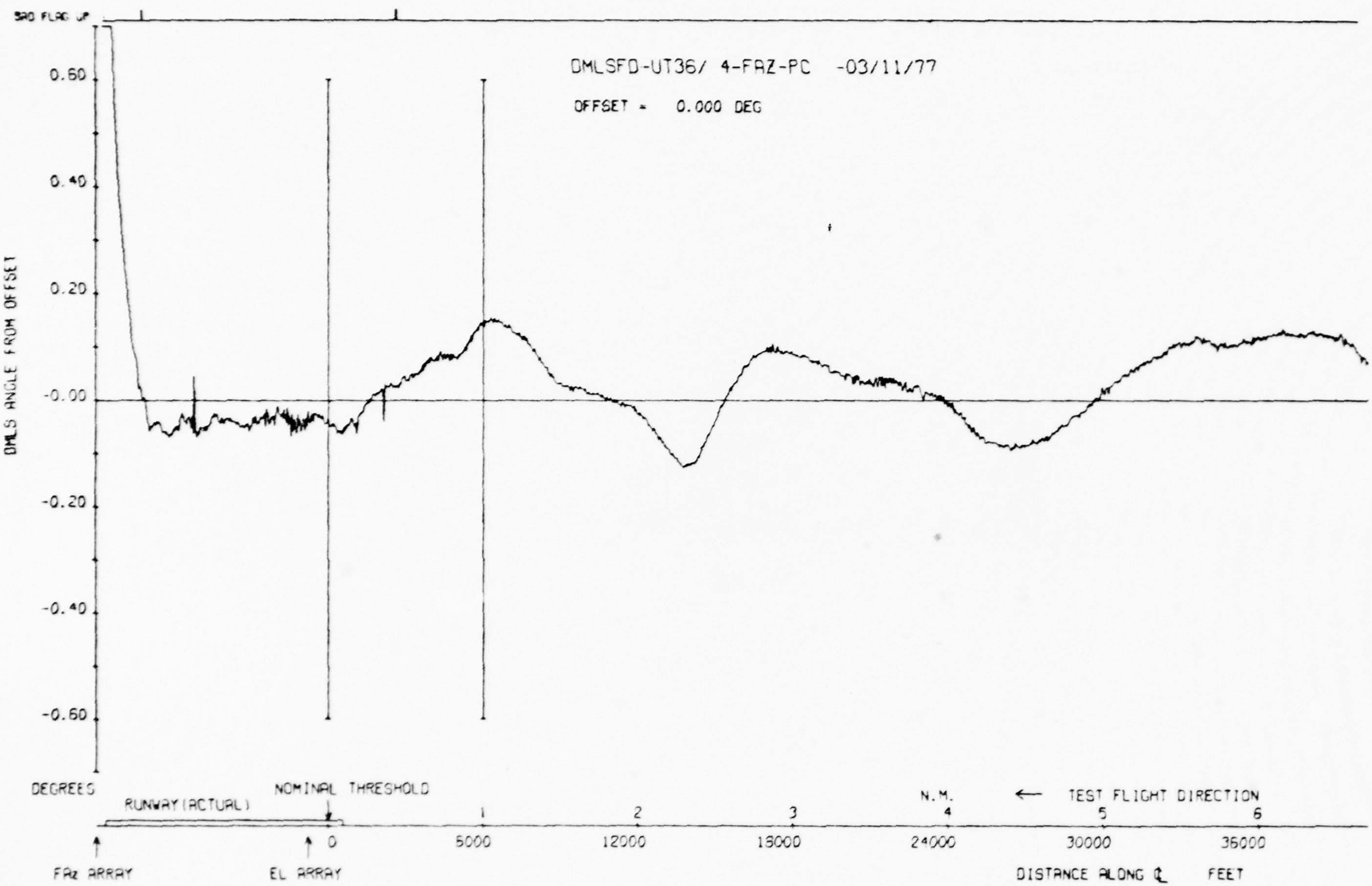


Fig 29a Manchester International Airport – azimuth centre line approach, 27λ aperture

TR 78144

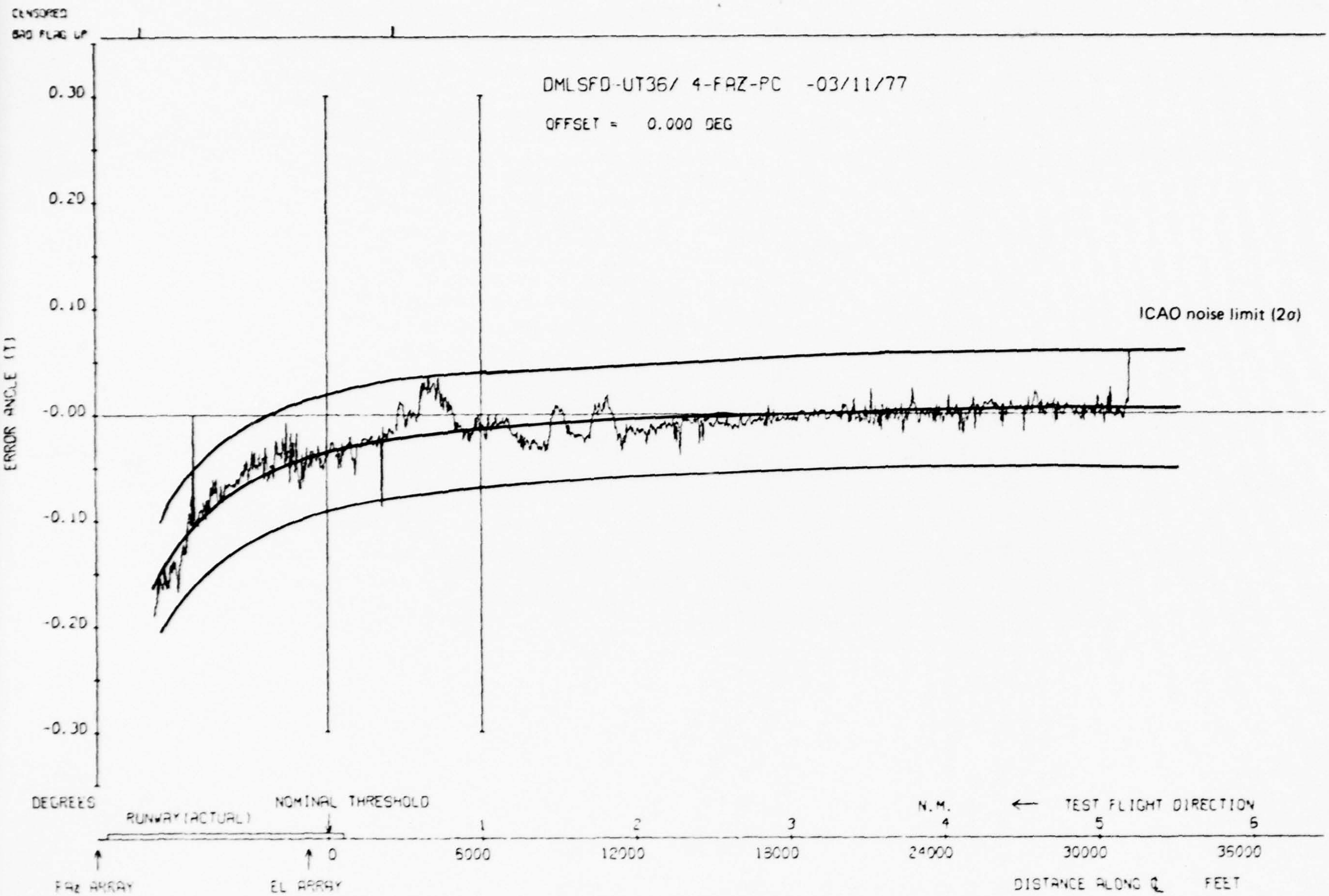


Fig 29b Manchester International Airport – azimuth centre line approach, 27λ aperture

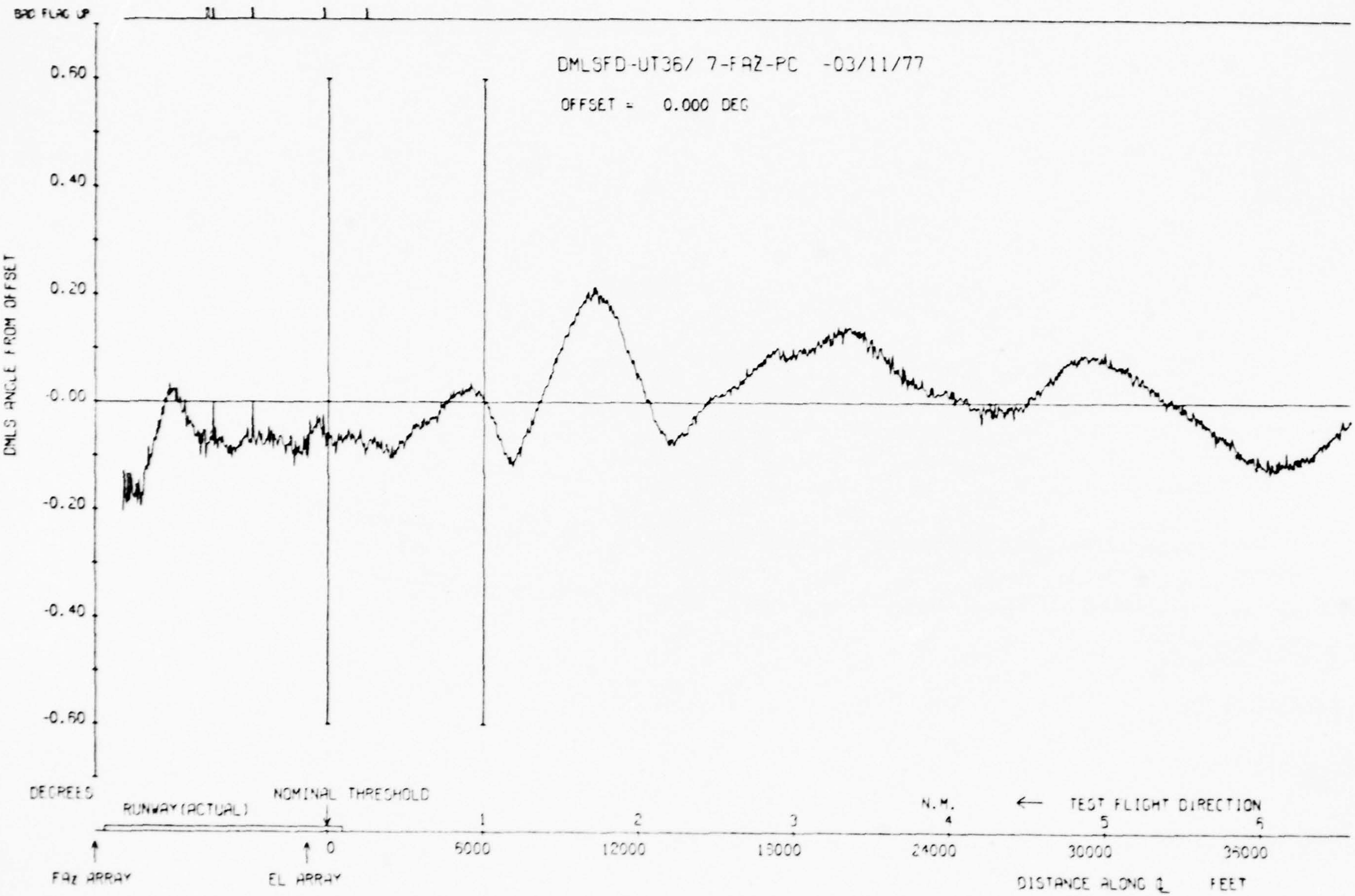


Fig 30a Manchester International Airport – azimuth centre line approach, 20λ aperture

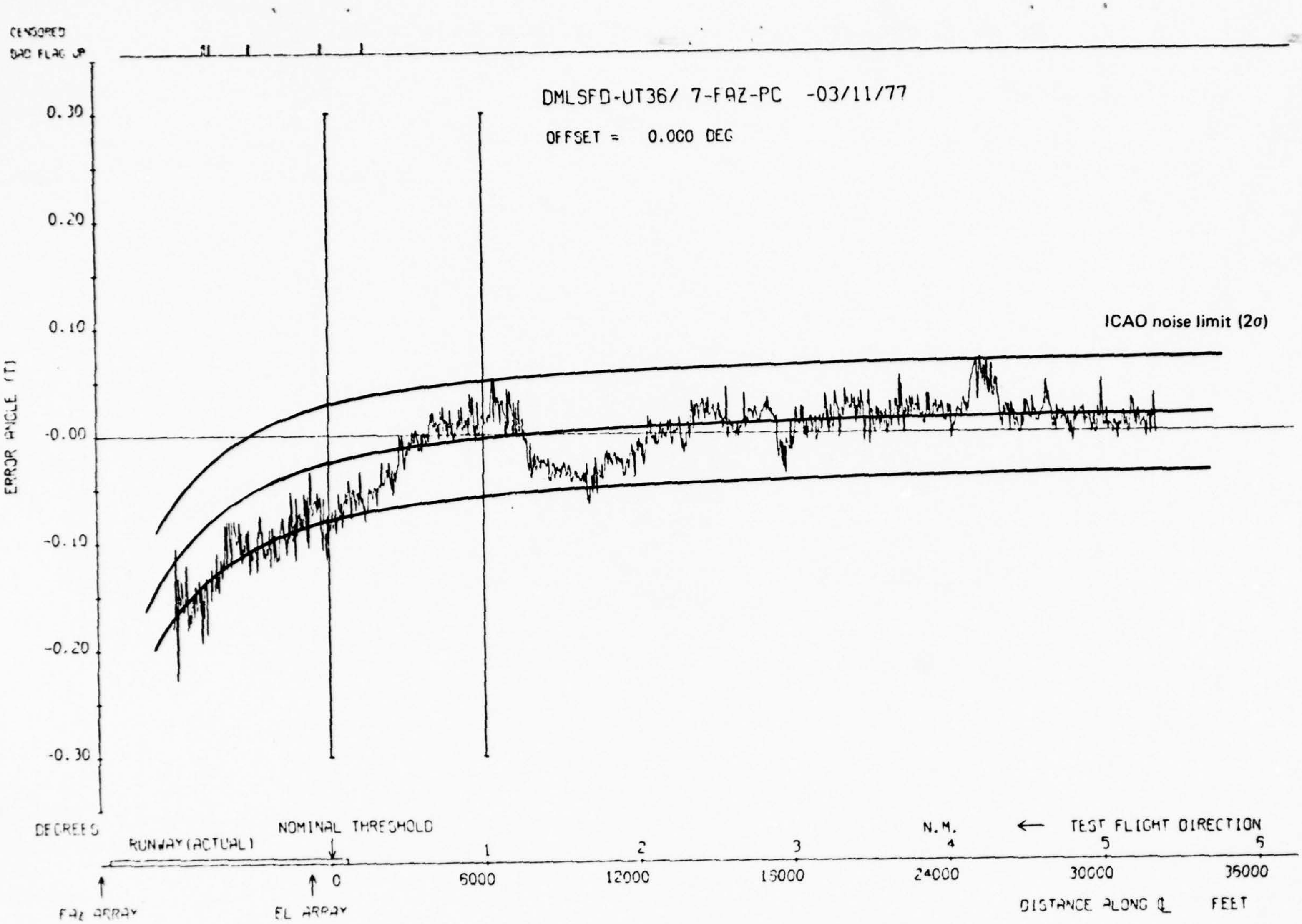


Fig 30b Manchester International Airport – *azimuth centre line approach*, 20λ aperture

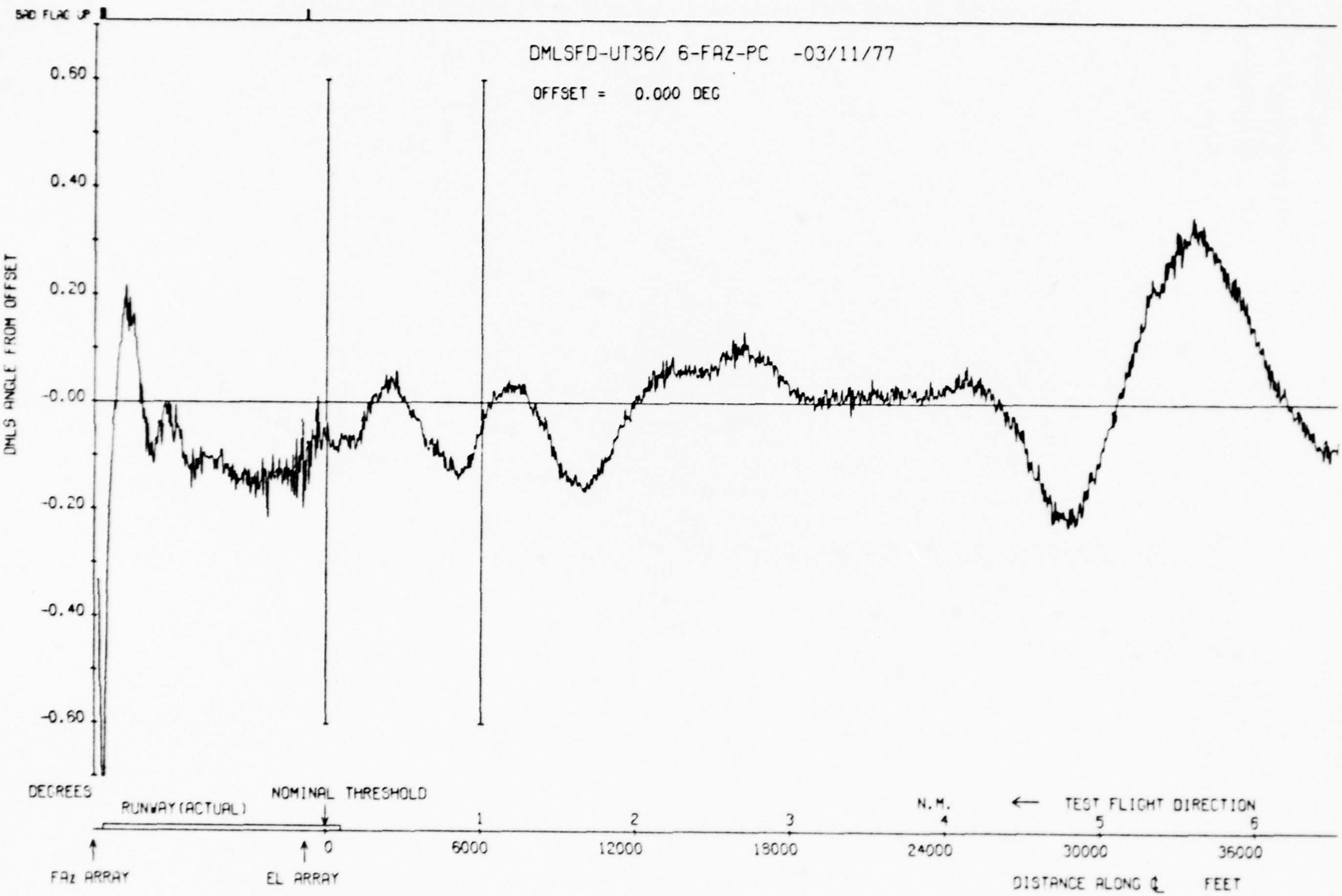


Fig 31a Manchester International Airport – azimuth centre line approach, 15λ aperture

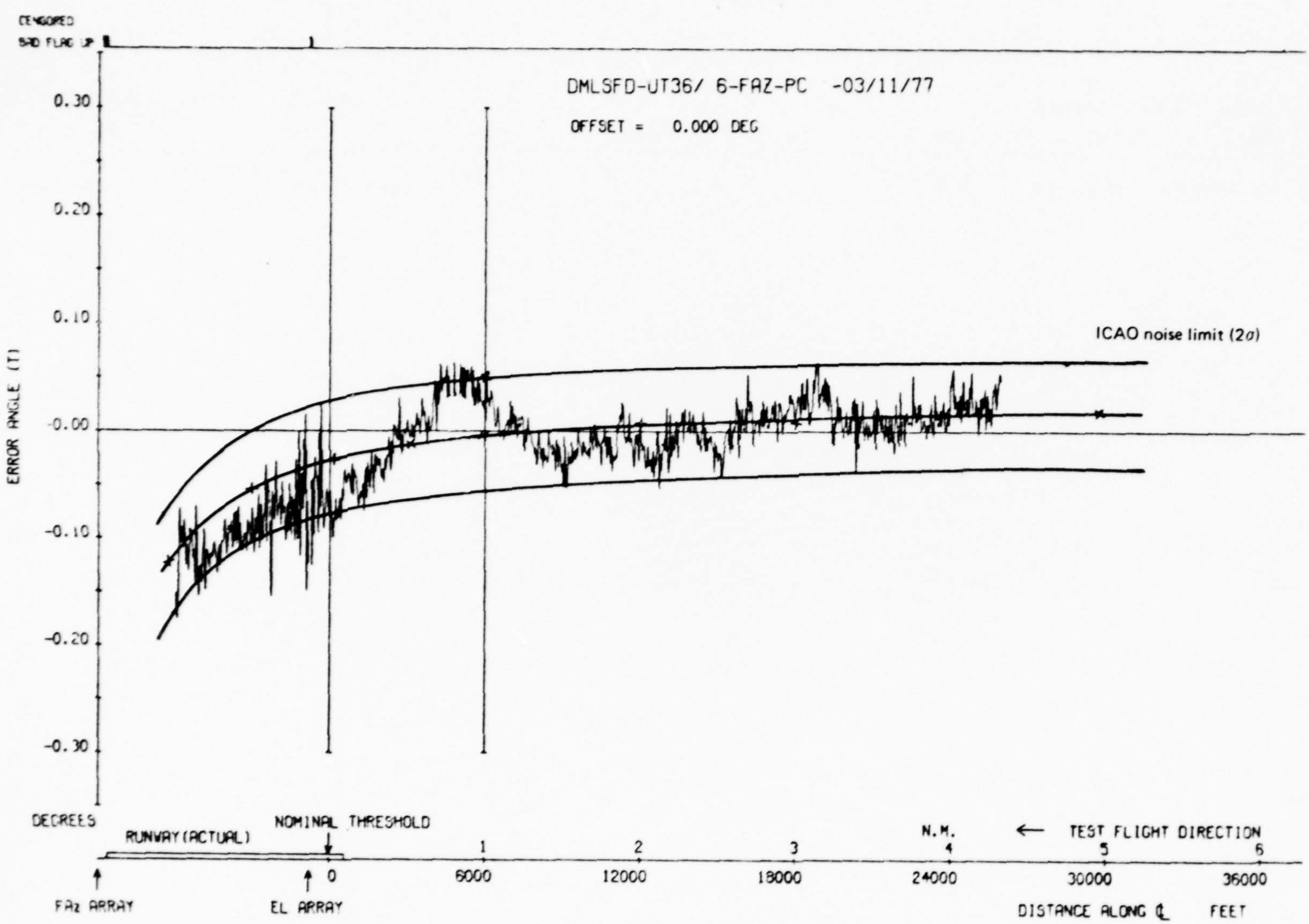


Fig 31b Manchester International Airport – azimuth centre line approach, 15λ aperture

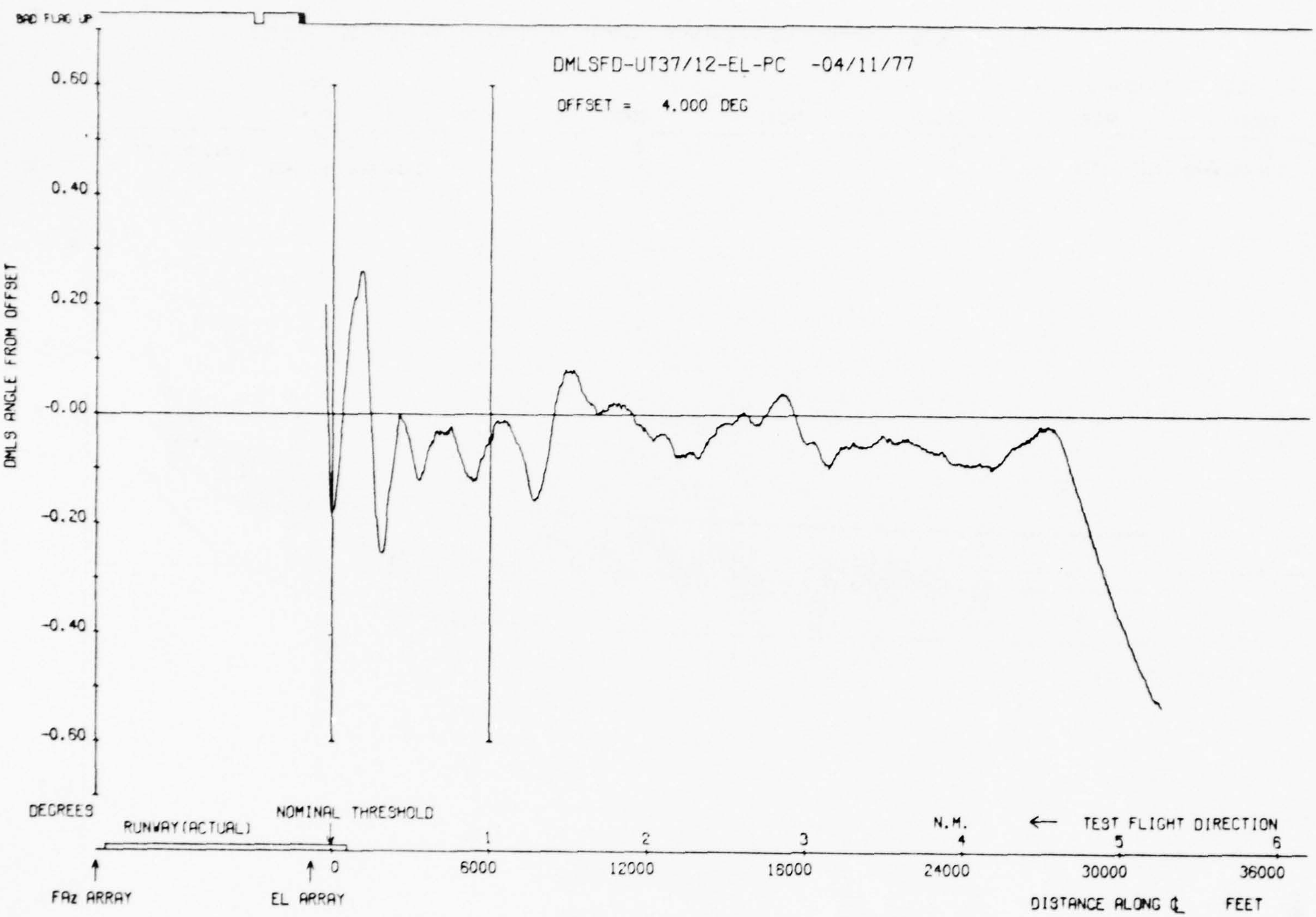


Fig 32a Manchester International Airport – elevation 4 degree approach, 54λ aperture

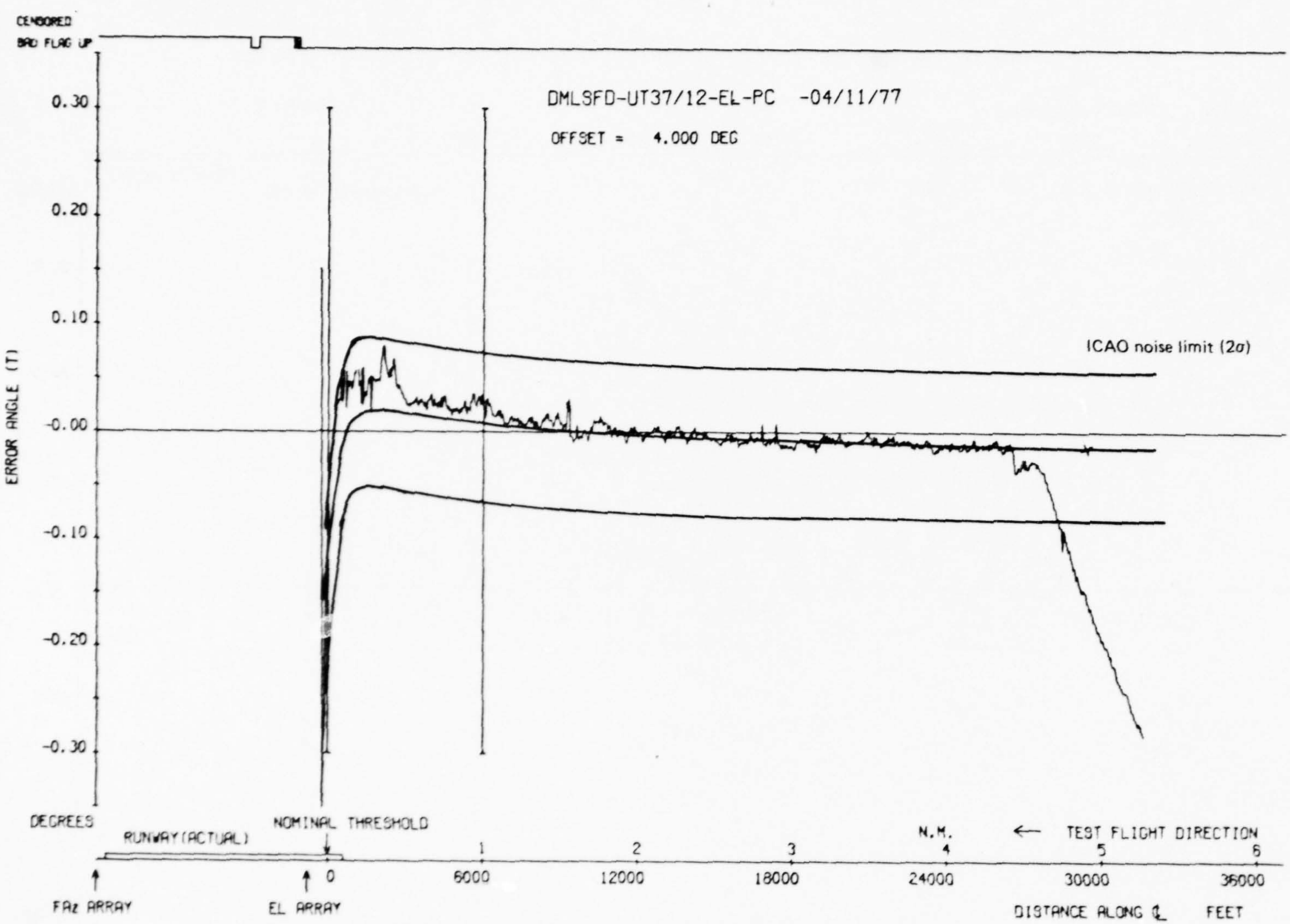


Fig 32b Manchester International Airport – elevation 4 degree approach, 54λ aperture. Telecroscope induced errors censored by hand

Fig 32b

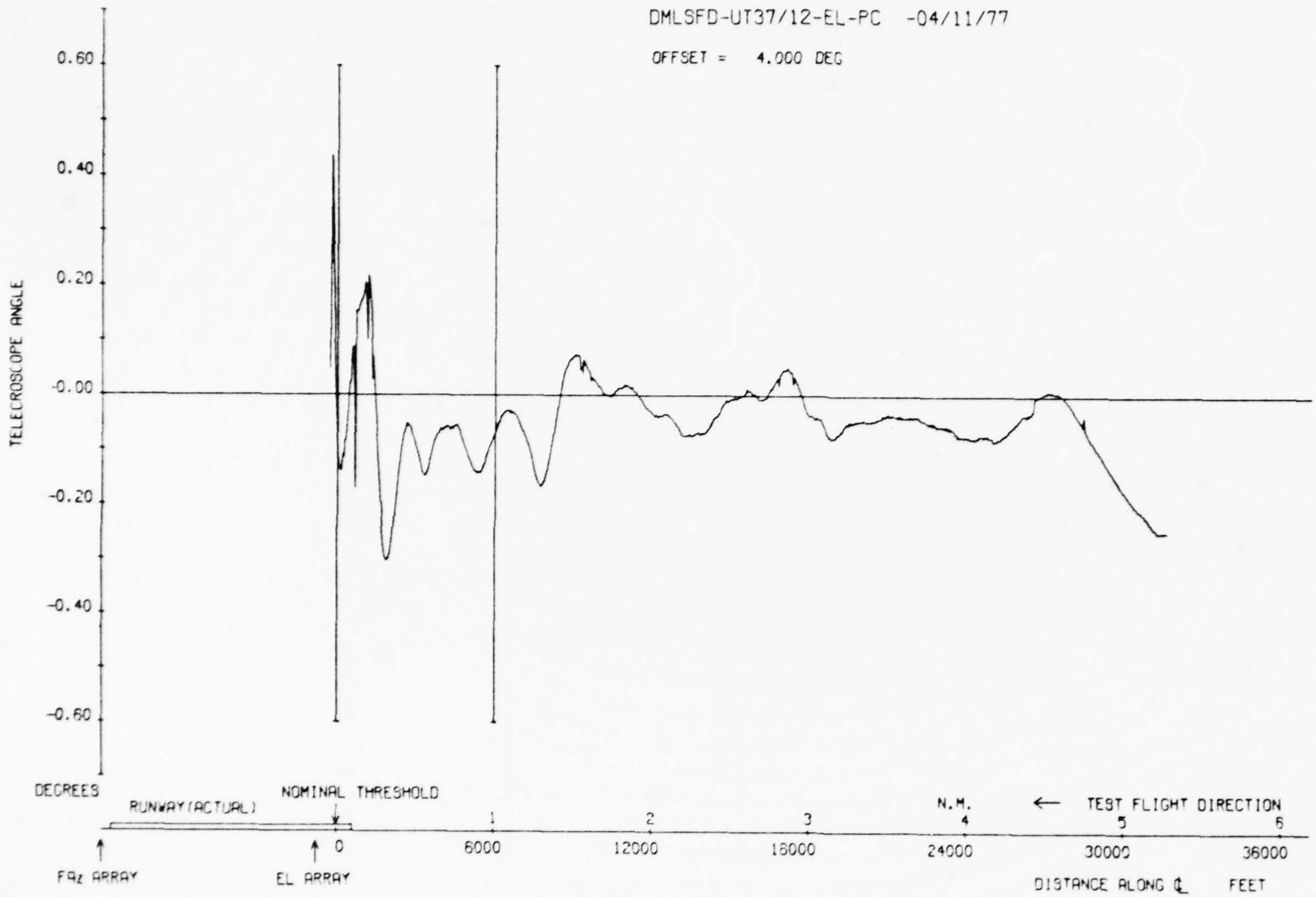


Fig 32c Manchester International Airport – elevation 4 degree approach, 54λ aperture

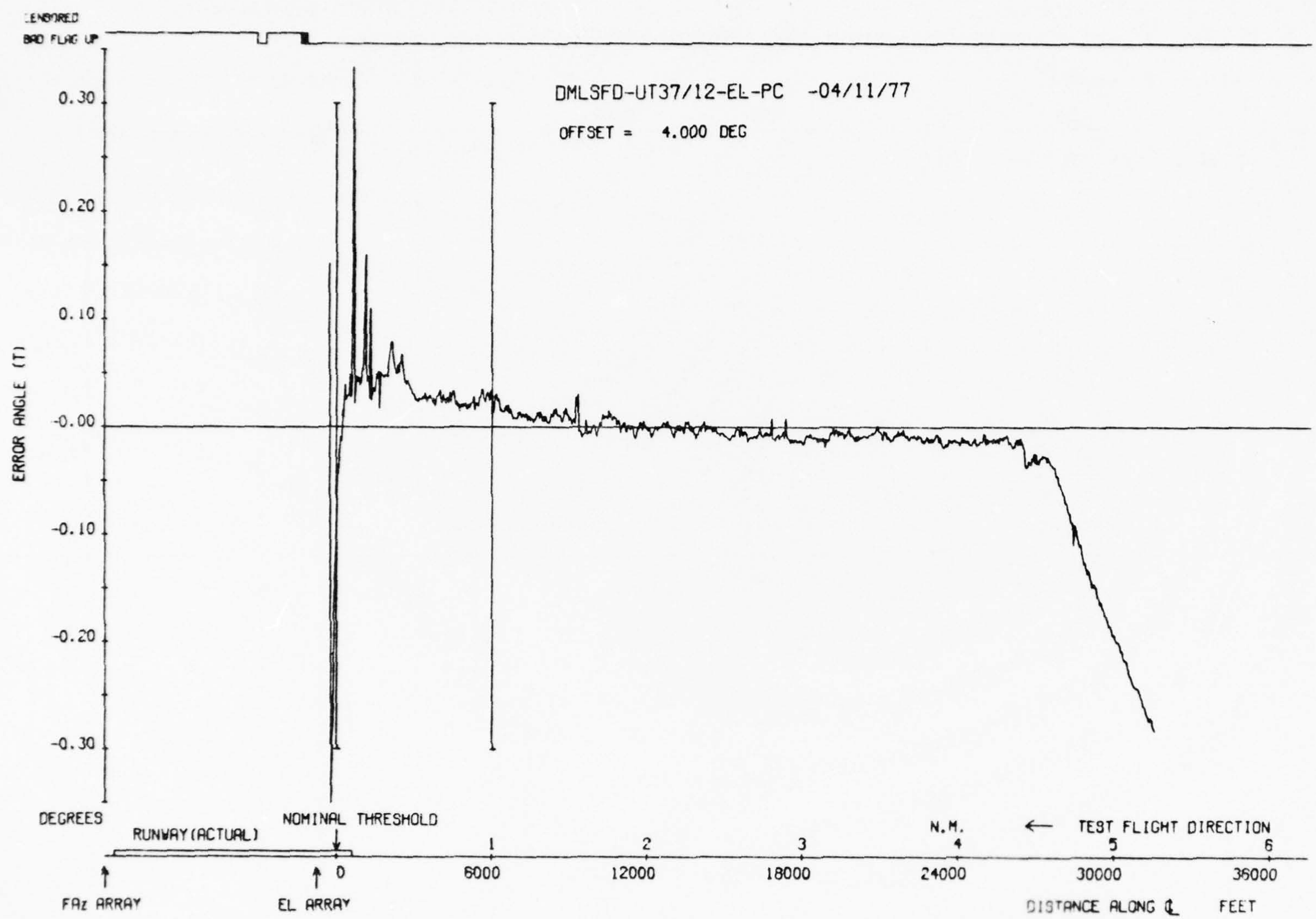


Fig 32d Manchester International Airport – elevation 4 degree approach, 54λ aperture. Telecroscope induced errors uncensored

Fig 32d

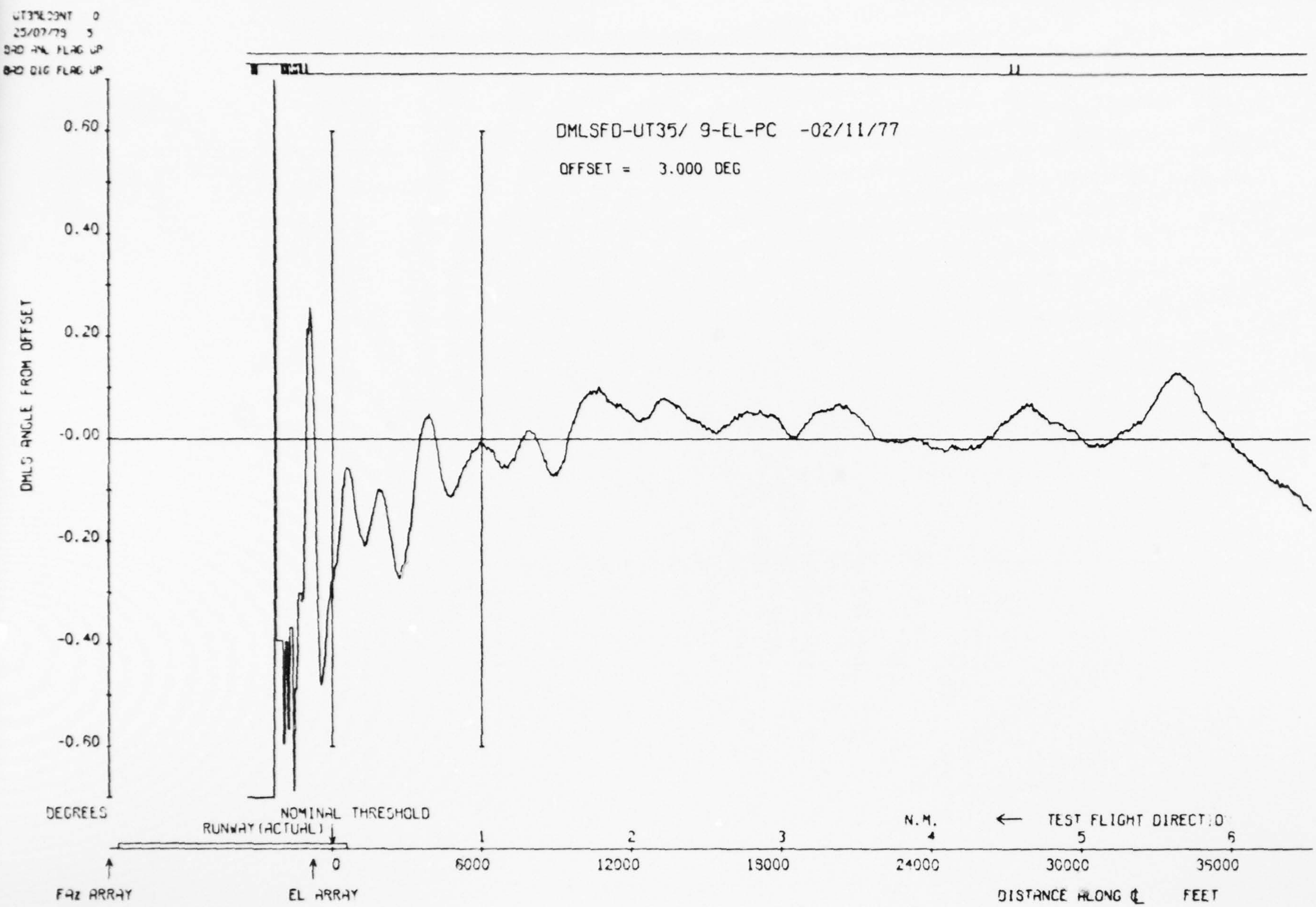


Fig 33a Manchester International Airport – elevation 3 degree approach, 54λ aperture

TR 78144

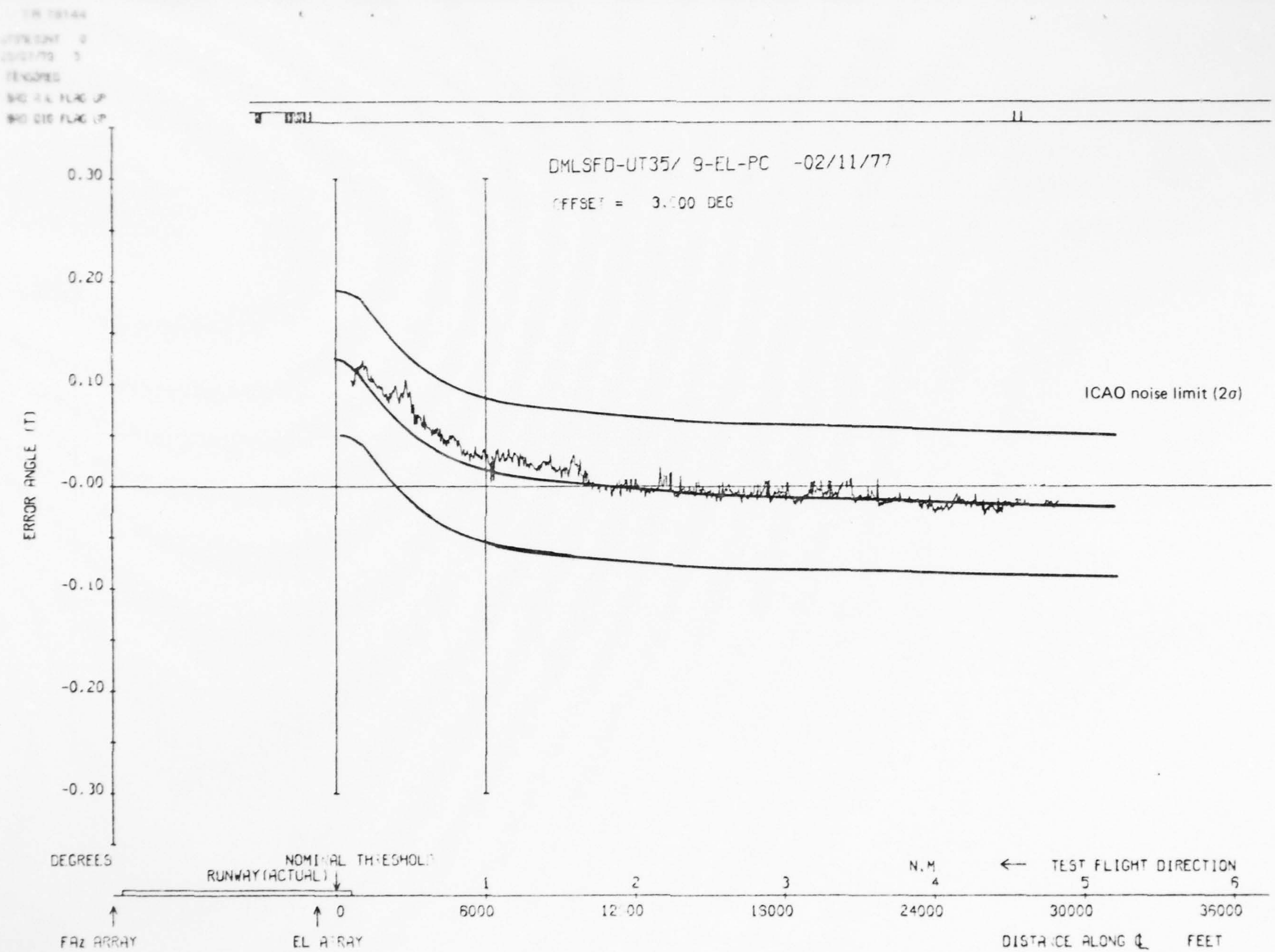


Fig 33b Manchester International Airport – elevation 3 degree approach, 54λ aperture

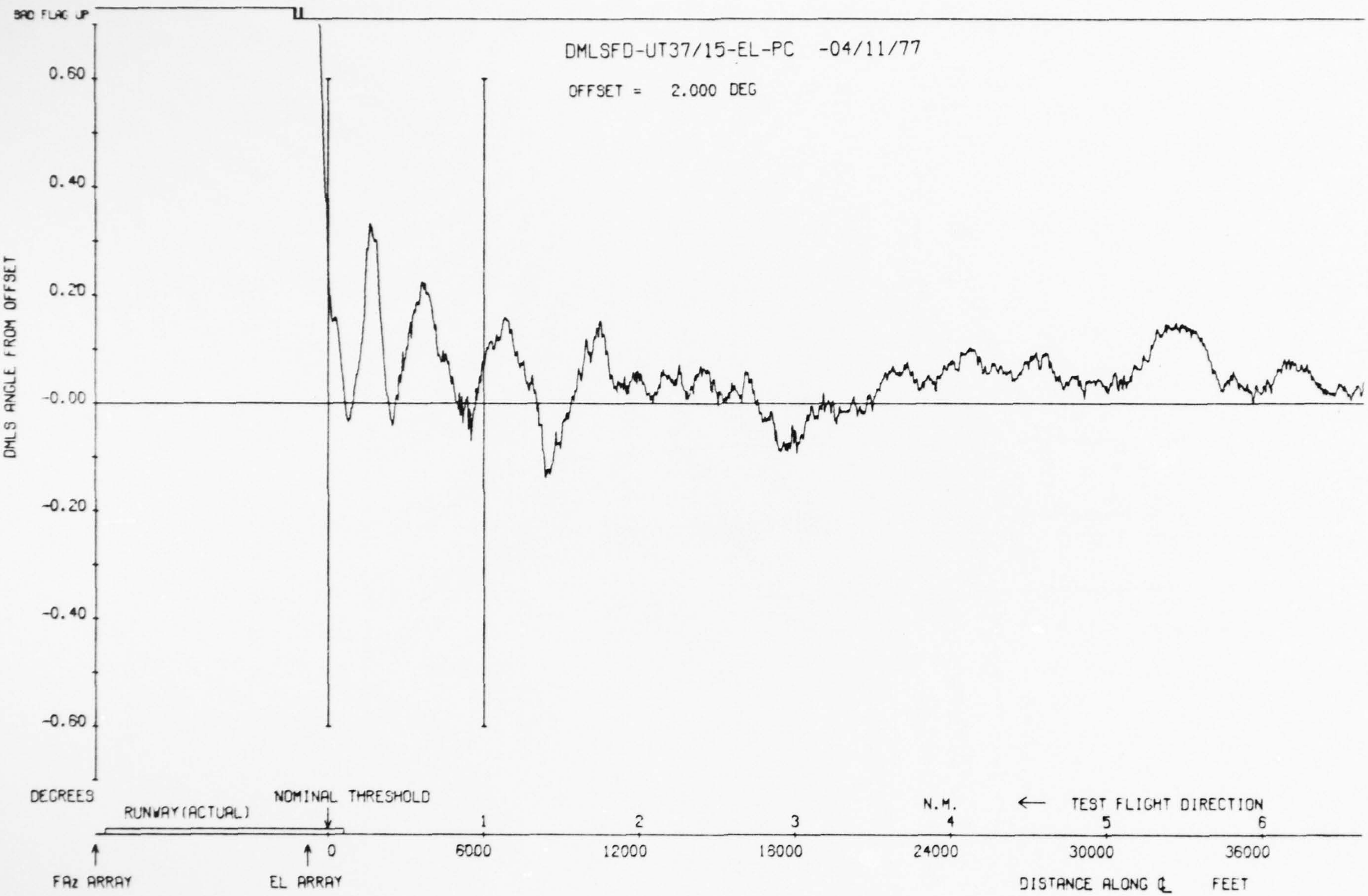


Fig 34a Manchester International Airport – elevation 2 degree approach, 54λ aperture

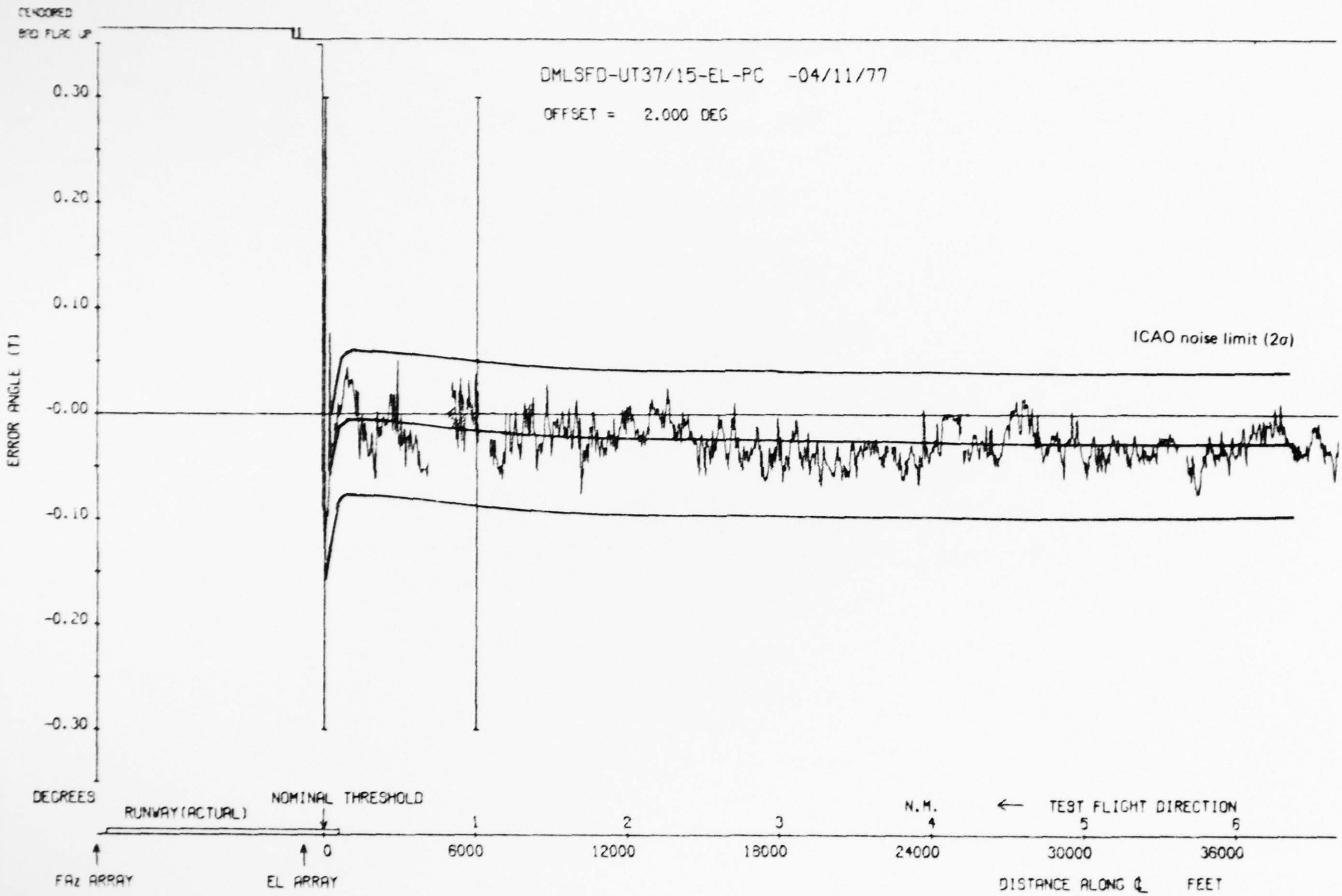


Fig 34b Manchester International Airport – elevation 2 degree approach, 54λ aperture

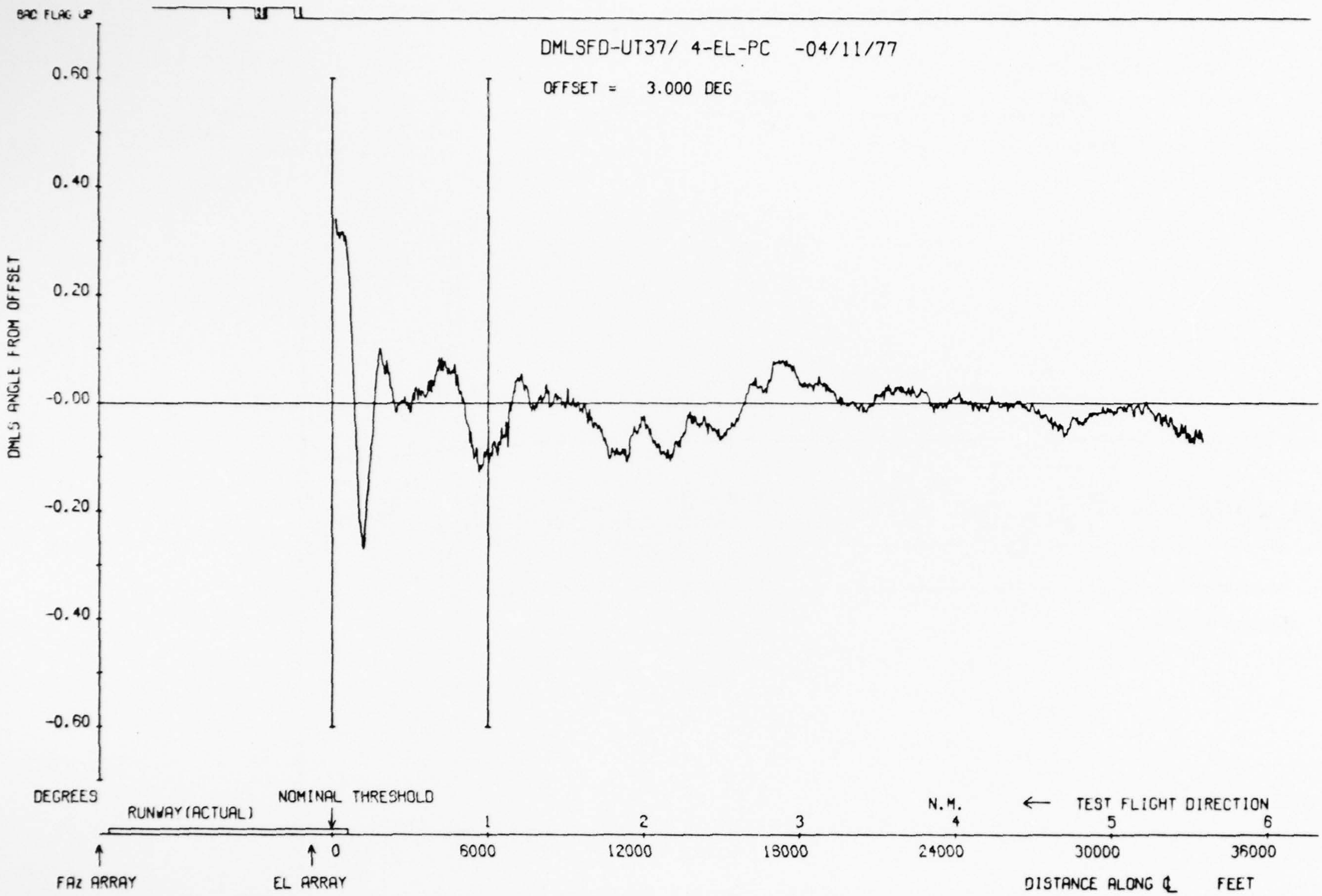


Fig 35a Manchester International Airport – elevation 3 degree approach, 39λ aperture

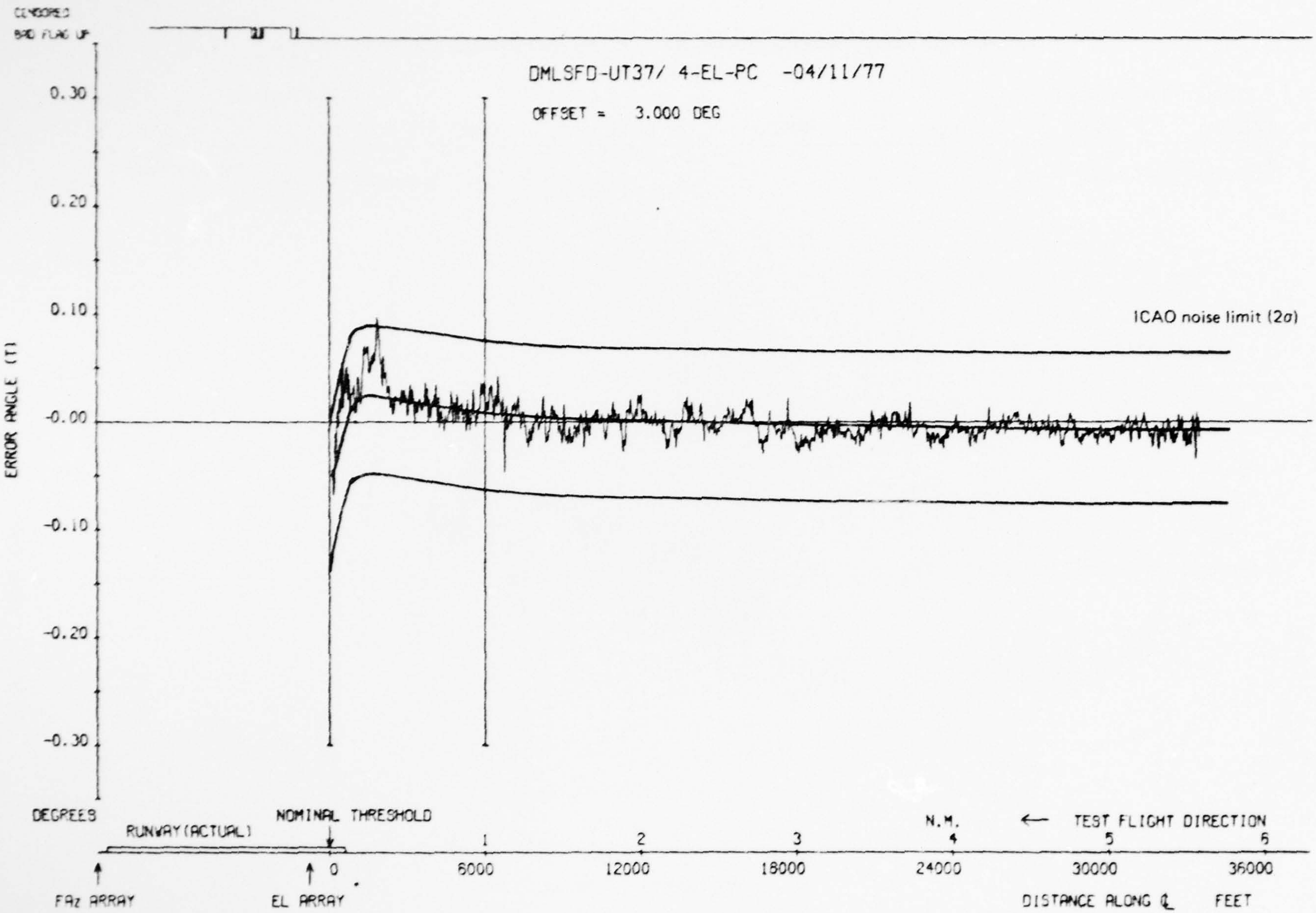


Fig 35b Manchester International Airport – elevation 3 degree approach, 39λ aperture

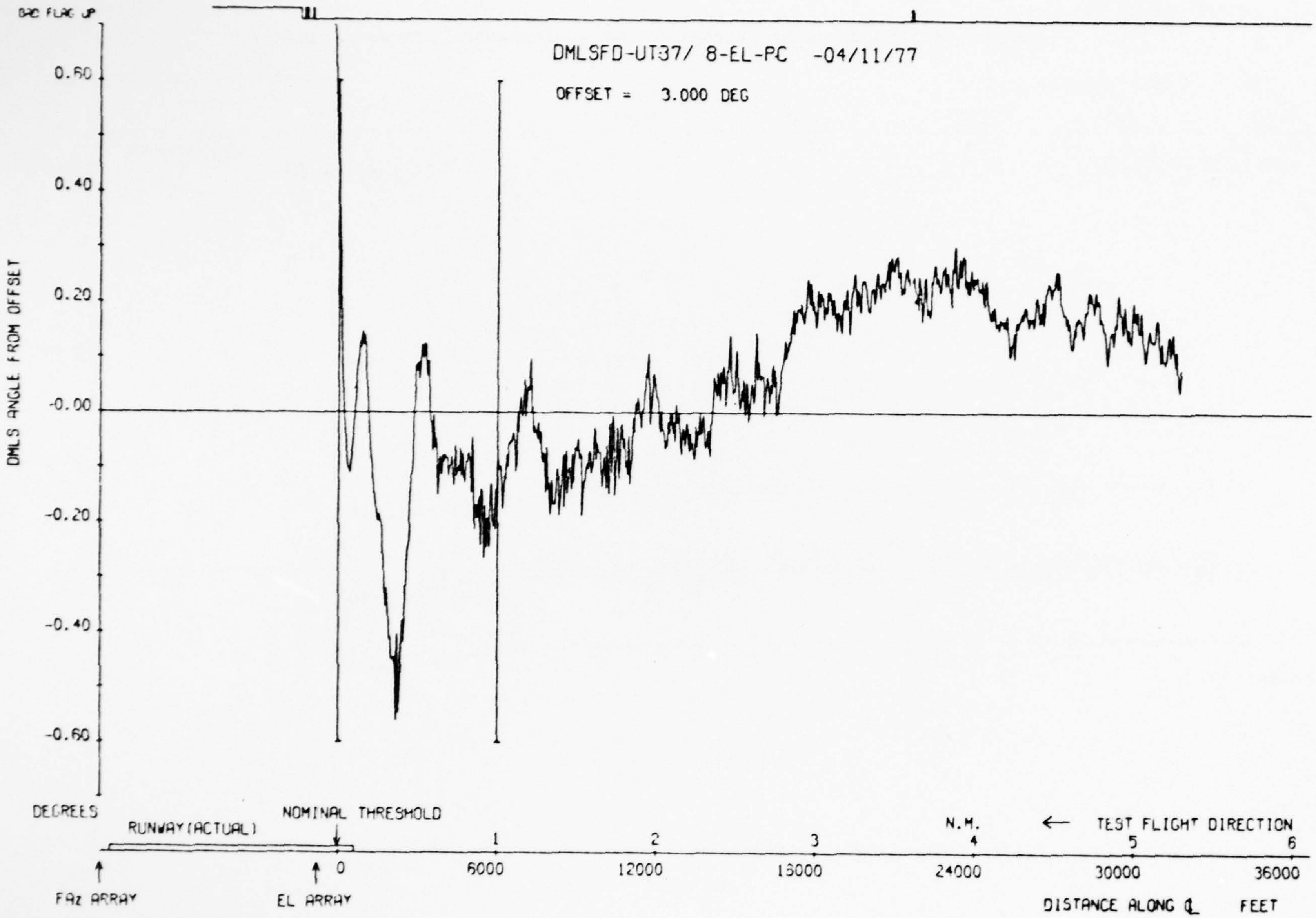


Fig 36a Manchester International Airport – elevation 3 degree approach, 30λ aperture

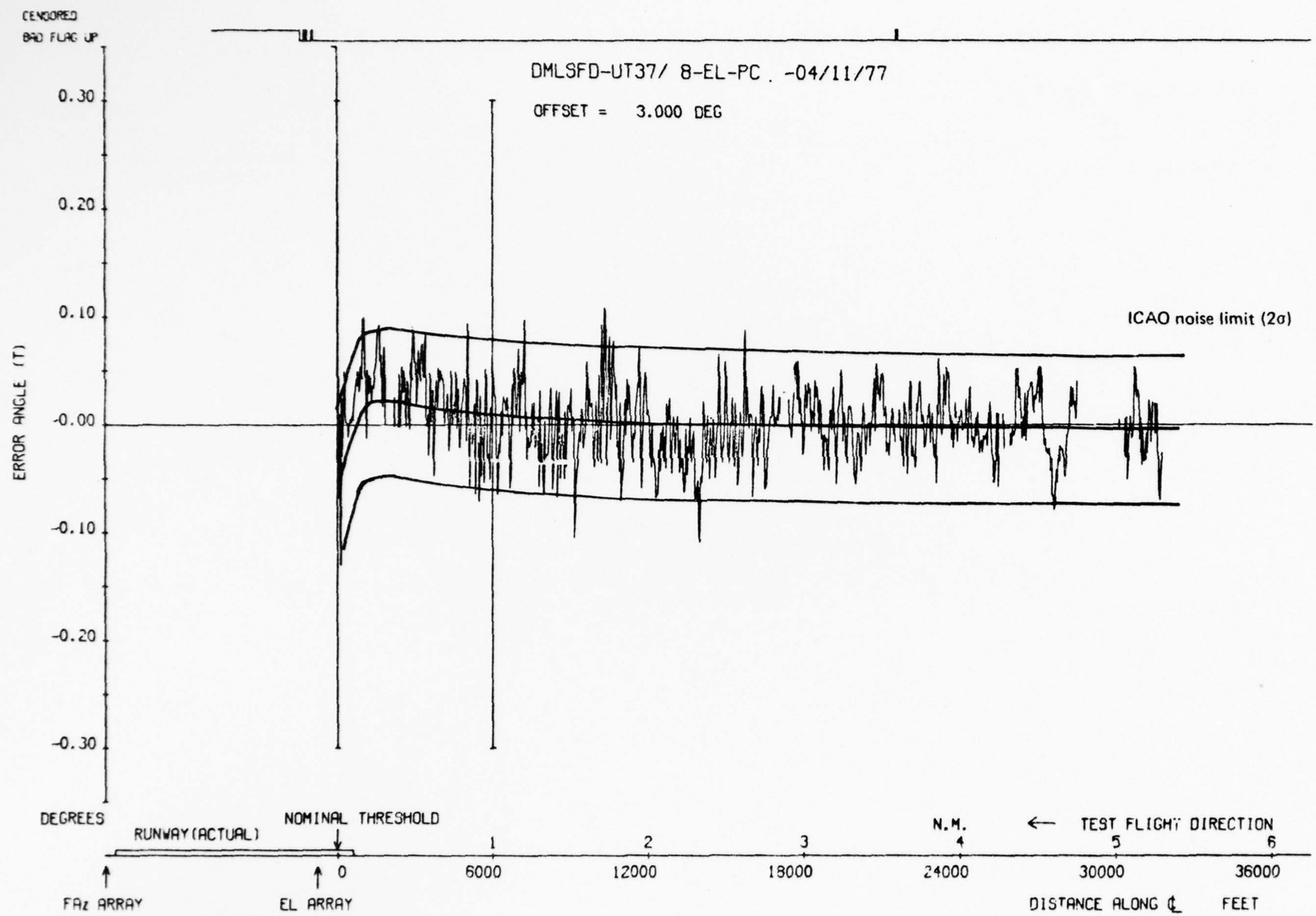


Fig 36b Manchester International Airport – elevation 3 degree approach, 30λ aperture

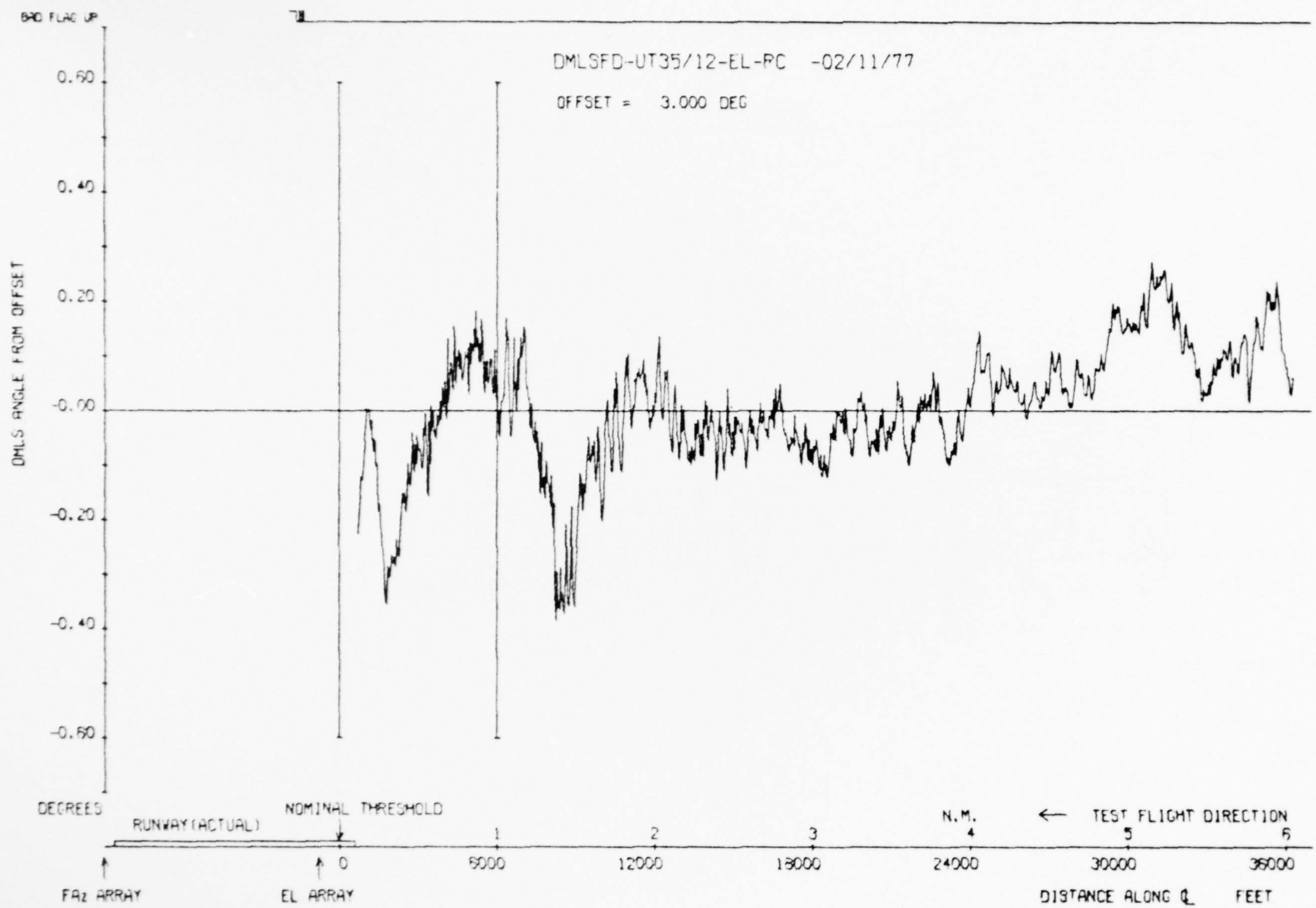


Fig 37a Manchester International Airport – elevation 3 degree approach, 27λ aperture

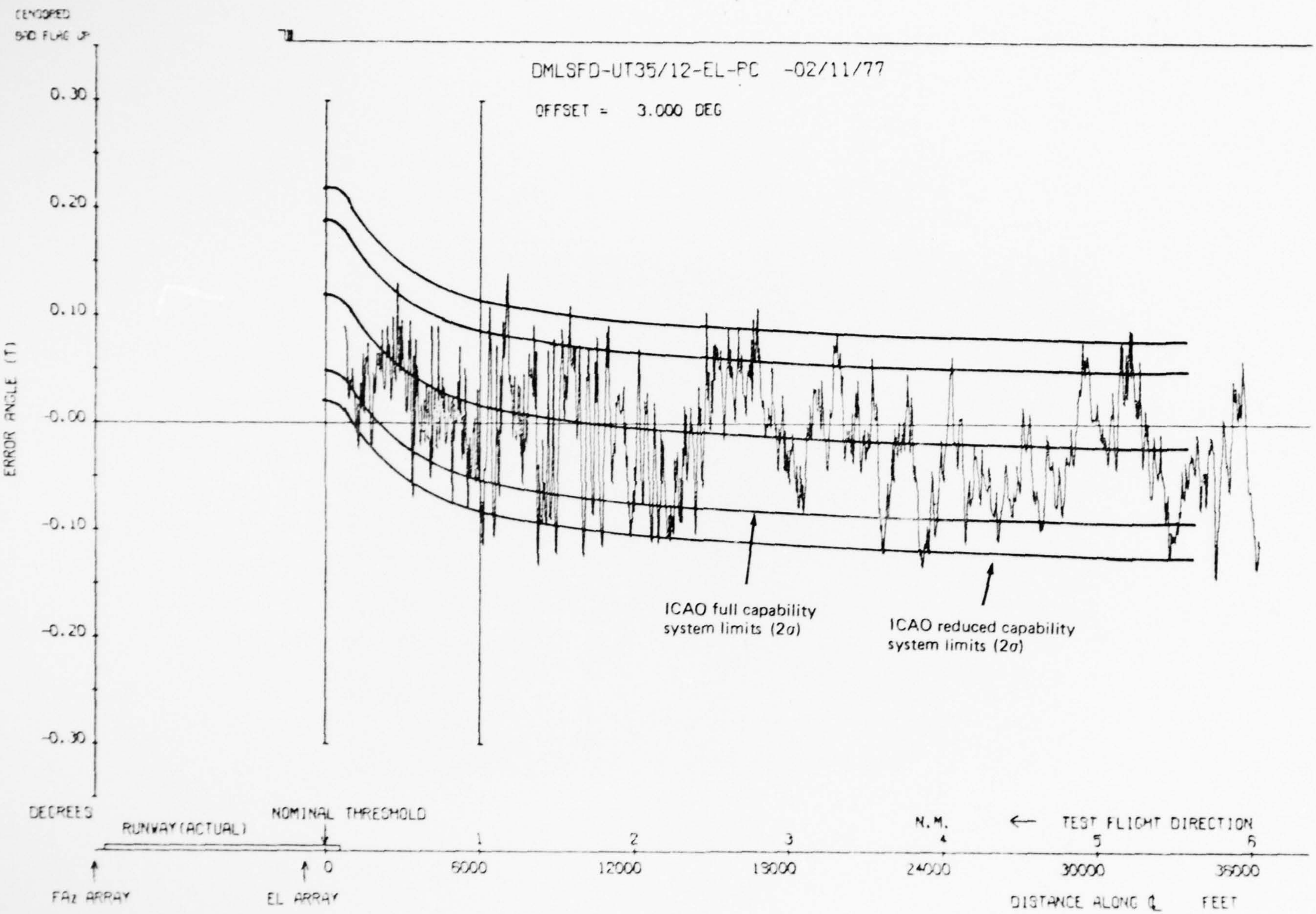


Fig 37b Manchester International Airport – elevation 3 degree approach, 27λ aperture

Fig 38

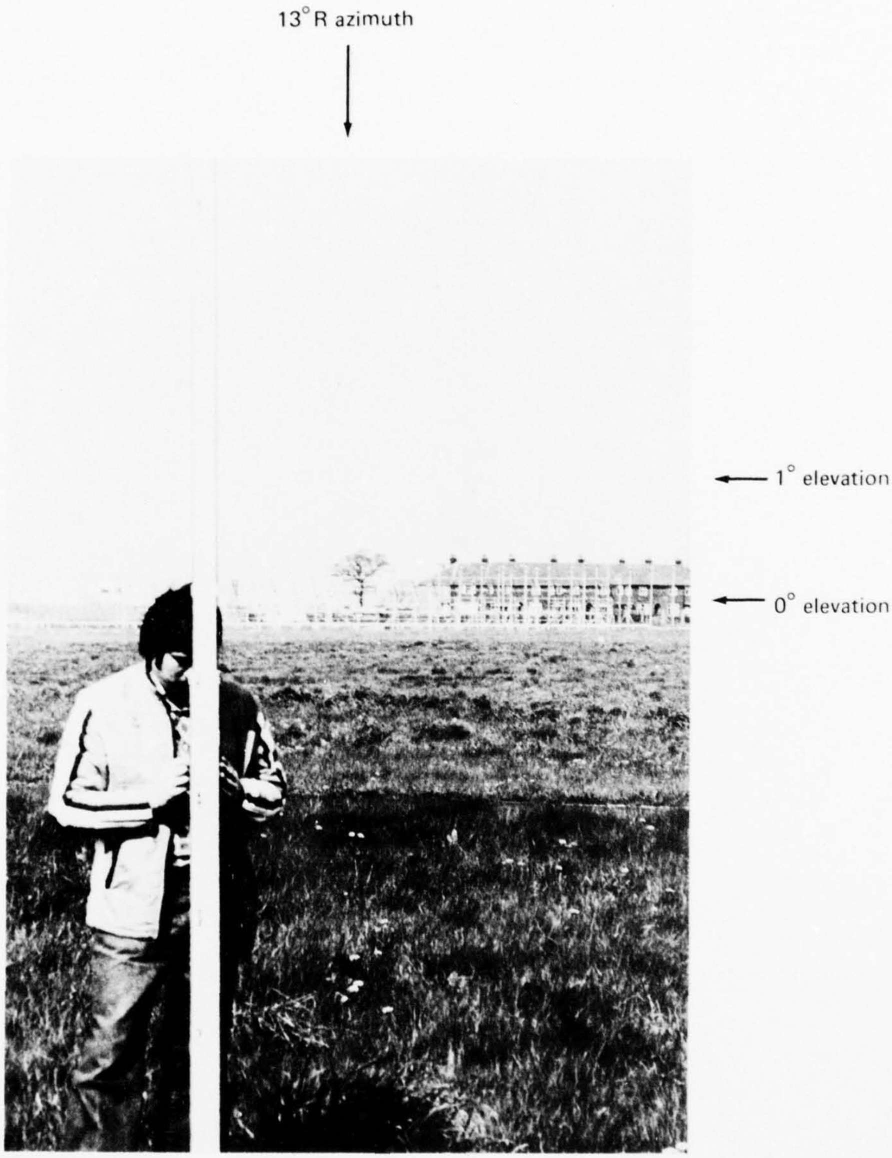


Fig 38 View from elevation array towards centre line

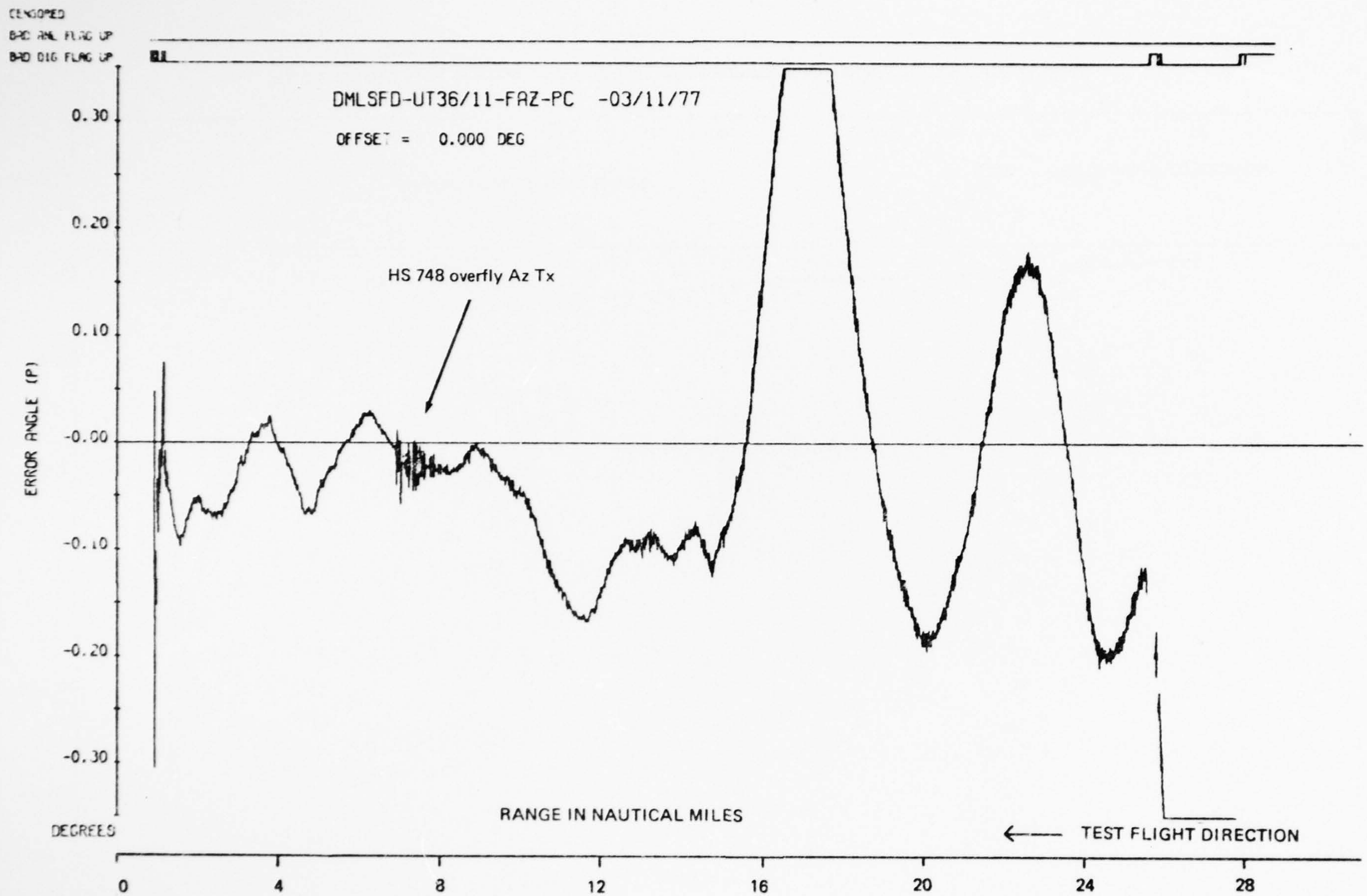


Fig 39 Manchester International Airport – azimuth coverage radial, 54λ aperture, 3500 ft, 0° azimuth

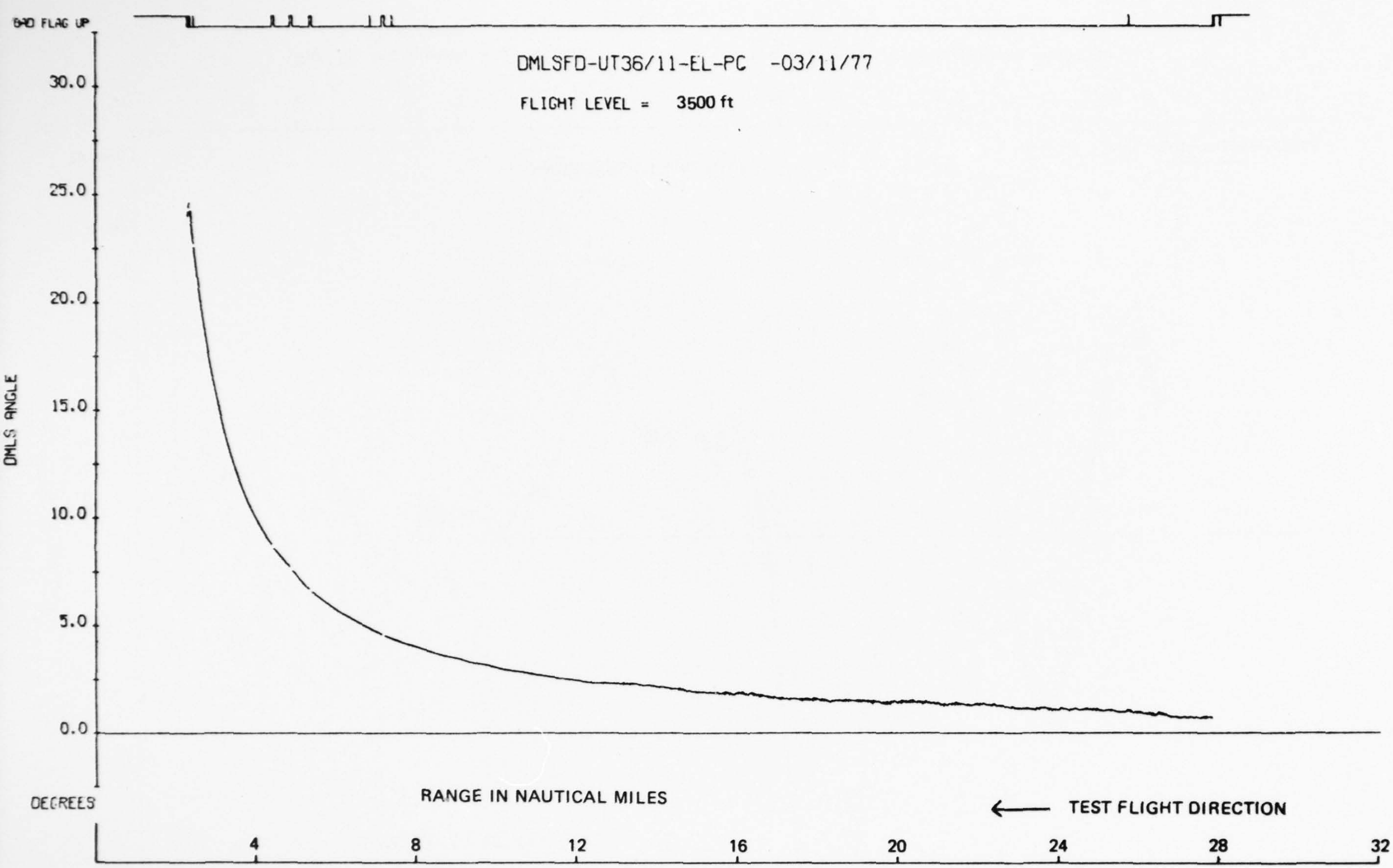


Fig 40 Manchester International Airport – elevation coverage radial, 54λ aperture, 3500 ft, 0° azimuth

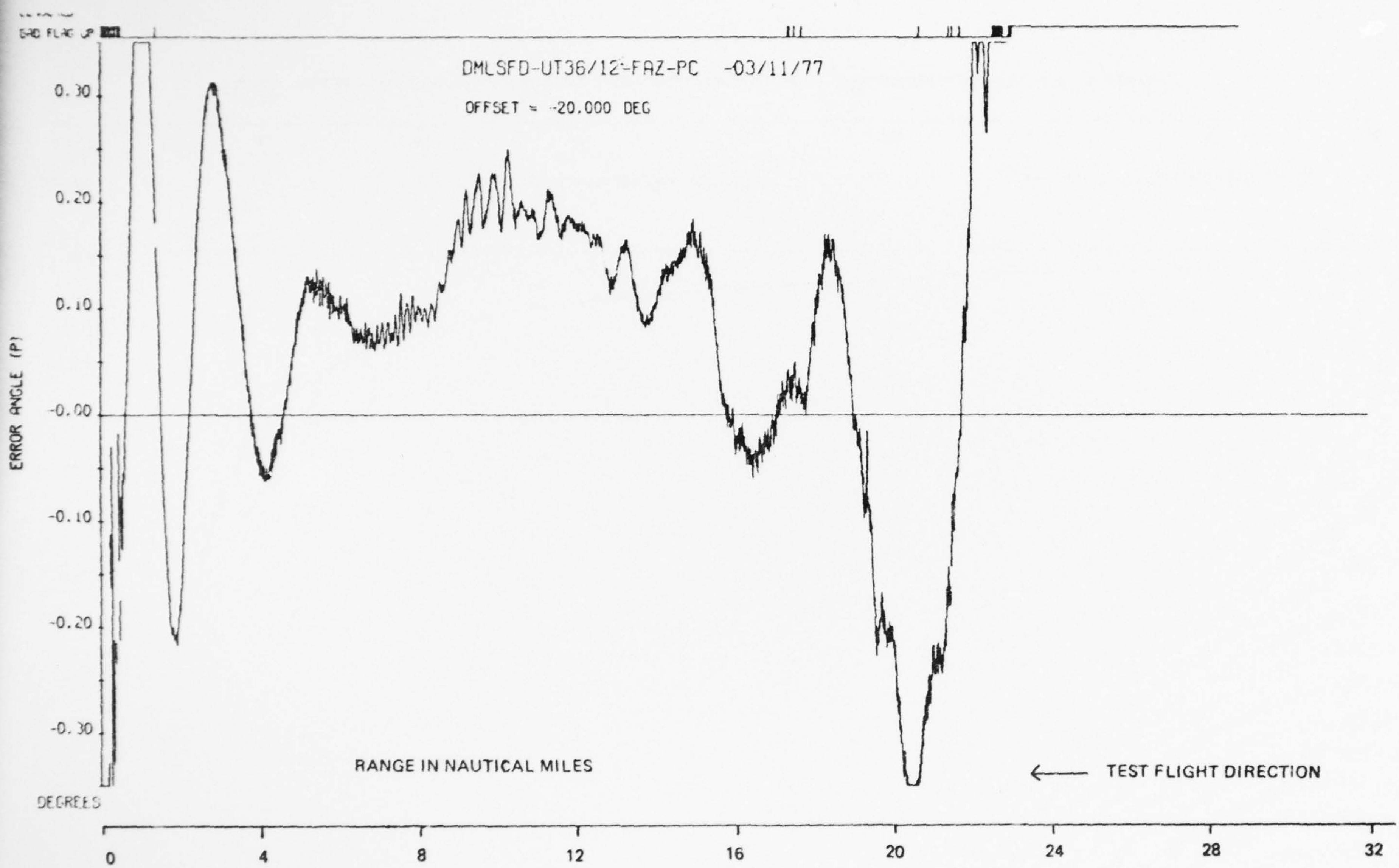


Fig 41 Manchester International Airport – azimuth coverage radial, 54λ aperture, 3500 ft, –20° azimuth

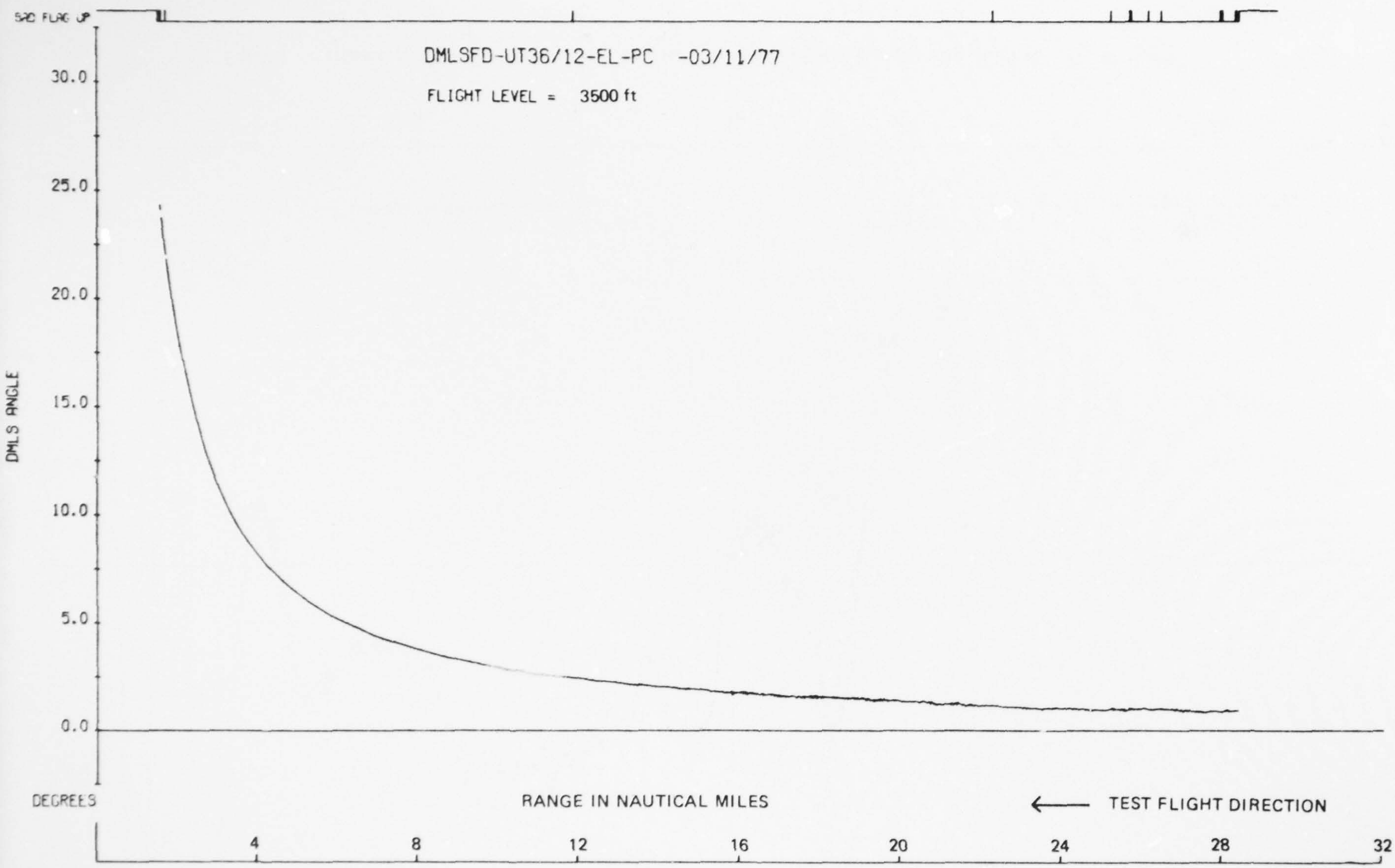


Fig 42 Manchester International Airport – elevation coverage radial, 54λ aperture, 3500 ft, –20° azimuth

AD-A070 291 ROYAL AIRCRAFT ESTABLISHMENT FARNBOROUGH (ENGLAND) F/G 17/7
TRIALS OF THE DOPPLER MICROWAVE LANDING SYSTEM AT MANCHESTER IN--ETC(U)
NOV 78 D WALKER
UNCLASSIFIED RAE-TR-78144 DRIC -BR-67351 NL

2 OF 2
AD A070291

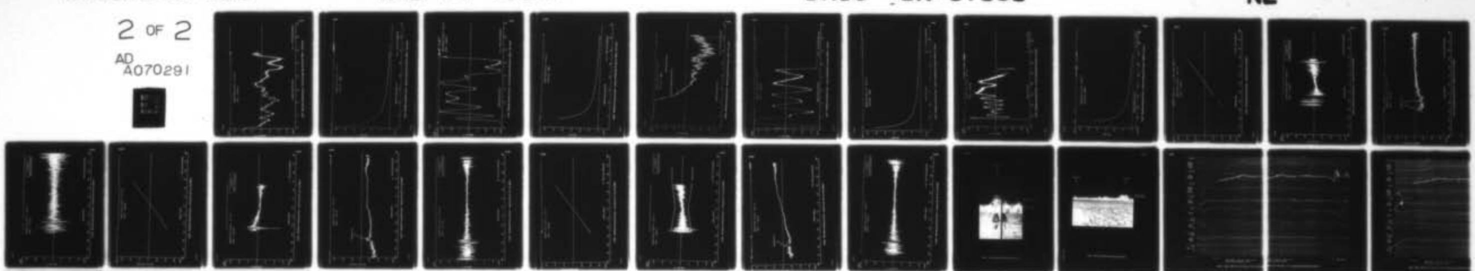

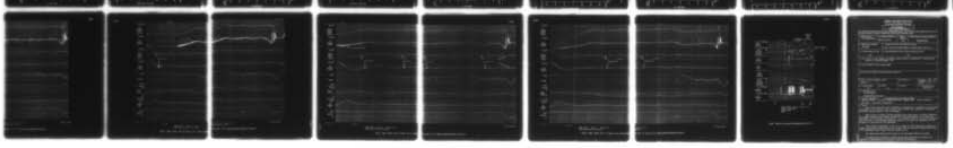

END
DATE FILMED
7-79
DDC

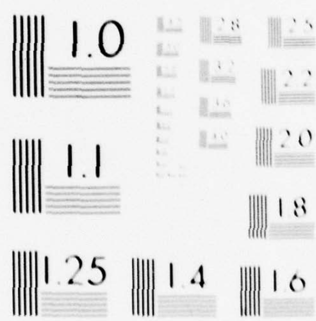


MICROCOPY RESOLUTION TEST CHART
NATIONAL BUREAU OF STANDARDS-1963-A

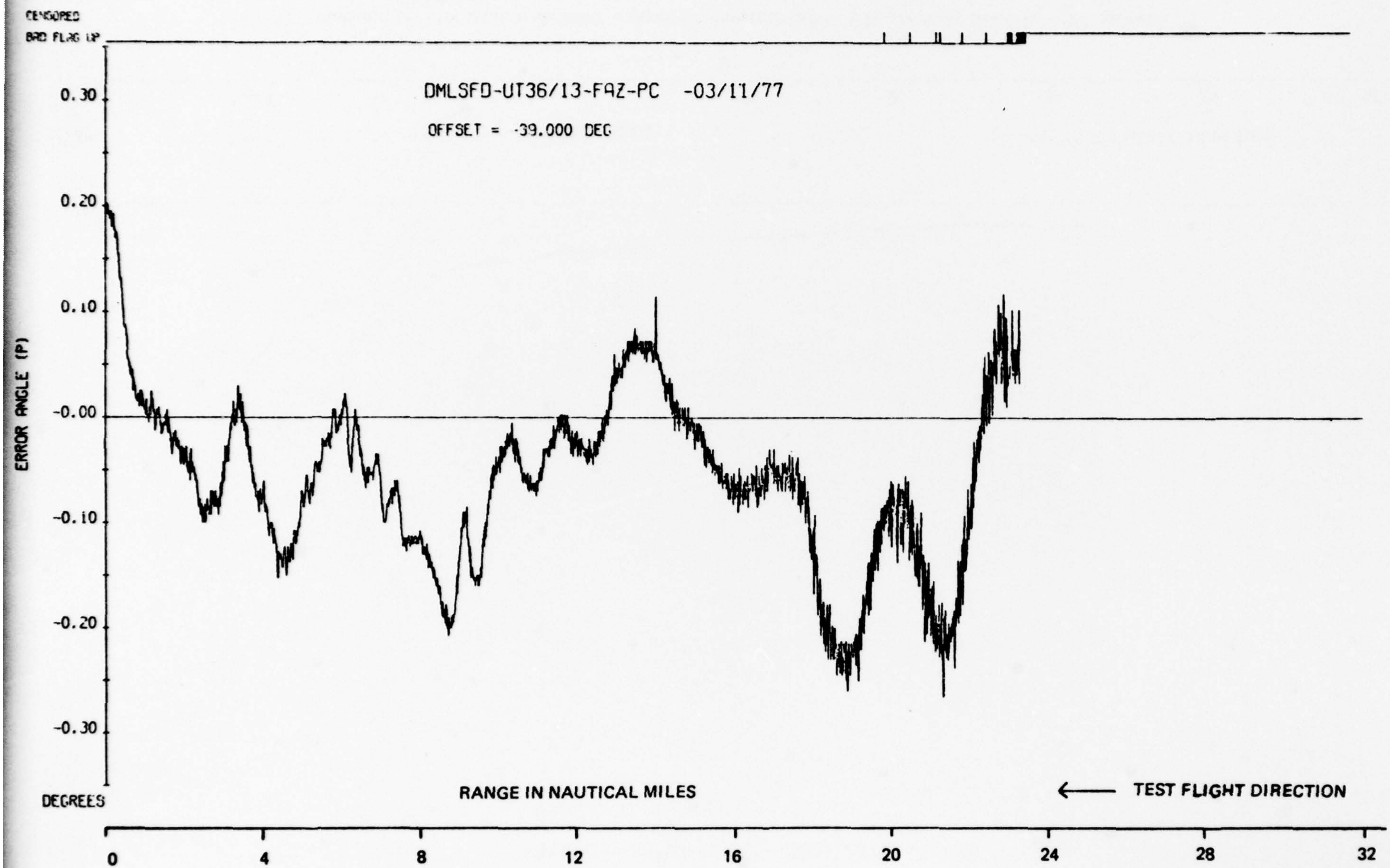


Fig 43 Manchester International Airport – azimuth coverage radial, 54λ aperture, 3500 ft, –39° azimuth

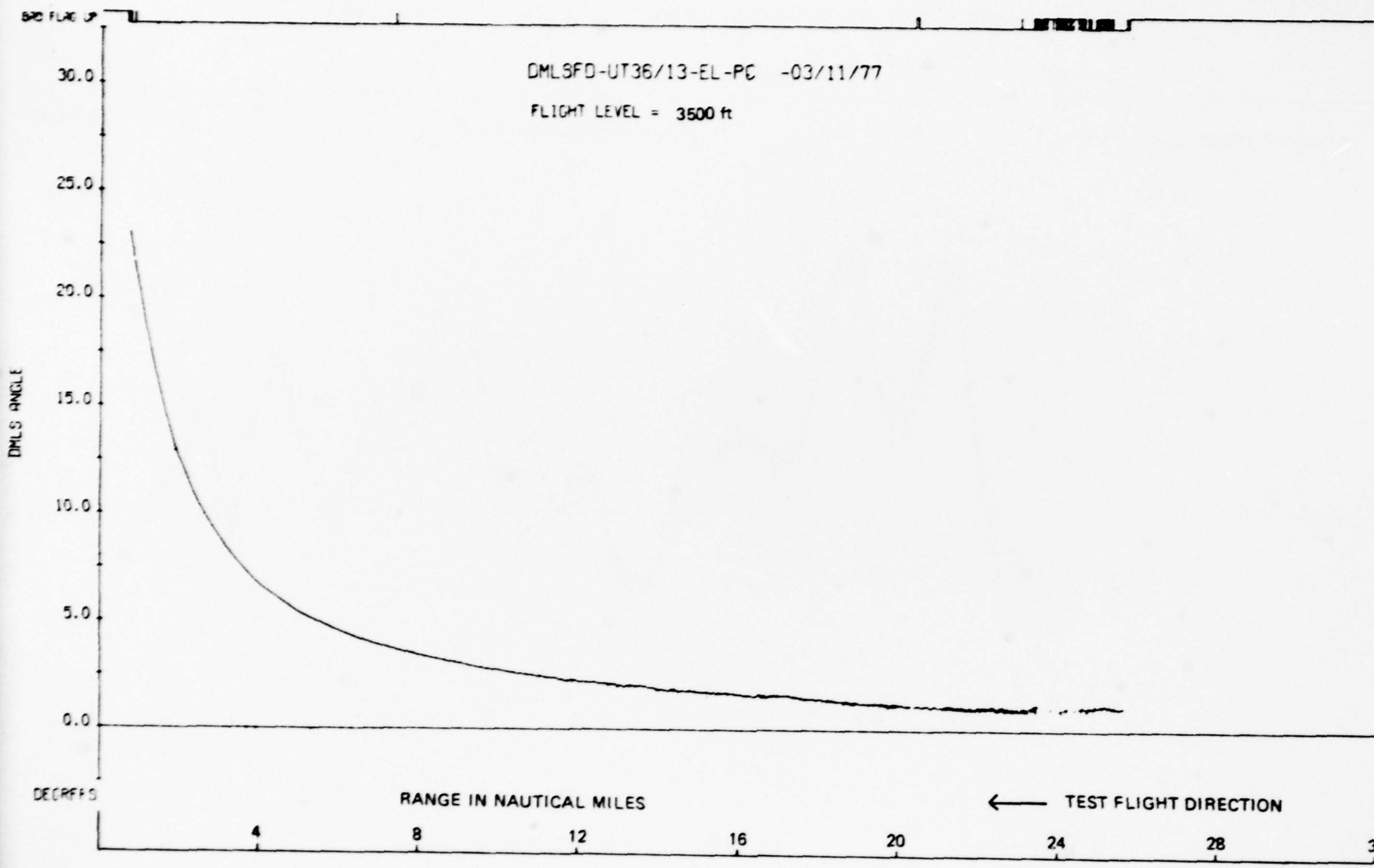


Fig 44 Manchester International Airport – elevation coverage radial, 54λ aperture, 3500 ft, –39° azimuth

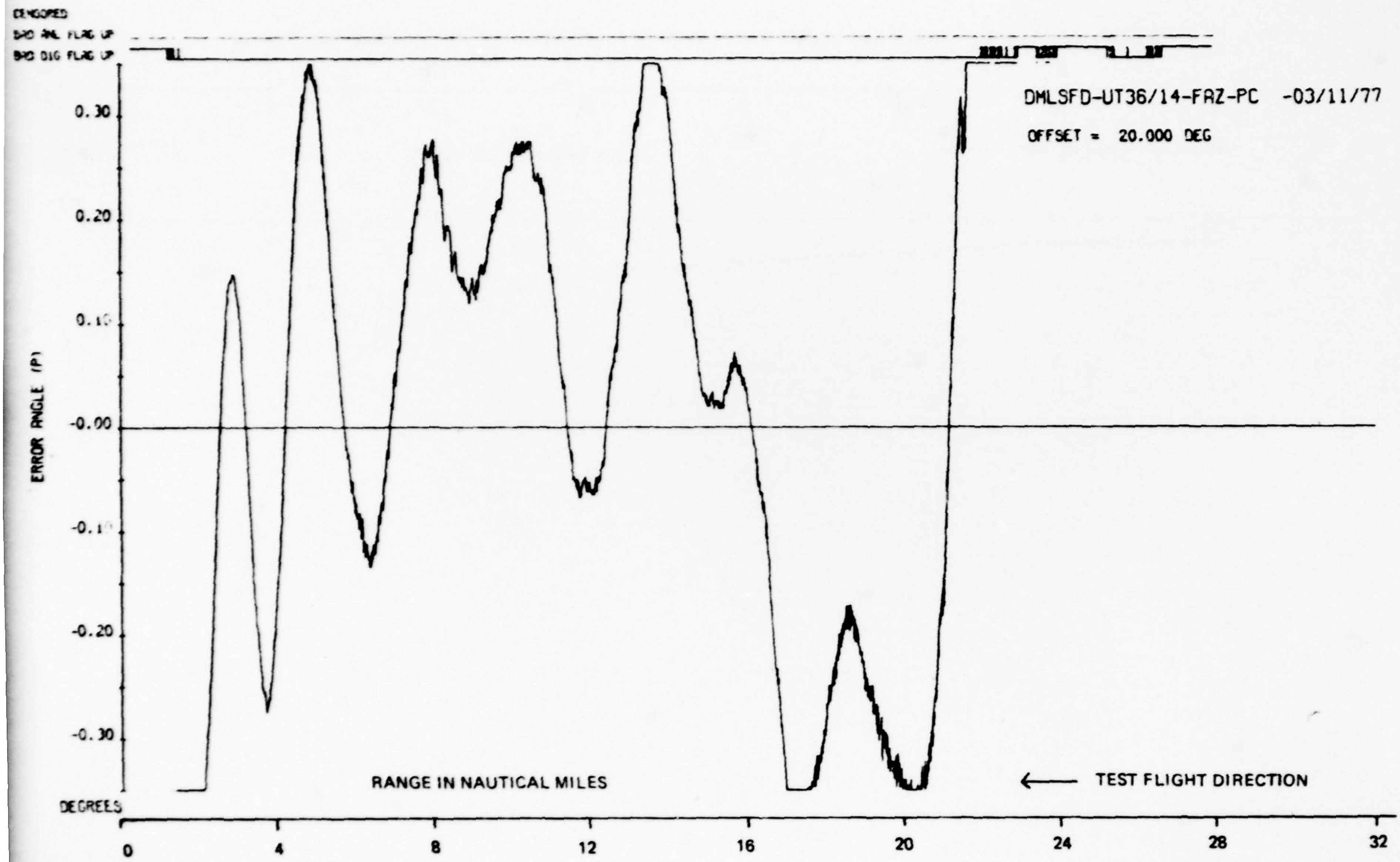


Fig 45 Manchester International Airport – azimuth coverage radial, 54λ aperture, 3500 ft, +20° azimuth

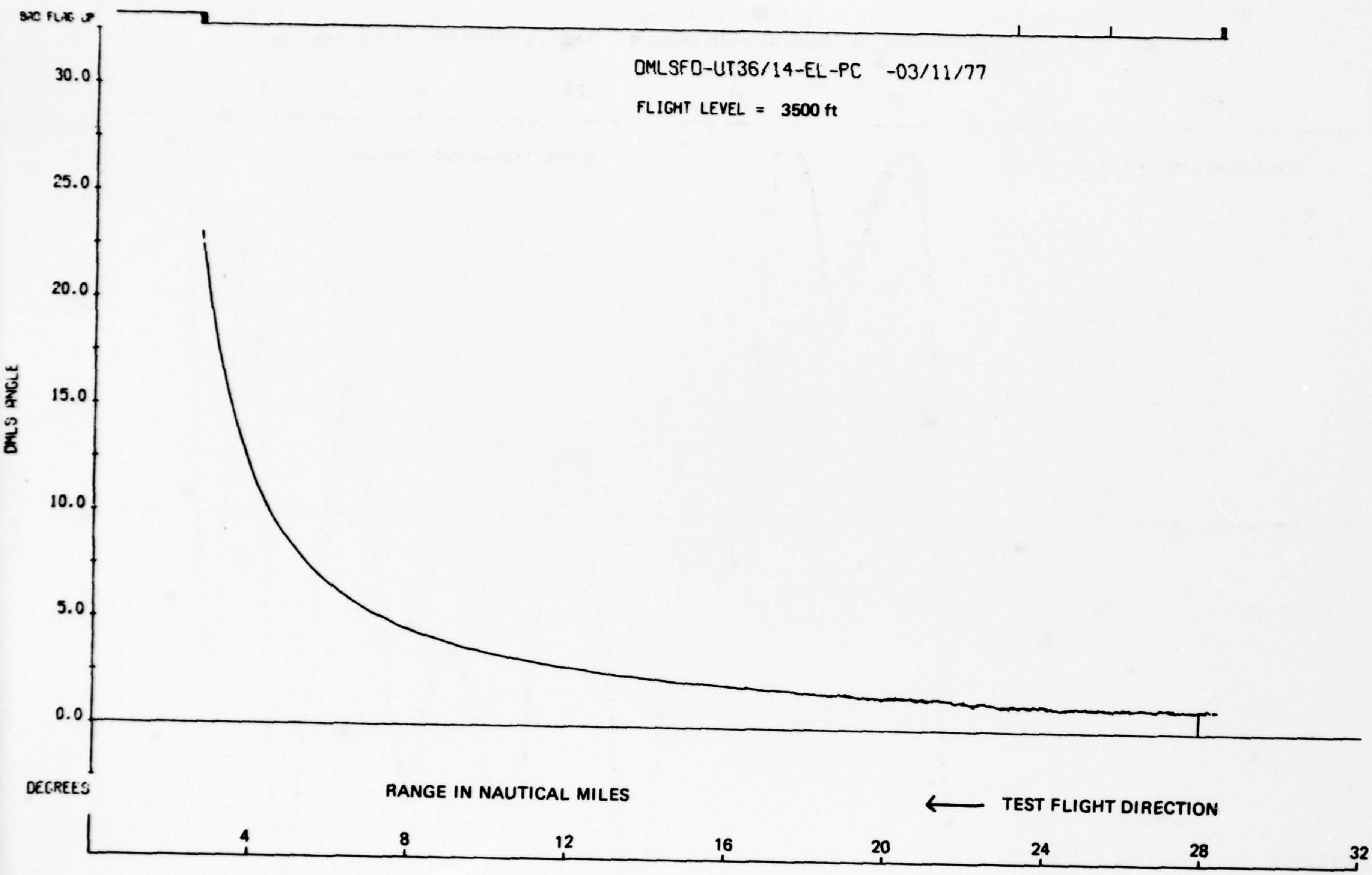


Fig 46a Manchester International Airport – elevation coverage radial, 54λ aperture, 3500 ft, +20° azimuth

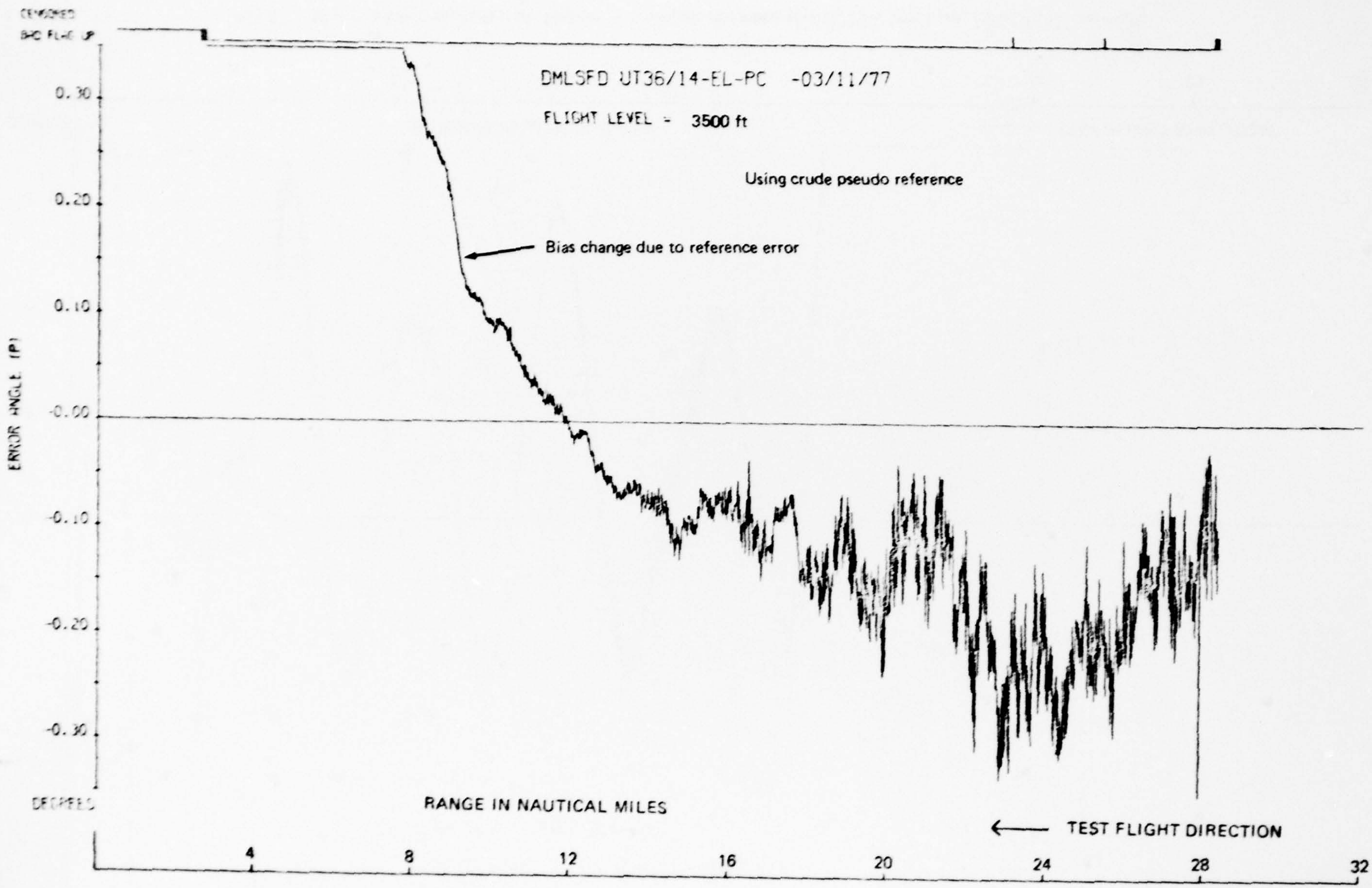


Fig 46b Manchester International Airport – elevation coverage radial, 54λ aperture, 3500 ft, +20° azimuth

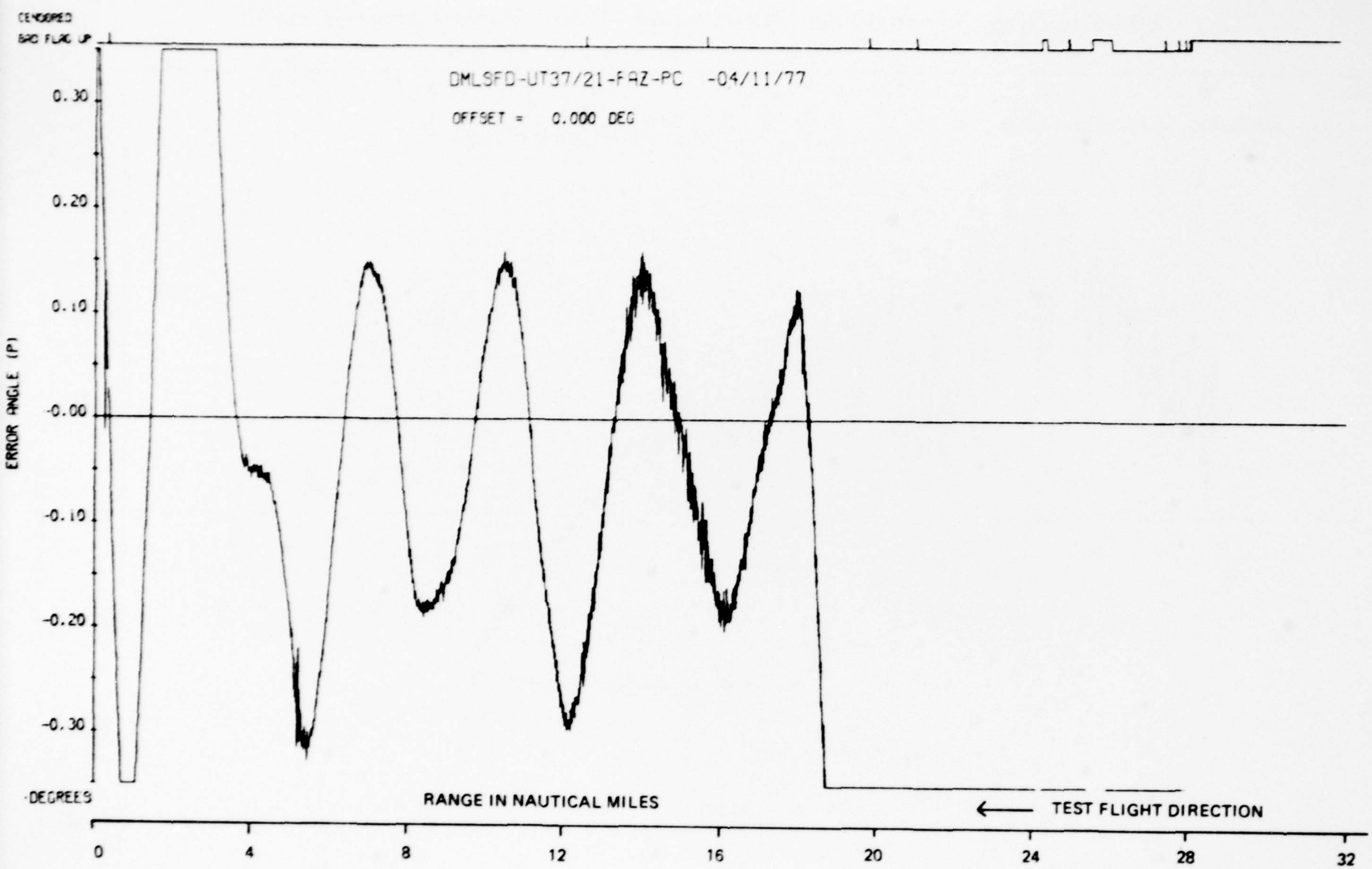


Fig 47 Manchester International Airport – azimuth coverage radial, 27λ aperture, 3000 ft, 0° azimuth

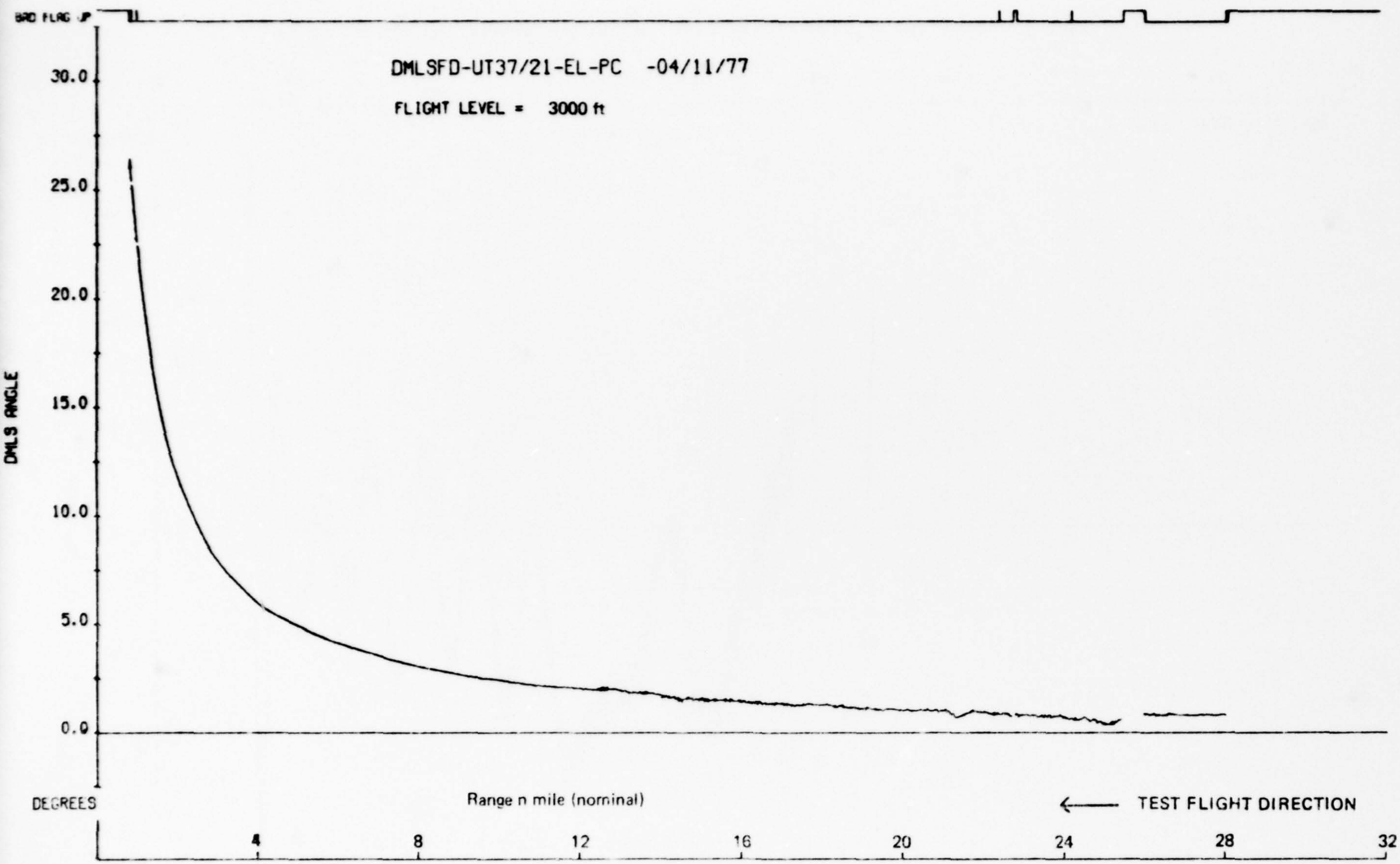


Fig 48 Manchester International Airport – elevation coverage radial, 54λ aperture, 3000 ft, 0° azimuth

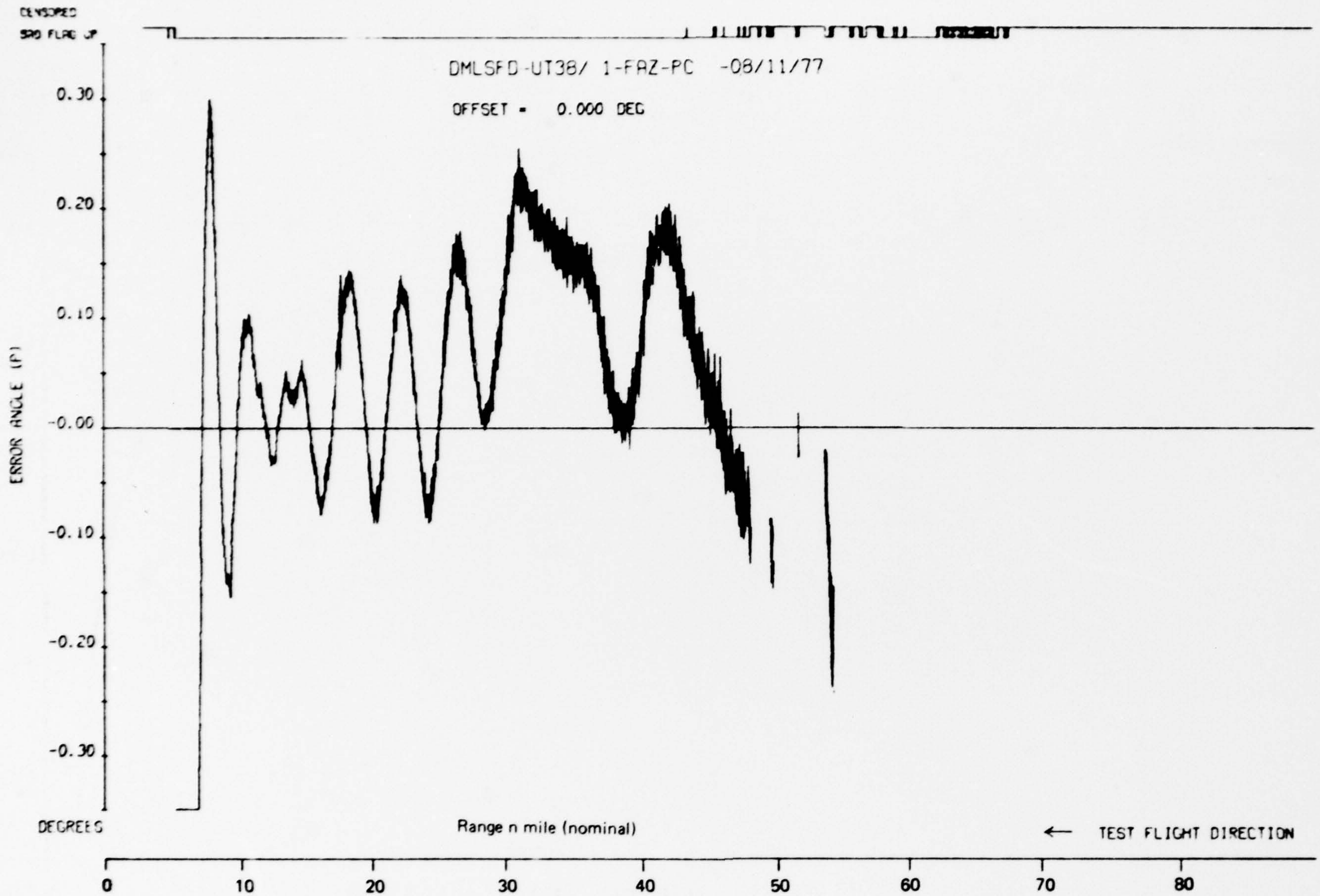


Fig 49 Manchester International Airport – azimuth coverage radial, 54λ aperture, 0° azimuth

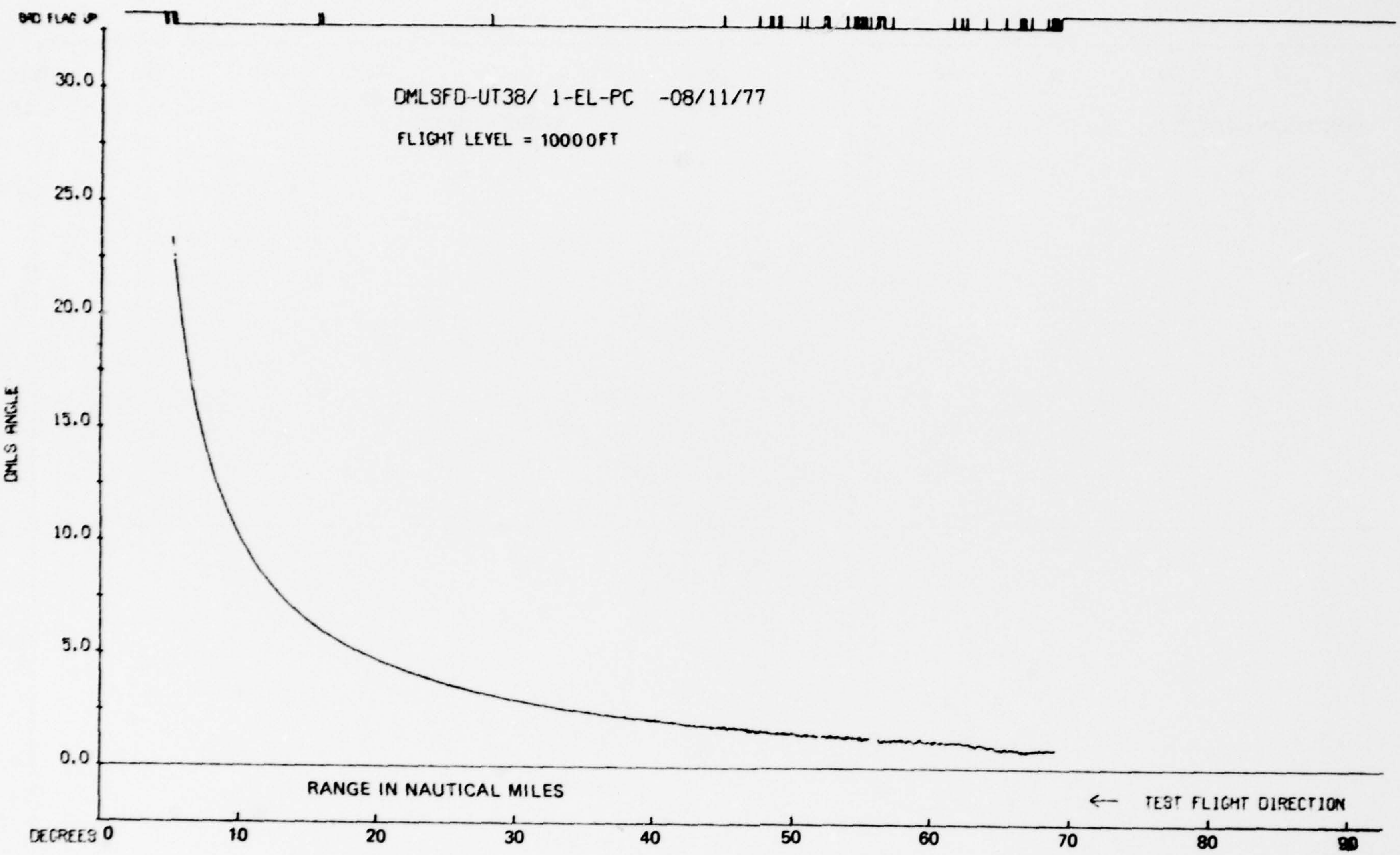


Fig 50 Manchester International Airport – elevation coverage radial, 54λ aperture, 10000 ft, 0° azimuth

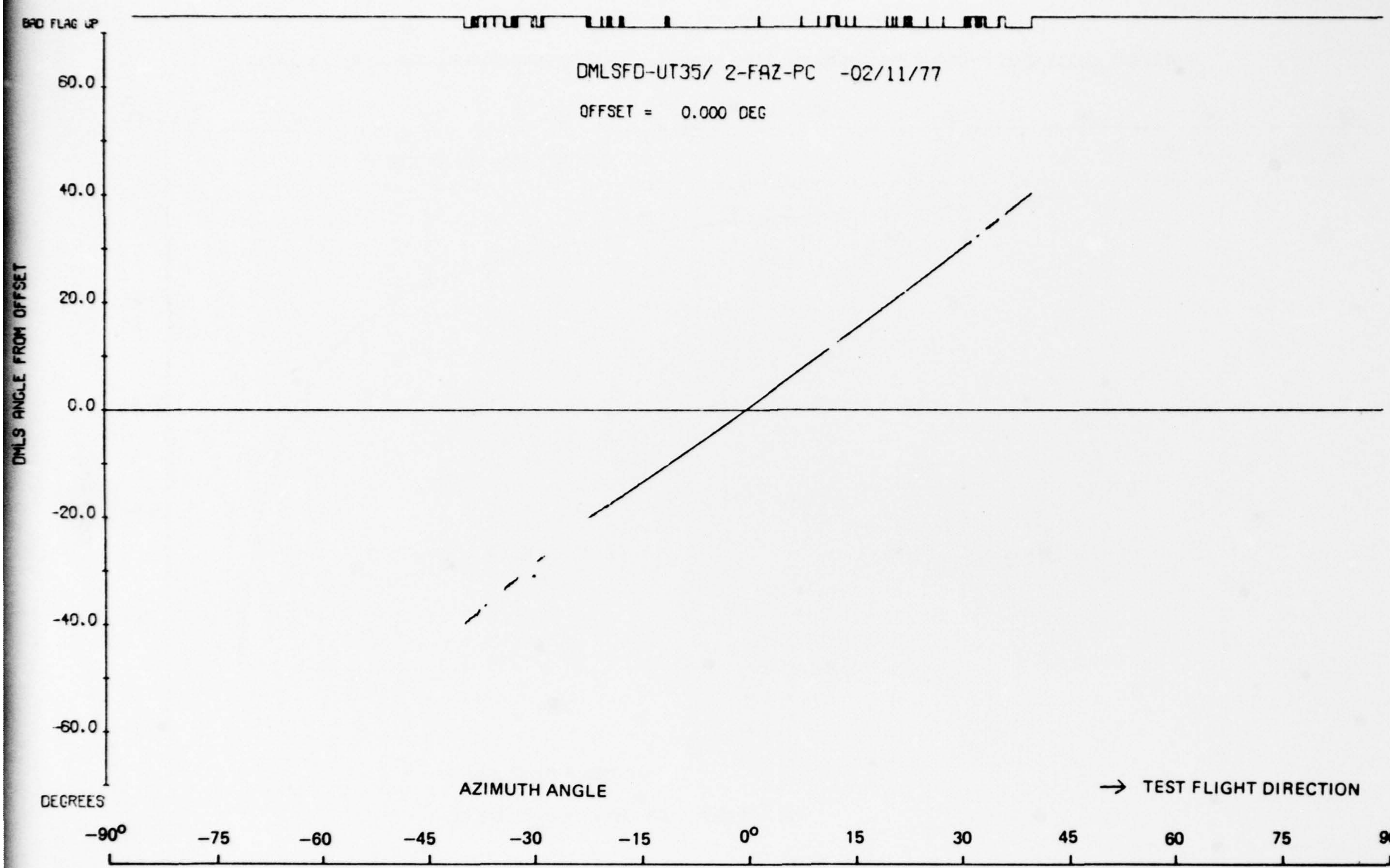


Fig 51a Manchester International Airport – azimuth orbit, 20 n mile, 3000 ft

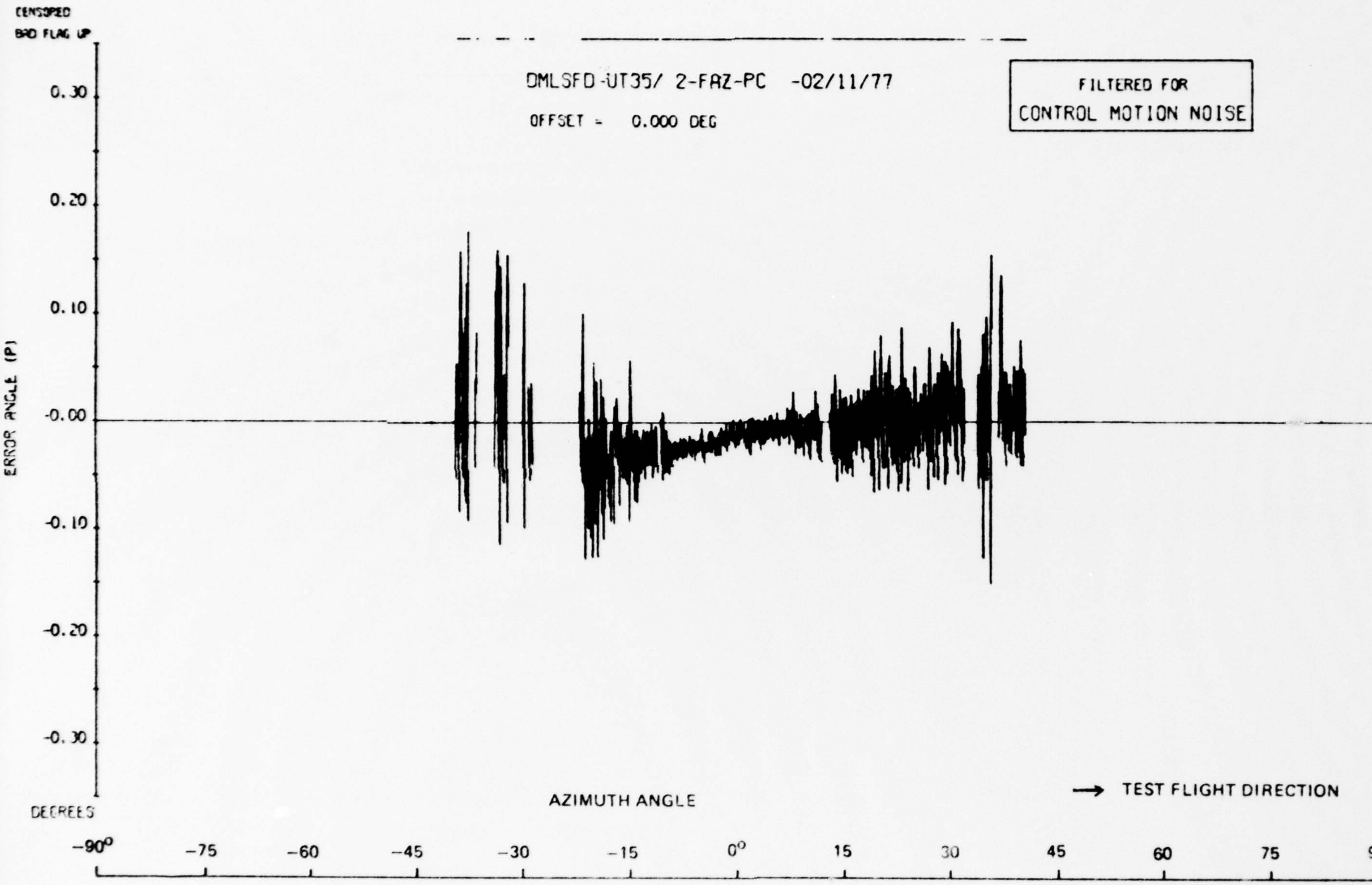


Fig 51b Manchester International Airport – azimuth orbit, 20 n mile, 3000 ft

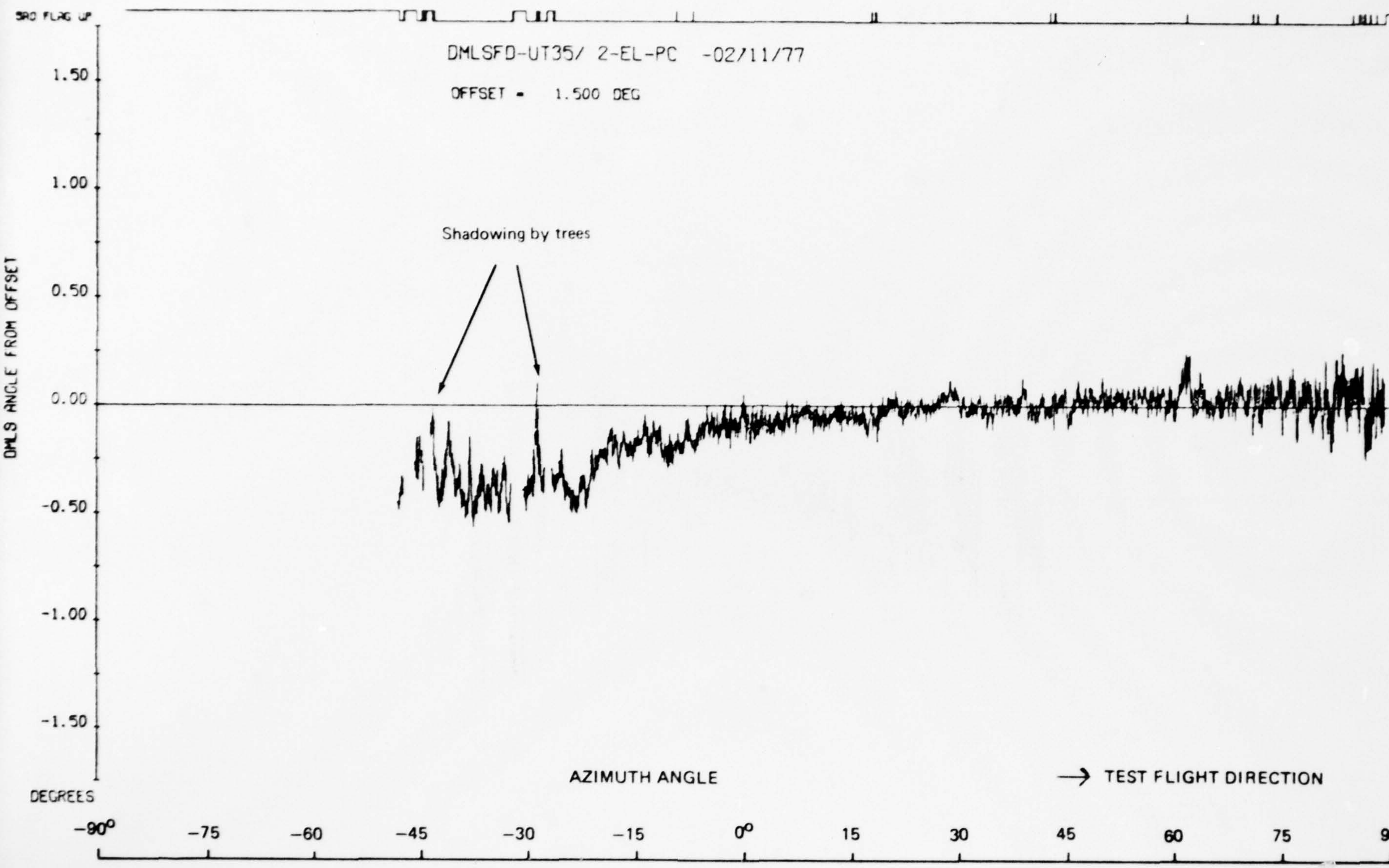


Fig 52a Manchester International Airport – elevation orbit, 20 n mile, 3000 ft

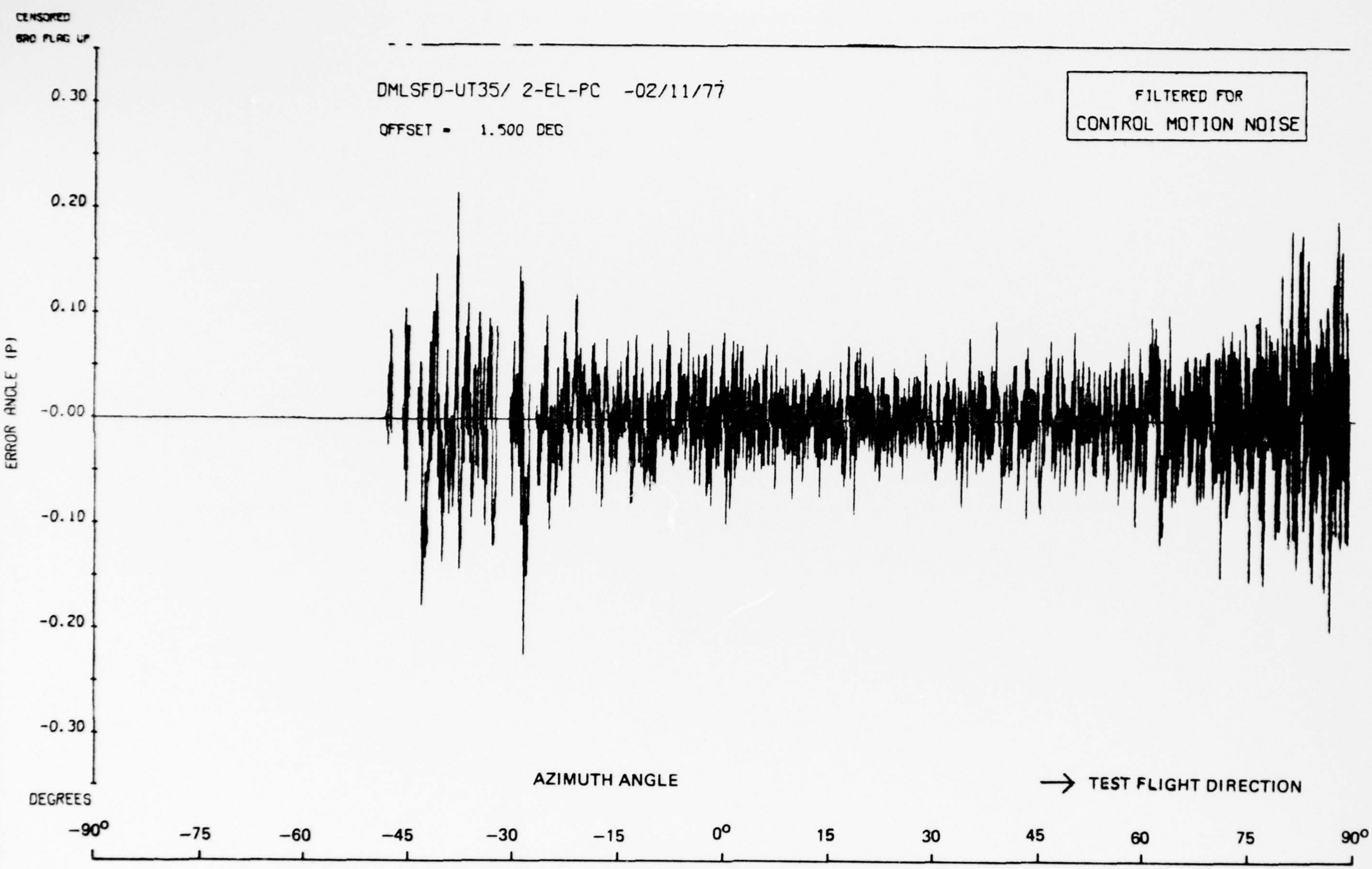


Fig 52b Manchester International Airport – elevation orbit, 20 n mile, 3000 ft

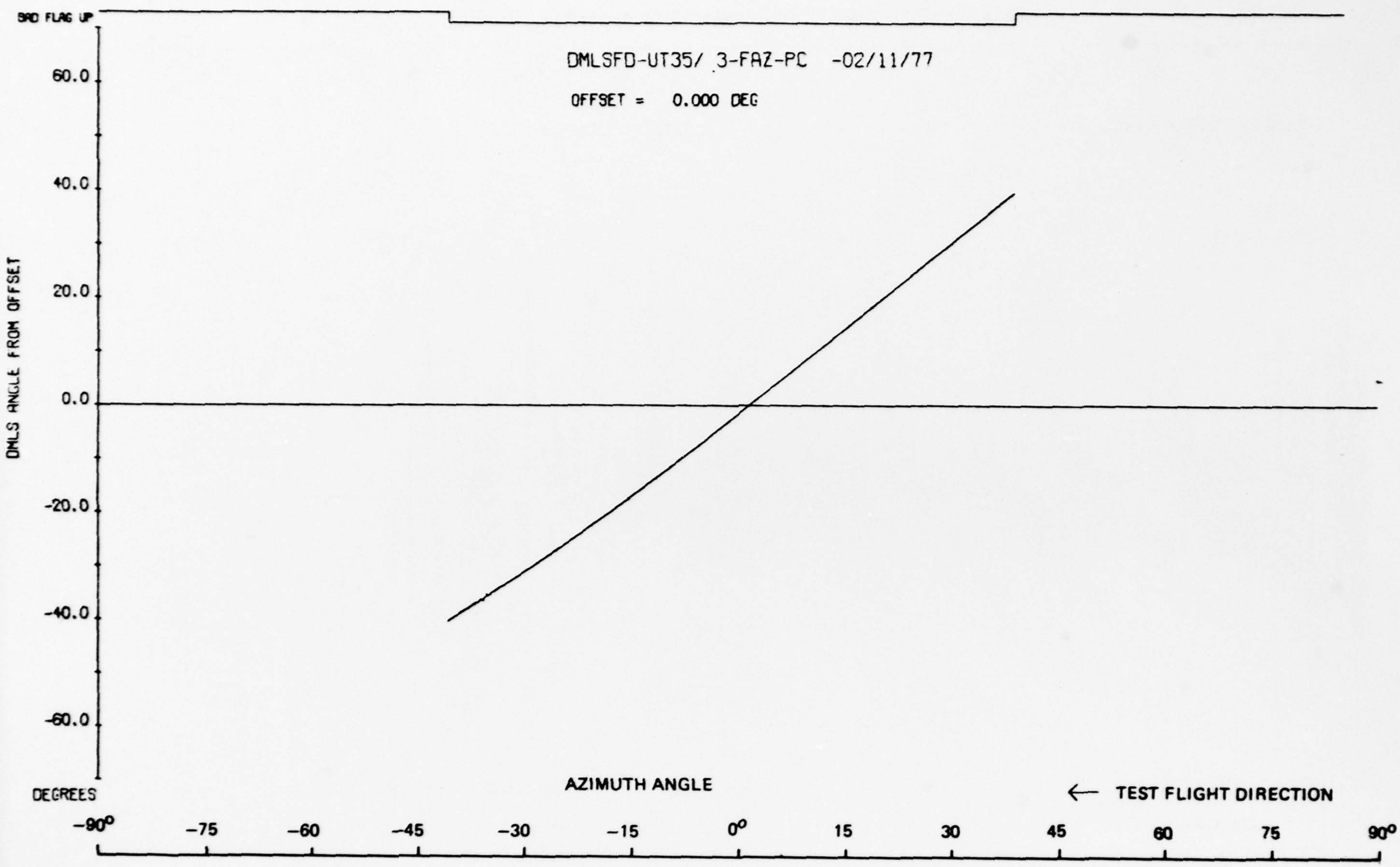


Fig 53a Manchester International Airport – azimuth orbit, 54λ, 20 n mile, 6000 ft

TR 78144

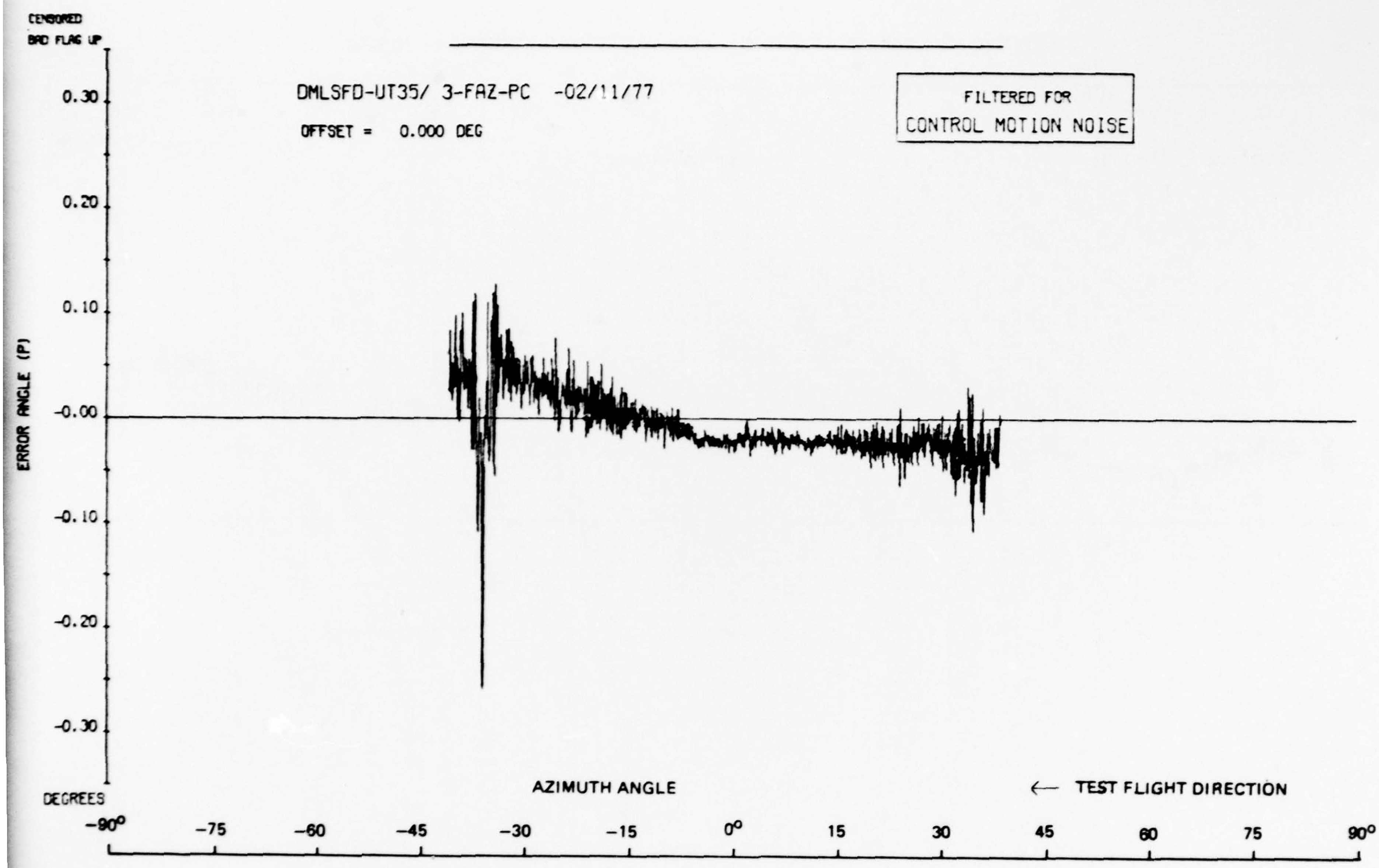


Fig 53b Manchester International Airport – azimuth orbit, 54λ, 20 n mile, 6000 ft

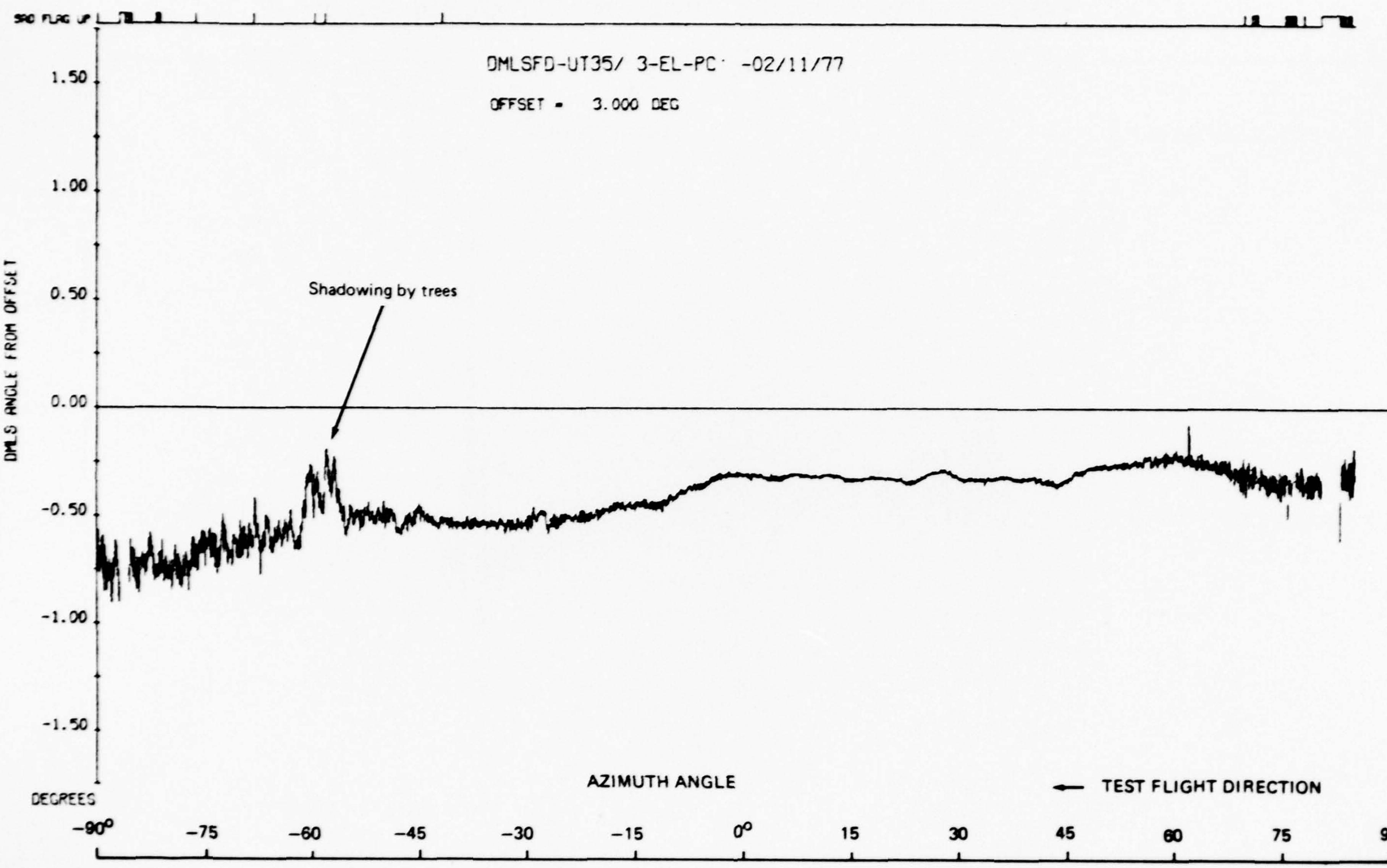


Fig 54a Manchester International Airport – elevation orbit, 54λ, 20 n mile, 6000 ft

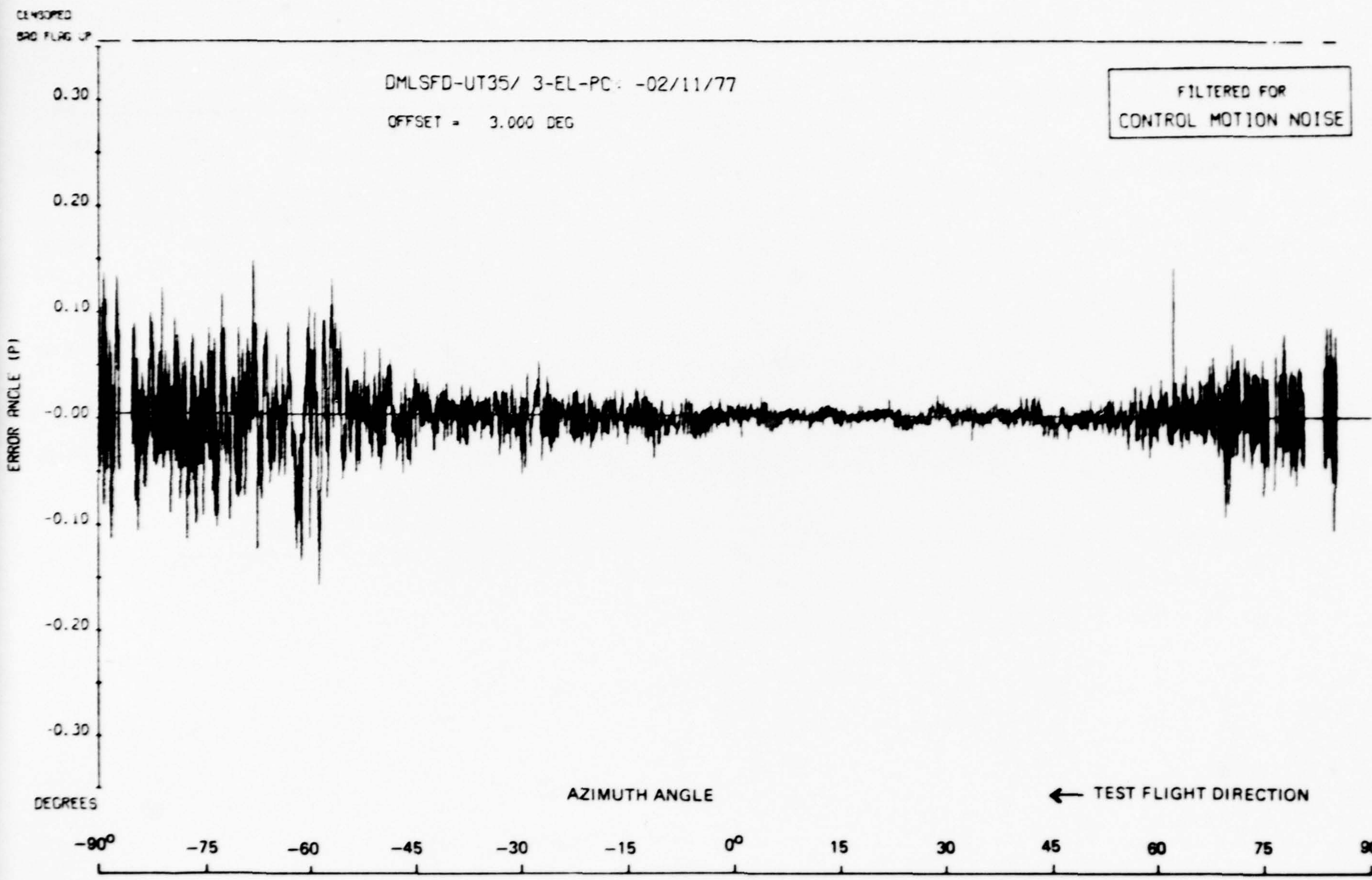


Fig 54b Manchester International Airport – elevation orbit, 54λ, 20 n mile, 6000 ft

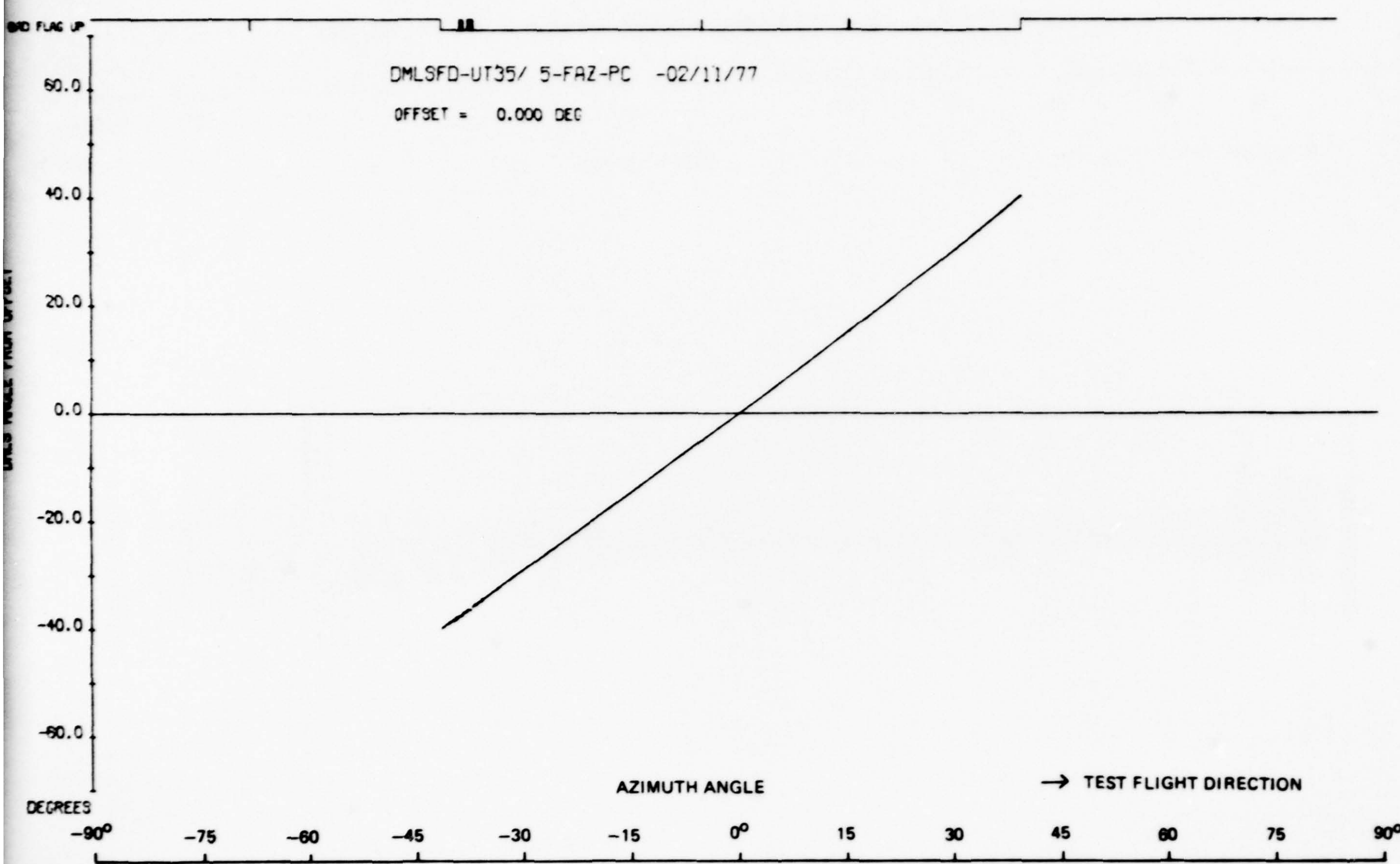


Fig 55a Manchester International Airport – azimuth orbit, 27λ, 20 n mile, 6000 ft

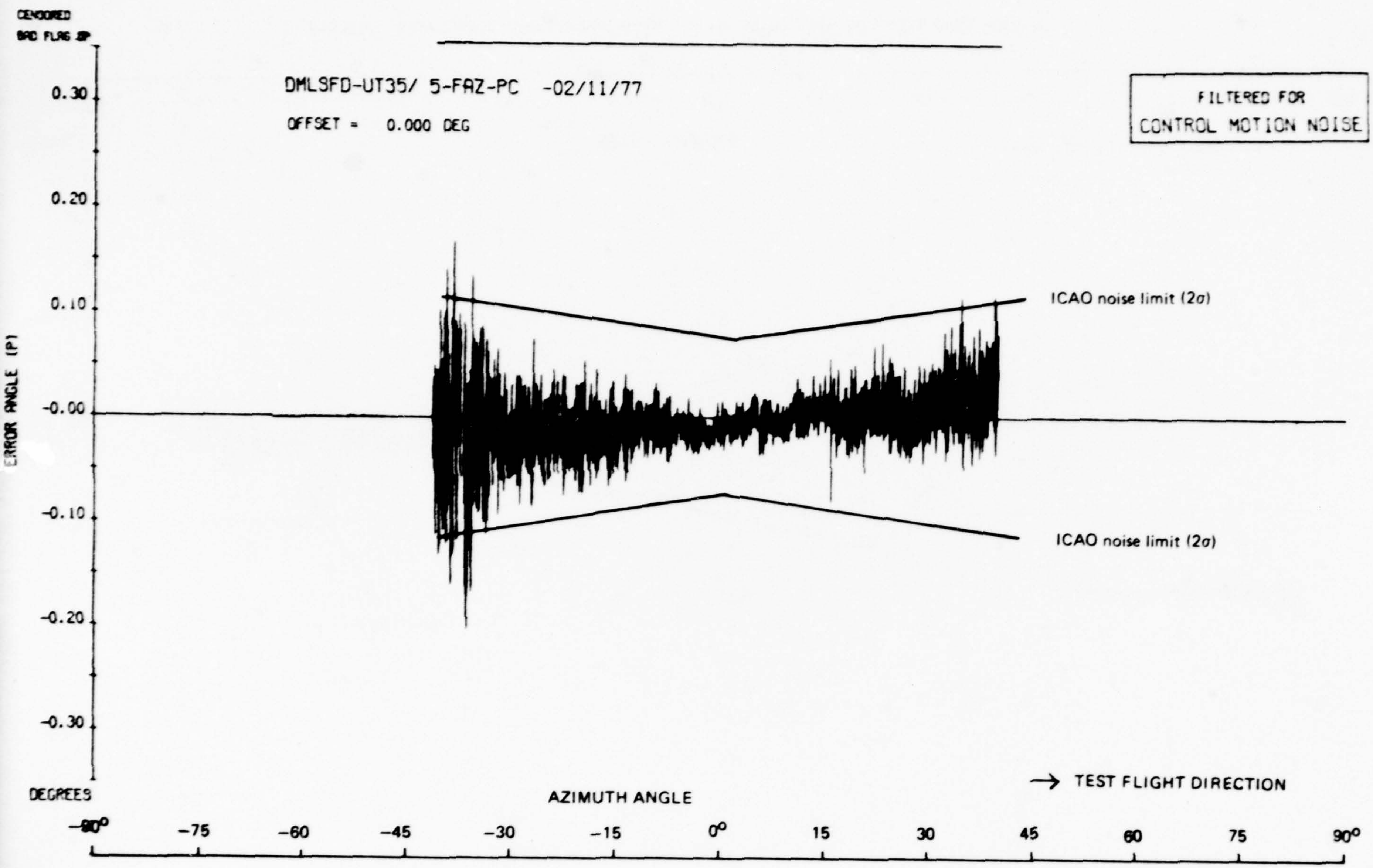


Fig 55b Manchester International Airport – azimuth orbit, 27λ, 20 n mile, 6000 ft

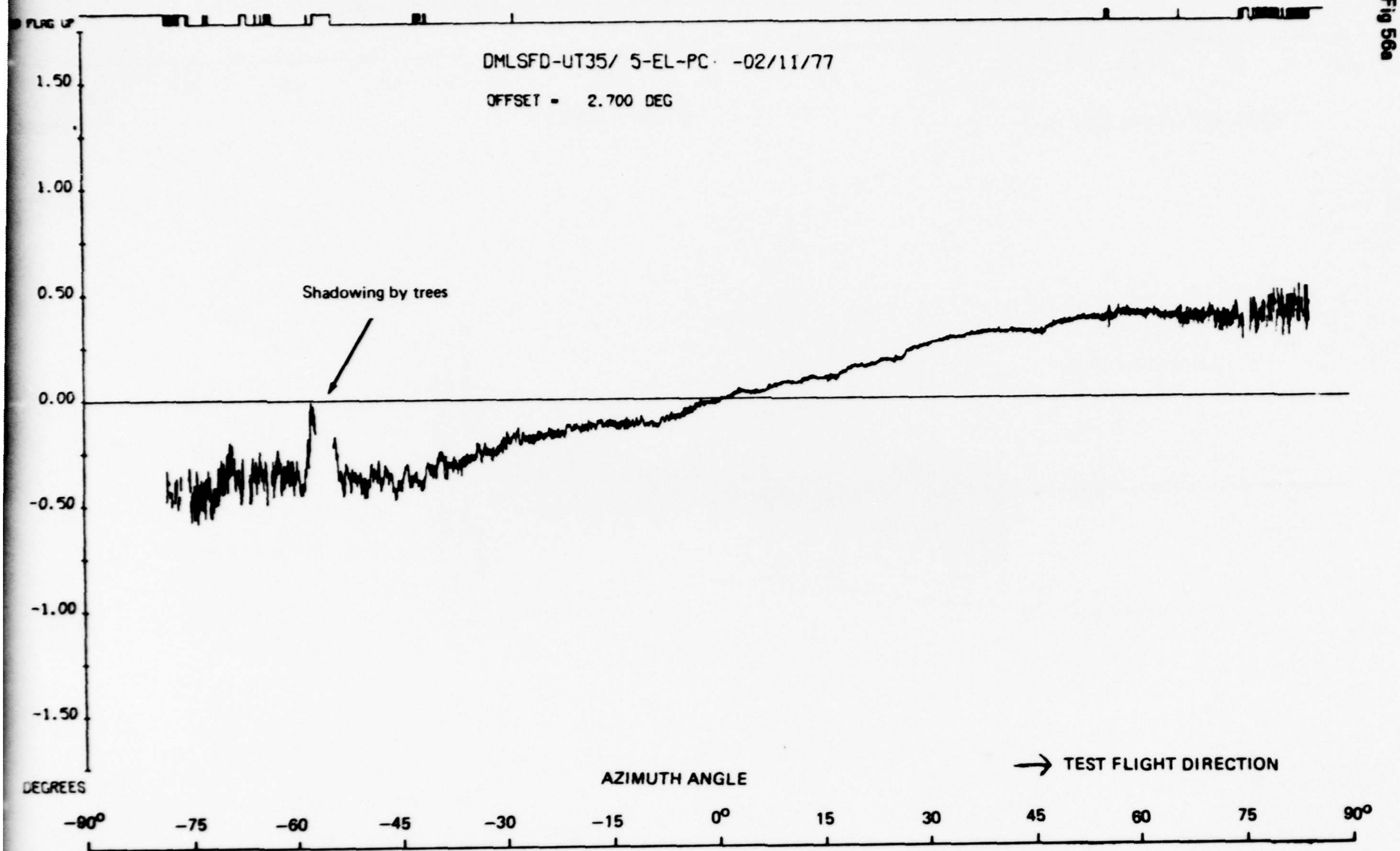


Fig 56a Manchester International Airport – elevation orbit, 54λ, 20 n mile, 6000 ft

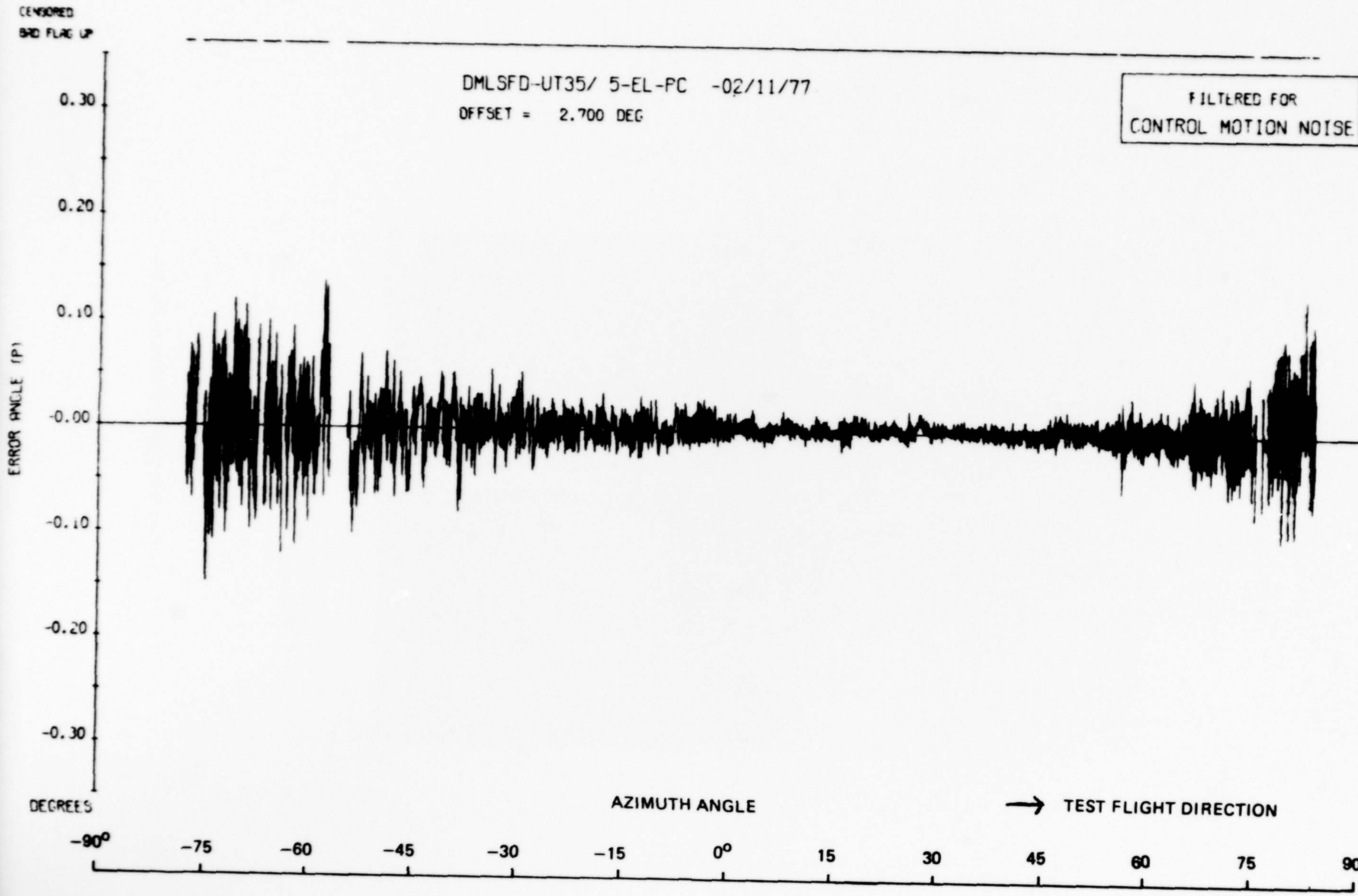


Fig 56b Manchester International Airport – elevation orbit, 54λ, 20 n mile, 6000 ft

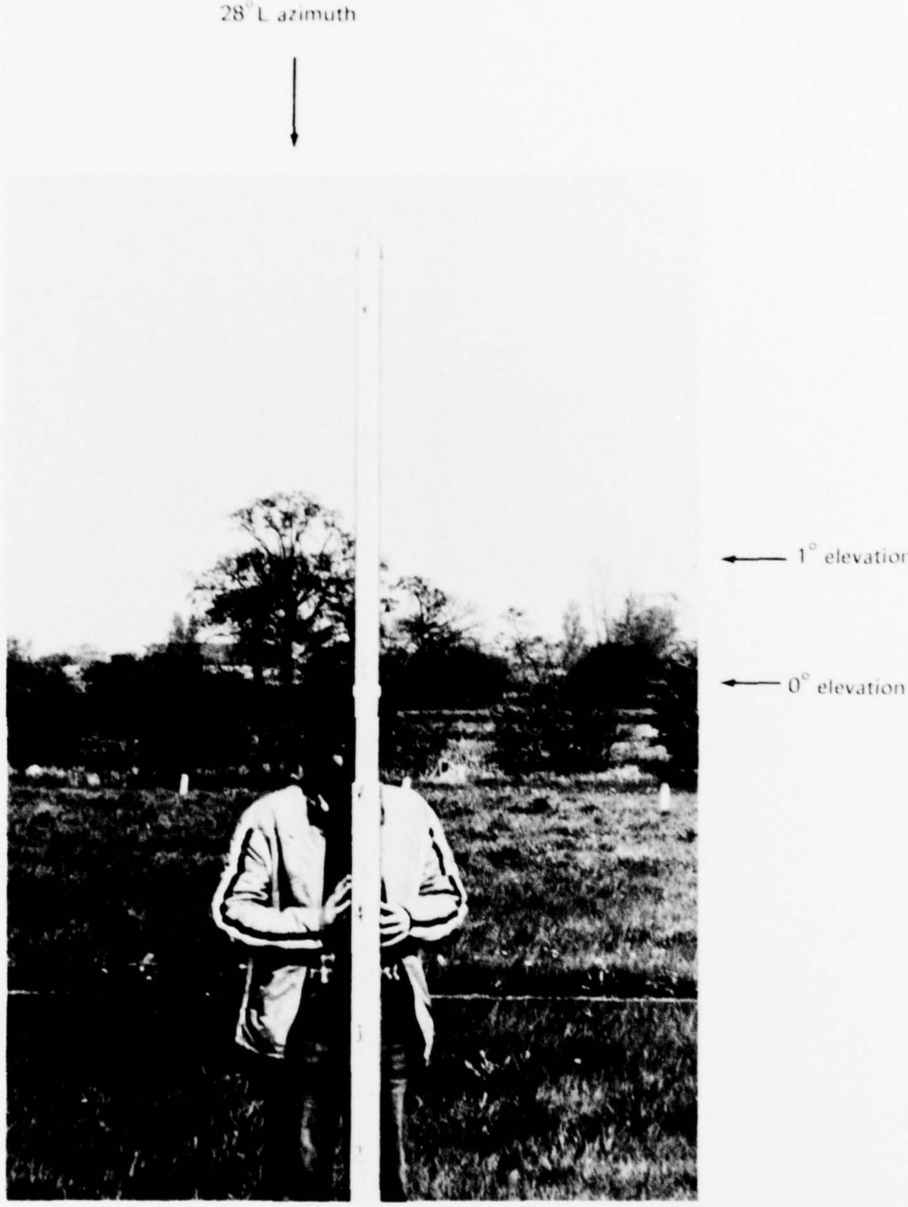


Fig 57 Tree on elevation system skyline at 28° left


Fig 58 View from elevation site showing tree skyline

Fig 59

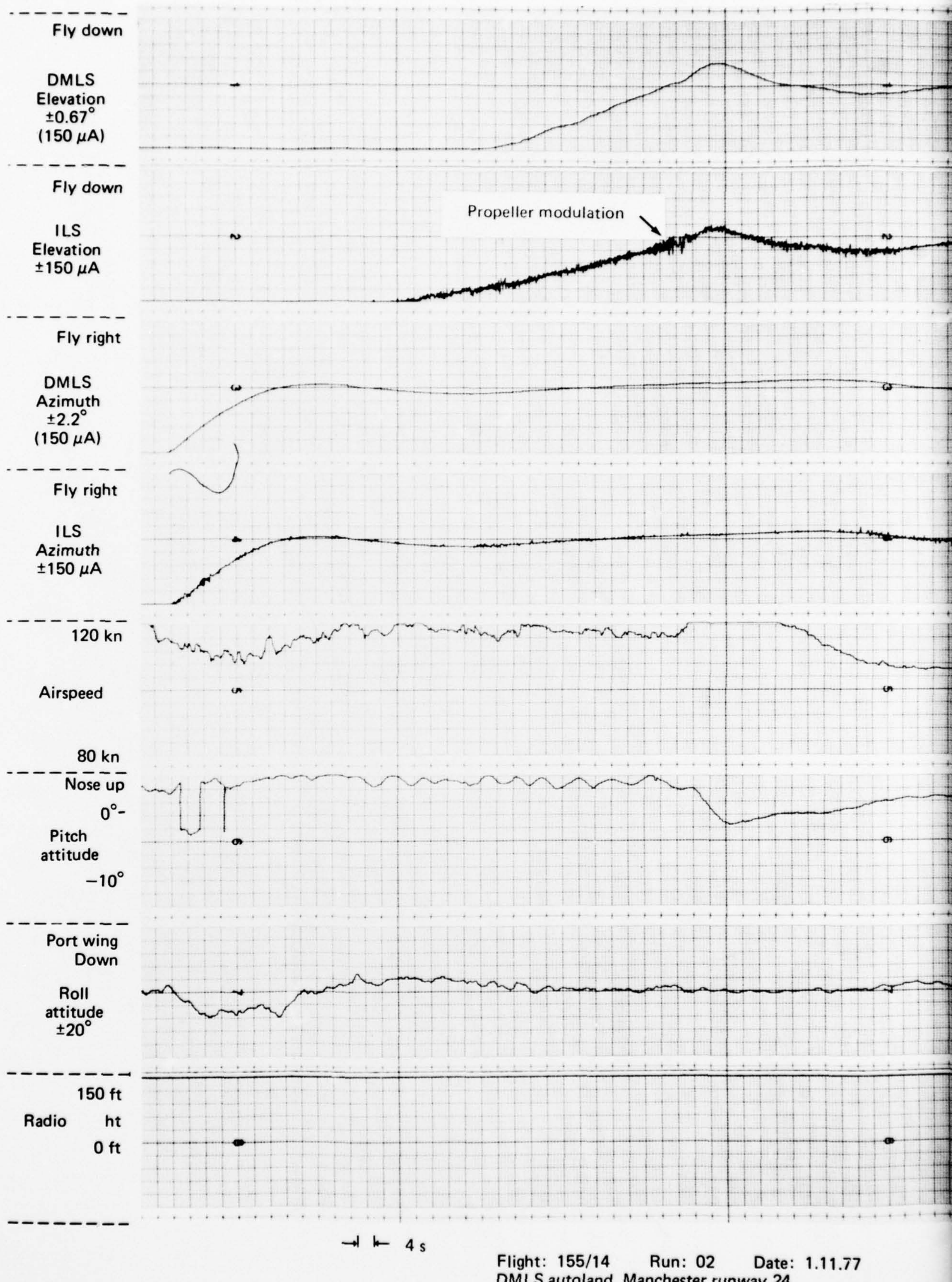


**Fig 59 Flight: 155/14, Run: 02, Date: 1.11.77. DMLS auto**

1

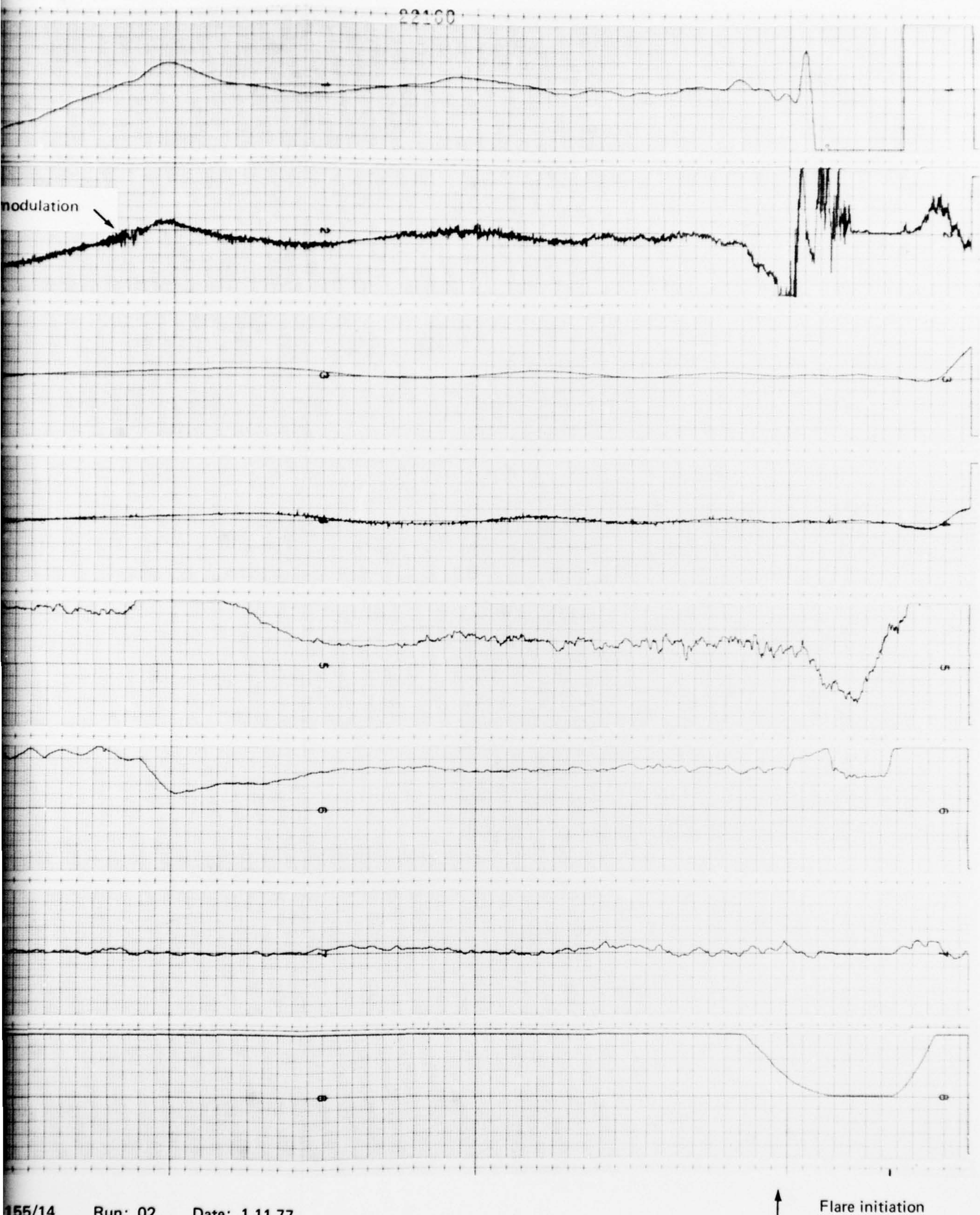


155/14 Run: 02 Date: 1.11.77
utoland, Manchester runway 24

55/14, Run: 02, Date: 1.11.77. DMLS autoland, Manchester runway 24

2

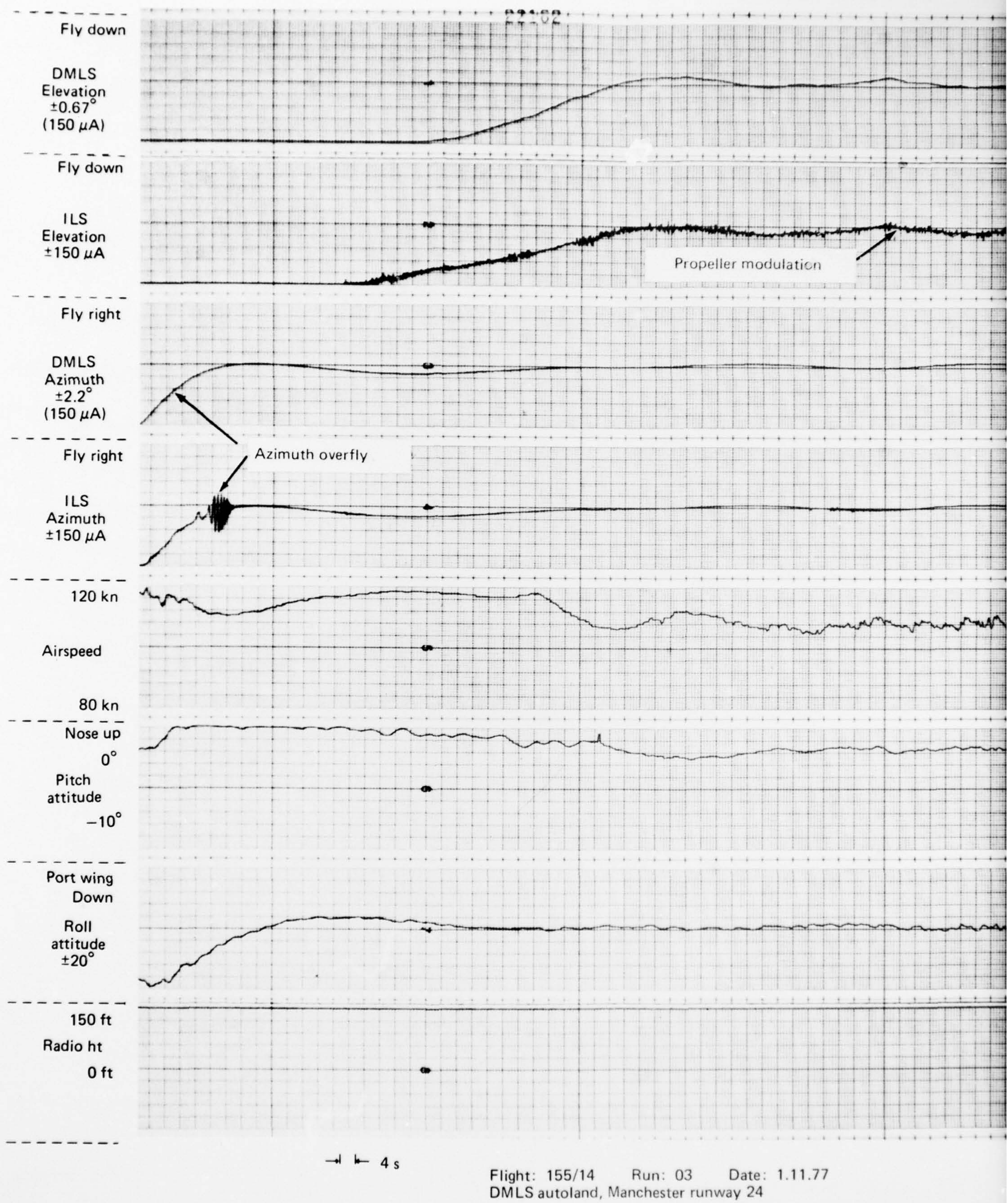


**Fig 60 Flight: 155/14, Run: 03, Date: 1.11.77. DMLS autoland, Manchester runw**

Fig 60

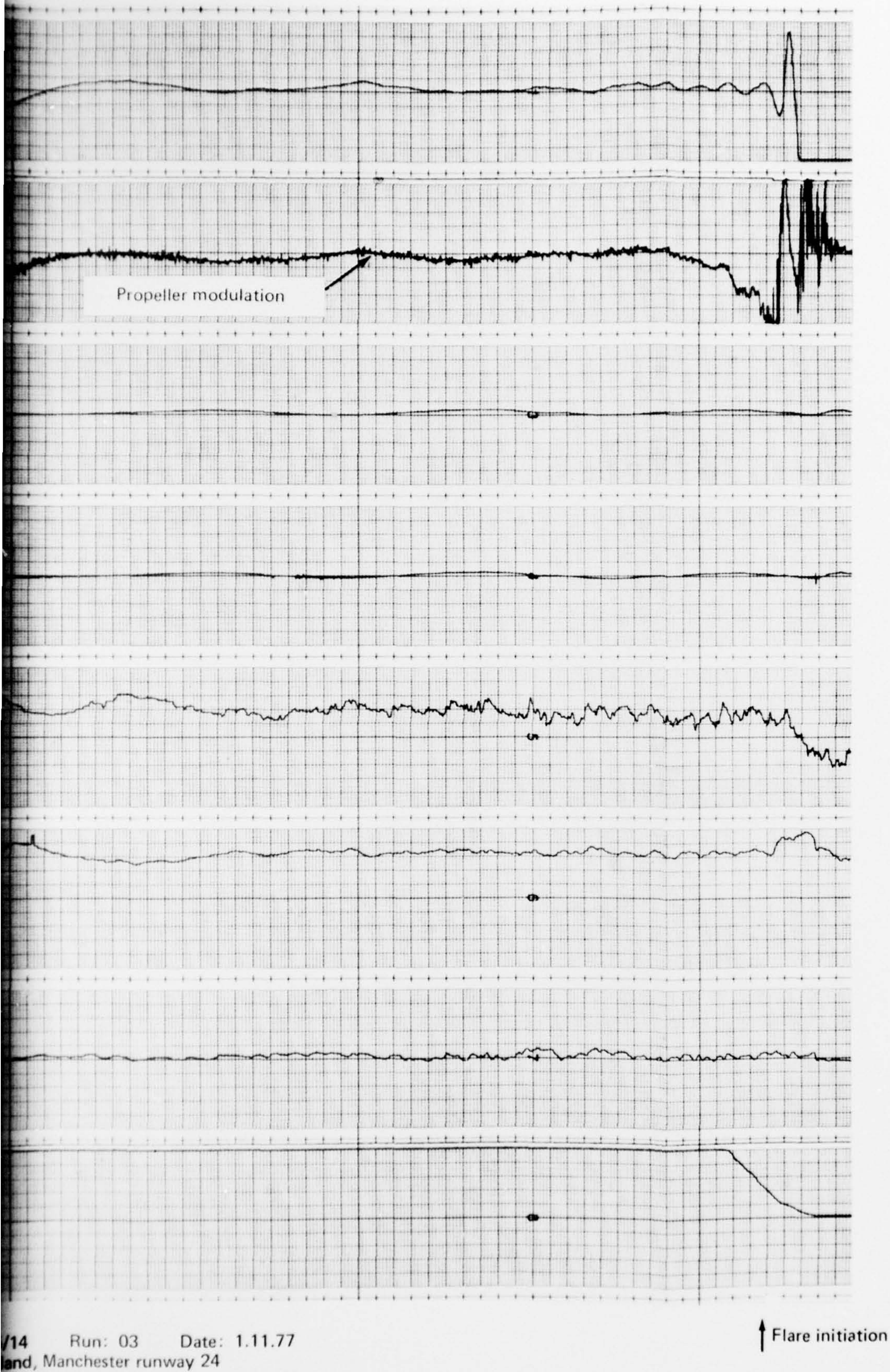


/14 Run: 03 Date: 1.11.77
land, Manchester runway 24

3, Date: 1.11.77. DMLS autoland, Manchester runway 24

Fig 61

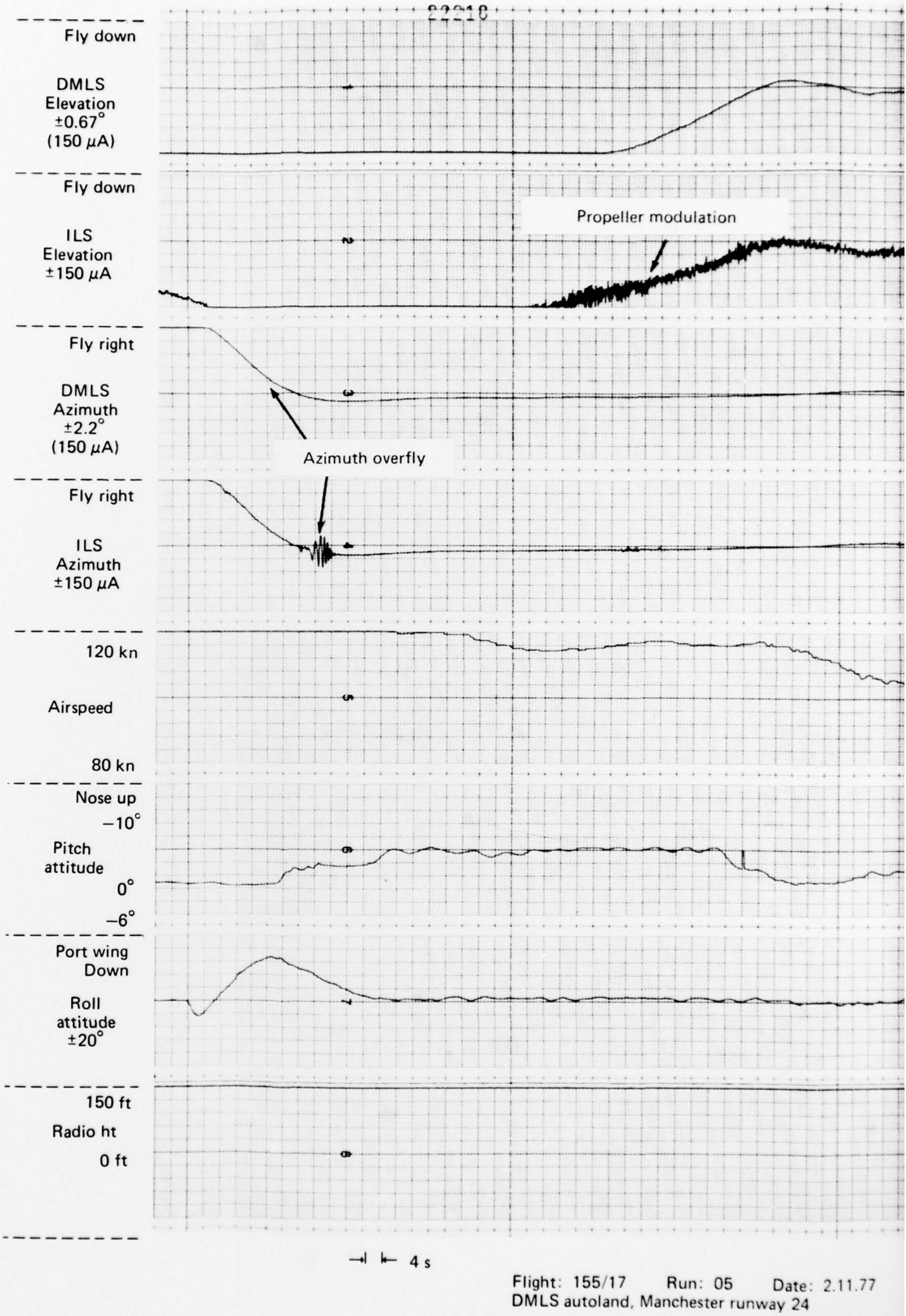


**Fig 61 Flight: 155/17, Run: 05, Date: 2.11.77. DMLS auto**


Flare initiation

/17 Run: 05 Date: 2.11.77
nd, Manchester runway 24

: 05, Date: 2.11.77. DMLS autoland, Manchester runway 24

TR 78144

TR 78144


Flight: 155/17 Run: 07 Date: 2.11.77
DMLS autoland, Manchester runway 24

**Fig 62 Flight: 155/17, Run: 07, Date: 2.11.77. DM**

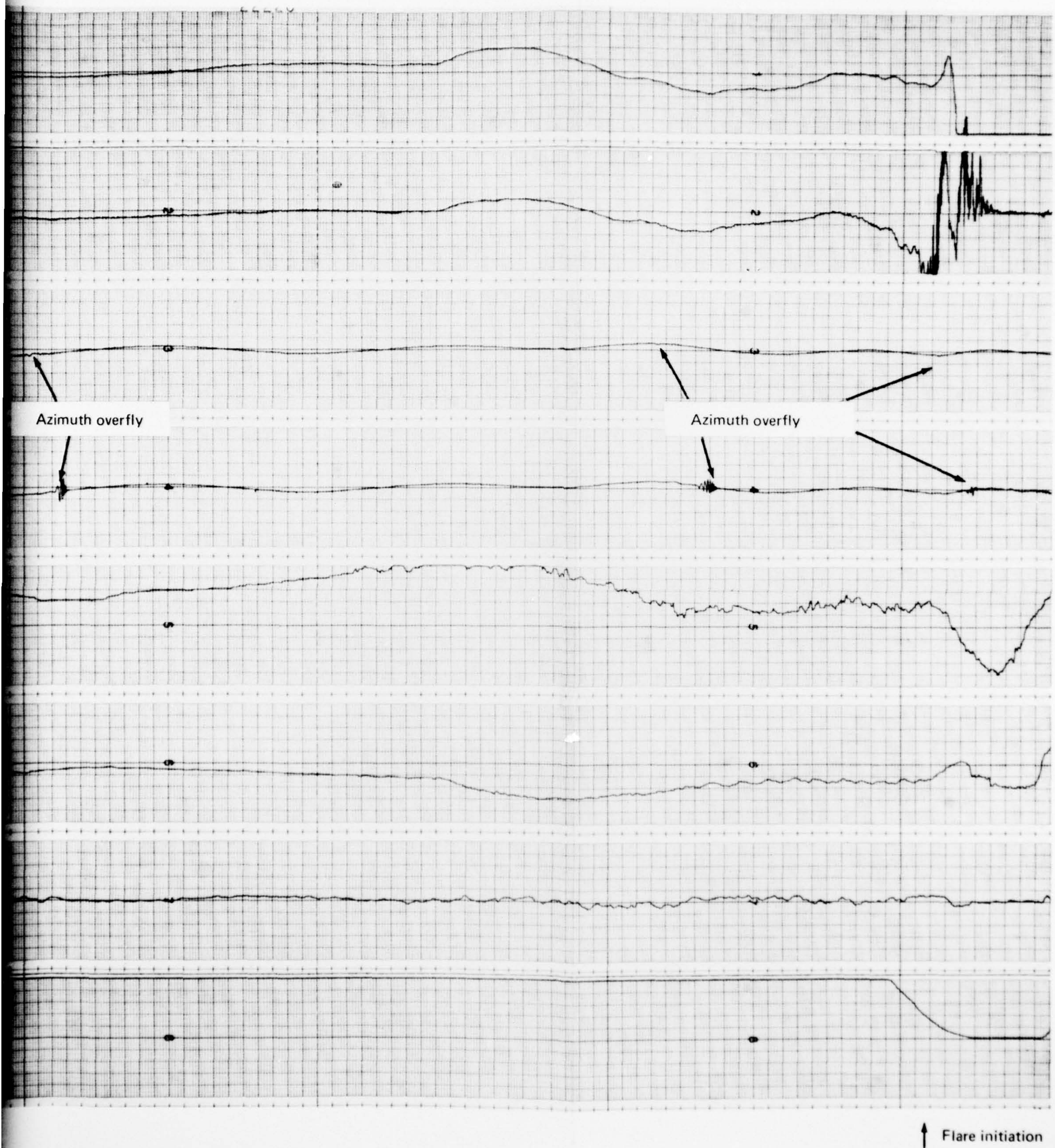


07, Date: 2.11.77. DMLS autoland, Manchester runway 24

Fig 63

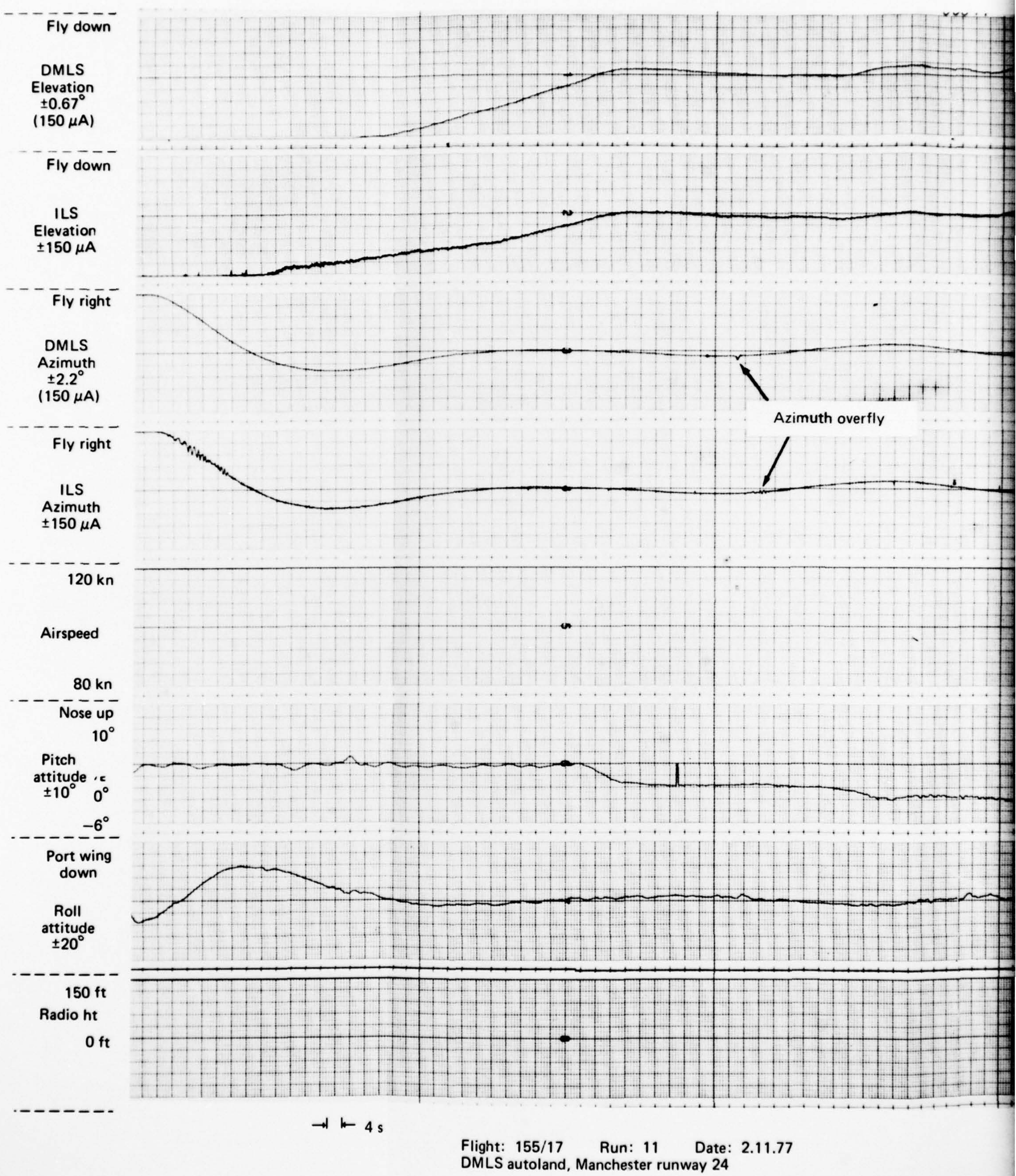


**Fig 63 Flight: 155/17, Run: 11, Date: 2.11.77. DMLS autola**

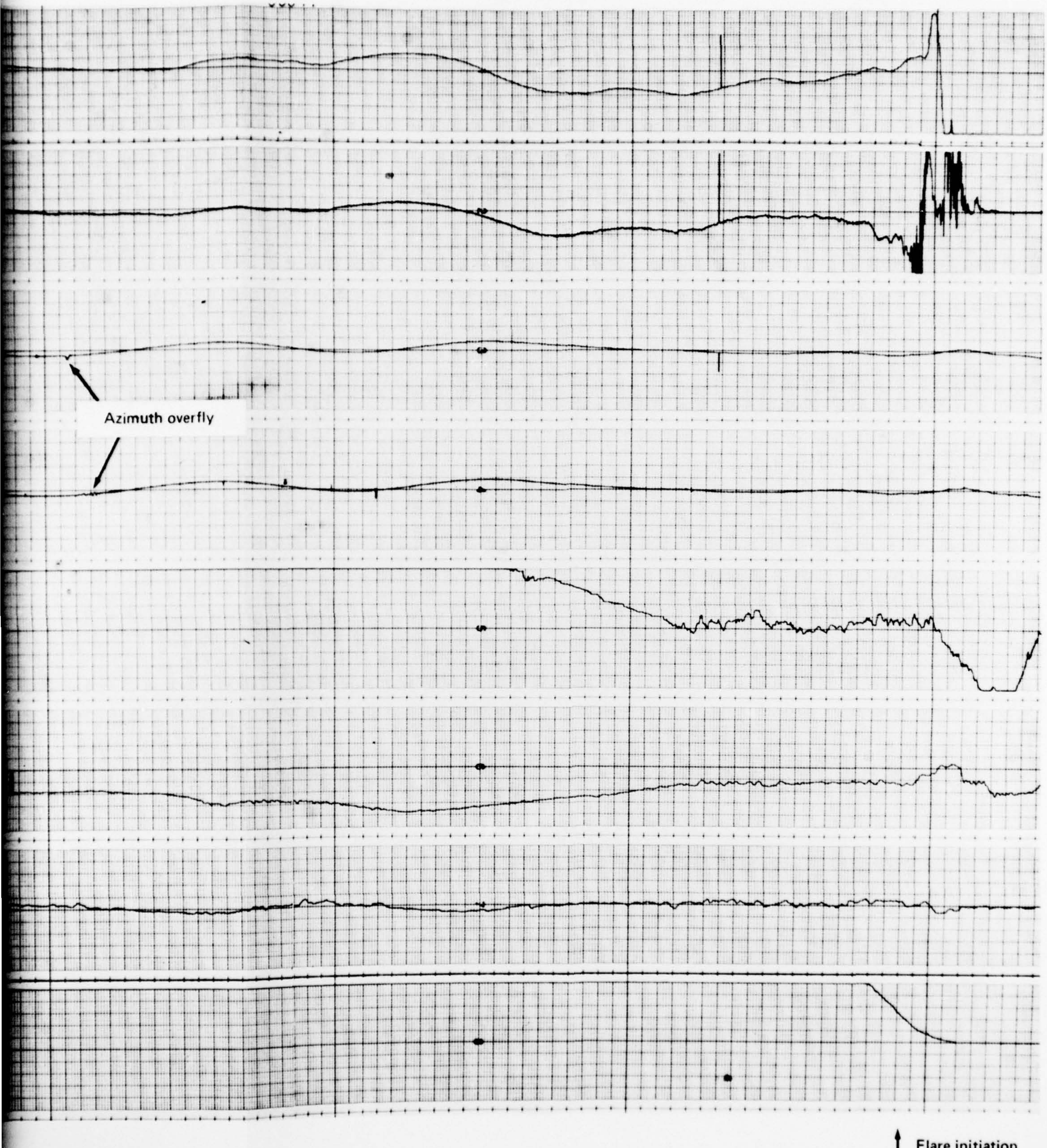


Date: 2.11.77
nway 24

**7, Run: 11, Date: 2.11.77. DMLS autoland, Manchester runway 24**

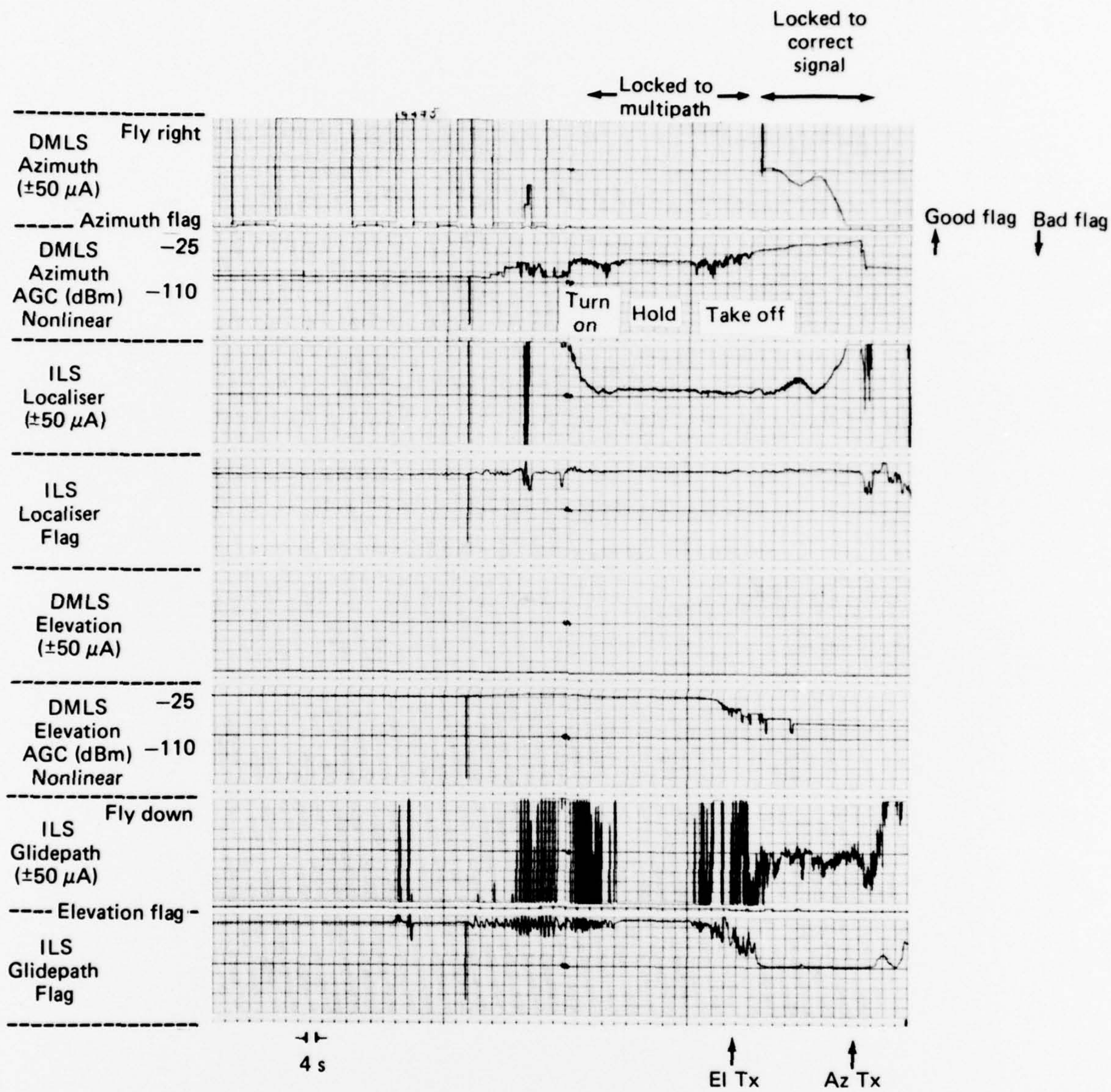


Flight: 155/18 Run: 01 Date: 2.11.77
DMLS Trials, Manchester
Elevation angle:
Wind:

**Fig 64 Take off from runway 24, Bedford HS 748, 2.11.77**

## REPORT DOCUMENTATION PAGE

**Overall security classification of this page**

UNCLASSIFIED

UNLIMITED

As far as possible this page should contain only unclassified information. If it is necessary to enter classified information, the box above must be marked to indicate the classification, e.g. Restricted, Confidential or Secret.

| 1. DRIC Reference (to be added by DRIC) | 2. Originator's Reference | 3. Agency Reference | 4. Report Security Classification/Marking |
|---|---|---|---|
| | RAE TR 78144 | N/A | UNCLASSIFIED |

| 5. DRIC Code for Originator | 6. Originator (Corporate Author) Name and Location |
|---|---|
| 7673000W | Royal Aircraft Establishment, Farnborough, Hants, UK |
| **5a. Sponsoring Agency's Code** | **6a. Sponsoring Agency (Contract Authority) Name and Location** |
| N/A | N/A |

7. Title Trials of the Doppler microwave landing system at Manchester International Airport, October/November 1977

7a. (For Translations) Title in Foreign Language

7b. (For Conference Papers) Title, Place and Date of Conference

| 8. Author 1. Surname, Initials | 9a. Author 2 | 9b. Authors 3, 4 .... | 10. Date | Pages | Refs. |
|---|---|---|---|---|---|
| Walker, D. | | | November 1978 | 124 | 8 |

| 11. Contract Number | 12. Period | 13. Project | 14. Other Reference Nos. |
|---|---|---|---|
| N/A | N/A | | Rad-Nav 67 |

15. Distribution statement
(a) Controlled by –
(b) Special limitations (if any) –

16. Descriptors (Keywords) (Descriptors marked * are selected from TEST)
Landing systems. Microwave landing systems. Doppler MLS. Radio navigation. Multipath. Microwave propagation.


17. Abstract

This Report describes tests performed at Manchester to determine the multipath environment at the airport, and to assess the accuracy and coverage of the Doppler Microwave Landing System in this environment.

High levels of azimuth system multipath were found close to runway threshold, but azimuth systems with as small an aperture as 20 wavelengths (1.2 m) gave the equivalent of ILS Catetory III accuracy. No isolated sources of elevation multipath were found and a 39 wavelength aperture system (2.3 m) gave the equivalent of ILS Category III accuracy for $3^{\circ}$ approaches.

The coverage requirement of 20 n mile range and $\pm 40^{\circ}$ azimuth was achieved at heights sufficient to give clear line of sight, but at elevation angles below about $1.5^{\circ}$, shadowing caused signal loss and large errors.

Autolands were demonstrated using the 54 wavelength aperture systems.

No specifically technique related effects were seen and the results are regarded as representative of typical C-band MLS performance.


F5910/1